Lawrence Berkeley National Laboratory
Recent Work

Title

THE INTERACTIONS OF BENZO(A)PYRENE WITH MOUSE EPITHELIAL CELLS IN CULTURE

Permalink

https://escholarship.org/uc/item/1th8c8sg

Author

Landolph Jr., Joseph Richard

Publication Date

1976-09-01

THE INTERACTIONS OF BENZO(A)PYRENE WITH
MOUSE EPITHELIAL CELLS IN CULTURE

Joseph Richard Landolph, Jr.
(Ph. D. thesis)

September 1976

For Reference

Not to be taken from this room

DISCLAIMER

TABLE OF CONTENTS

THE INTERACTIONS OF BENZO(A)PYRENE

WITH MOUSE EPITHELIAL CELLS IN CULTURE

Joseph Richard Landolph, Jr. *

Lawrence Berkeley Laboratory, Department of Chemistry
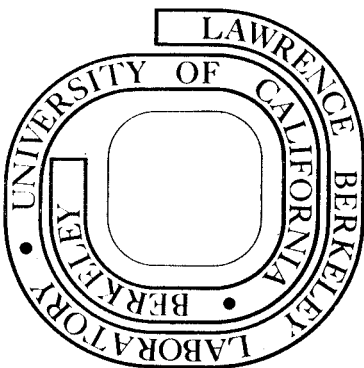University of California
Berkeley, California

ABSTRACT

This thesis represents investigation along four interrelated lines.

Firstly, the mechanisms of the toxicity of Benzo(a)pyrene (BaP) to a mouse liver epithelial cell line (NMuLi) in culture was studied. The toxicity and growth inhibition effects of the carcinogen were exponential with the time of exposure to BaP, with BaP concentration, and with the number of cell divisions in the presence of the carcinogen. Levels of aryl hydrocarbon hydroxylase (AHH), the enzyme responsible for metabolizing BaP to its toxic and mutagenic derivatives, were 1-3 times greater in log phase cells than in confluent cells. An activated derivative of BaP, the diol-epoxide, was 130 times more toxic to exponentially growing cells than to confluent cells. This implied that cellular division or some growth-associated function and not AHH levels was responsible for the greater toxicity of BaP to log phase cells. 7,8 benzoflavone (BF) inhibited the toxicity of BaP to cells and inhibited the AHH from the cells in approximately the same dose-dependent manner, suggesting that the activation of BaP to toxic metabolites was responsible for the cell killing effects of BaP.

Variants resistant to the toxic effects of BaP arose spontaneously at high rates in cloned sensitive lines derived from these epithelial

cells. These resistant variants appeared to possess a selective growth
advantage over the sensitive parent cells from which they were derived.
Cloning analyses showed that sensitive clones shed both sensitive and
resistant subclones, and hence did not breed true. The acquisition of
resistance did not appear to be correlated with chromosome loss, cloning
efficiencies, or population doubling times. In addition, there was no
correlation between the resistant and malignant states, since both
sensitive and resistant clones produced tumors upon injection into
isologous mice.

An exactly exponential relationship was found for the survival
fraction of cells treated with BaP and their maximum inducible AHH
levels, suggesting that the epoxidation and hydroxylation of BaP in
sensitive clones was greater than that in resistant clones and was
responsible for the toxicity. In addition, clones resistant to BaP
were not resistant to the diol-epoxide of BaP, suggesting further
that enzyme loss was responsible for the acquisition of resistance.
In a sensitive clone derived from NMuLi, variants resistant to BaP
increased with passage, but these were extremely sensitive to the
7,8-dihydro-diol of BaP and to the diol-epoxide of BaP. This sug-
gested that these resistant cells had lost an enzyme activity that can
hydroxylate BaP to the dihydrodiol (enzyme A). The killing curve for
the sensitive clone by the dihydro-diol in the presence of BF re-
sembled the killing curve of the resistant clone by the dihydro-diol
without BF, suggesting that the particular resistant clone had lost an
enzyme with a high K_m for the dihydrodiol as substrate (enzyme B),
but retained an enzyme with a low K_m for the dihydrodiol as substrate

(perhaps enzyme A or another enzyme). Hence, there could be two enzymes in this system, one that efficiently hydroxylates BaP to the 7,8-dihydro-diol and one that hydroxylates (epoxidates) the dihydro-diol to the diol-epoxide.

Finally, the effects of substituents on the aromatic ring system of BaP was studied by mass, absorption, and fluorescence spectroscopy. The guiding principle in the mass spectra of the derivatives of BaP was that the aromatic system was very stable, since the parent ions of the derivatives in many cases were the base peaks in the spectra. Loss of simple, small molecules also predominated, followed by ring closure to retain the aromatic system where possible. Doubly charged ions were abundant in the mass spectra, again attesting to the stability of the aromatic system. Fluorescence and absorption spectra could be rationalized where a double bond was saturated by substitution in considering the next lower aromatic from which BaP would be formally derived. Simple single-atom substitution resulted in general in red-shifts, and the magnitude of these paralleled the electron-donating inductive effect of the substituent. This could be rationalized on the basis of the substituent stabilizing a polar excited state of the molecule, i.e., the transition state dipole. The unusual stability of the aromatic system regardless of the substituent was the overwhelming conclusion reached from a study of these spectra, and might play a part in the toxicity and mutagenicity of this compound.

I. QUANTITATIVE STUDIES OF THE TOXICITY OF BENZO(A)PYRENE TO A MOUSE LIVER EPITHELIAL CELL STRAIN IN CULTURE[1]

A. Summary

The toxic effects of the carcinogen benzo(a)pyrene (BaP) were studied in a well-characterized epithelial cell strain NMuLi derived from the livers of weanling Namru mice. These cells were extremely susceptible to the toxicity, 99% dying after a six-day exposure to 5 ug/ml of BaP.

The toxic effects began between 11 and 24 hours post-application of BaP to the cells, and increased exponentially with the time of treatment. The toxicity was concentration-dependent in cells treated for a specific time period. The survival curves were exponential, and extrapolated to survival fraction of 1.0.

The toxic effects of BaP to logarithmically growing NMuLi were inhibited 40% by 7,8 benzoflavone (BF) and the inhibition was concentration-dependent. BF also inhibited aryl hydrocarbon hydroxylase (AHH) from NMuLi cell homogenates and microsomes by 99%. The concentration dependence for AHH inhibition by BF paralleled its inhibition of cellular toxicity.

The toxicity of BaP to these cells increased exponentially with the number of population doublings. Hence, the toxicity was 130 times greater in exponentially growing cells than in confluent cells. Levels of AHH, the enzyme that metabolizes BaP to its cytotoxic derivatives,

---

[1] The abbreviations used are: AHH, aryl hydrocarbon hydroxylase; BaP, benzo(a)pyrene; BF, 7,8 benzoflavone.

were only 2.4 times higher in exponentially growing than in confluent cells, suggesting that cell division or a growth-associated function was responsible for the large differential toxicity. In addition, a toxic BaP metabolic was preferentially toxic to log phase cells.

The results indicate that metabolism of BaP by AHH to produce cytotoxic metabolites, which may cause lesions that are expressed upon cell division, is responsible for the cytotoxicity of BaP to NMuLi.

B. Introduction

Analysis of a study carried out in Denmark showed that 92% of human cancer incidence is a result of carcinomas, which are of epithelial origin while the remaining 8% is due to leukemias and sarcomas, which are of connective tissue origin (4). Although more efforts should be devoted to study the effects of carcinogens on epithelial cells, it has been difficult to culture epithelial cells free of fibroblasts. Consequently, only a few malignant transformation studies with chemical carcinogens have been conducted on well-characterized epithelial systems, and many of these are plagued by high spontaneous transformation rates and difficulty in morphologically scoring transformants. Most of these investigations have been detailed in a comprehensive review of chemical transformation by Heidelberger (21). In addition, a temperature-sensitive mutant of chemically-transformed rat liver epithelial cells has been characterized by Yamaguchi and Weinstein (47).

Recently, Owens et al. have isolated a number of cell strains from Namru mice by selective trypsinization techniques and have characterized

them as epithelial by numerous morpologic and ultrastructural
criteria (26, 35). In other work, Whitlock and Gelboin have charac-
terized the induction parameters for aryl hydrocarbon hydroxylase
(AHH), the enzyme system responsible for metabolizing the carcinogen
benzo(a)pyrene (BaP) to cytotoxic derivatives (10, 16, 17), in an
epithelial cell strain cloned from Buffalo rat liver (45, 46). Huberman
and Sachs have shown that human embryo cell cultures containing greater
than 20% epithelial cells metabolized 3 to 25 times more BaP to water
soluble and alkali-soluble derivatives than did fibroblastic cell
cultures from the same embryos (22). Schwartz has shown that 7,12
dimethylbenz(a)anthracene inhibited the growth of rat liver epithelial
cells and depressed ^{3}H thymidine incorporation (40).

The production of malignantly transformed cells in culture generally
follows a different dose response relationship than does the toxicity of
carcinogens to cells, and no apparent correlation is evident (5, 25).
In fact, toxicity and transformation are competing processes and may
be wholly (11) or partially uncoupled (20, 32). Nevertheless, there
are certain parallels between malignant transformation and toxicity.
Both processes require activated or proximate forms of the carcinogen
(2, 8, 16, 17, 21, 24), and are mitigated by inhibitors of enzyme
systems that metabolize carcinogens to proximate forms (10, 29, 34).
Further, many strong carcinogens are also very good cytotoxic agents,
such as BaP (1, 7, 10, 15, 17, 23, 25), 4-nitroquinoline-1-oxide
(43, 44), 3-methylcholanthrene (3, 32), N-methyl-N'-nitro-N-nitro-
soguanidine (37), and 7,12 dimethylbenz(a)anthracene (9, 11, 14, 33, 42).
It is known that cell division is necessary for the expression of

malignant transformation (5, 12, 27, 28, 39). _In vivo_, it is conceivable that the cytotoxicity of carcinogens aids their carcinogenicity by calling up a proliferative response in the target organ, thus allowing the number of divisions to fix and express the properties of transformation, although large toxic effects could also decrease the yield of transformed cells.

For these reasons and the ease of studying toxicity, we chose to further examine aspects of the toxic process exerted by the carcinogen BaP. In particular, was cell division also necessary for toxicity expression? This information would extend or rule out the use of toxicity as a crude model for transformation.

Bartholomew _et al._ have tested five of Owens' epithelial strains and found all to be very susceptible to BaP-induced cytoxicity, and more susceptible than two fibroblastic strains that were tested (1). The most sensitive strain tested, NMuLi, was derived from weanling liver. Possessing a wide variety of enzyme activities responsible for metabolizing carcinogens and xenobiotics, liver cells should be of particular relevance in toxicity studies. Consequently, we have extended the work of Bartholomew _et al._ by examining in detail the toxicity of BaP to these epithelial cells. In particular, we have defined the time and concentration dependence of the toxicity, the necessity for cell division in toxicity expression, and the inhibition of the toxicity by 7,8 benzoflavone (BF).

C. Materials and Methods

1. Cells

The NMuLi cell strain is an epithelial derivative obtained from the

pooled livers of weanling Namru mice by Owens et al. (35, 36). The cells make aldolase A (muscle type aldolase) (Larry Anderson, personal communication), which predominated in developing or neoplastic cells from liver (41). As Owens originally reported, NMuLi produces predominantly differentiated cystadenomas when injected into newborn Namru mice (35, 36) with an occasional fibrosarcoma and adenocarcinoma at passage 10. At passage 28, Owens et al. (36) found that NMuLi produced two tumors out of four mice injected; one tumor was a differentiated cystadenoma and the second was a fibrosarcoma. In our laboratory, NMuLi did not grow in soft agar at passage 36 at innocula of 10^6 cells by the method of MacPherson (31). A positive control, Moloney murine sarcoma virus-transformed Balb 3T3 cells, grew well in agar in this assay. At passage 40, intrascapular injection of four clones from NMuLi at 1-3 $\times$ 10^6 cell/innocula, produced tumors which were mixtures of cystic structures and fibrosarcomas, with a latent period of one week. When explanted, the cells cultured from NMuLi tumors grew in soft agar and all possessed epithelial morphology (6/6 tumors explanted).

The cloning efficiency of NMuLi is 50 $\pm$ 10% (3 experiments) and the population doubling is 16 $\pm$ 1 hours (4 experiments). Unless otherwise indicated these experiments were performed on cells from passages 26 to 40.

2. General Culture Techniques

NMuLi was cultured in minimal Eagle's medium (13) fortified with 10% fetal calf serum (GIBCO, Grand Island, N.Y.) and 10 ug/ml of insulin under 5% CO_2 at 37°. Cells were seeded at 1 $\times$ 10^5 per 100 mm dish (Falcon Plastics, Oxnard, Calif.) and transferred weekly as previously

described (1). Cells were routinely checked for Mycoplasma-free by autoradiography using the method of Culp and Black (6), and the results were negative.

Growth curves were determined by seeding 3×10^4 cells per 35 mm dish in 1.5 ml of medium, and allowing the cells to recover for 24 hr. On each day of counting, the medium was aspirated off and the cells were washed with 0.25 mM Tris-HCl, pH 7.4, containing mM NaCl, and 0.7 mM Na_2HPO_4 (isotonic Tris buffer). The cells were then removed from the plates by incubating the 0.01% trypsin (Difco, 1:250, Detroit, Mich) in isotonic Tris buffer for 10 min at 37°C. An aliquot of the trypsin solution was counted in a model Fn Coulter counter (Coulter Electronics, Hialeah,Fla). Four plates were averaged for each point on the growth curves.

Saturation densities were determined from complete growth curves determinations by reading off the highest cell number attained. Medium was not renewed during growth curve determinations. The exponential portion of the growth curves was computer-fit, using a linear least-squares program, to determine the fractional growth rate, from which the doubling time was determined.

3. Toxicity Studies

Two general types of studies were conducted. For determining the concentration dependence of the toxicity, cell counting assays were performed as follows: Cells were seeded at 3×10^4 per 35 mm dish 1.5 ml of medium, and allowed to recover for 24 hr, at which time they were in log phase of growth. Then, 10 ul of a freshly prepared solution of BaP in acetone was added directly to the culture (0.66% acetone in the medium) for three days. After BaP treatment, cells were trypsinized

and counted as per growth curve determinations. This acetone concen-
tration caused no cell death relative to the untreated controls.

The concentration dependence of the toxicity was also verified by
clonal death assays, as follows; 300 single cells were plated in 60 mm
dishes in 5.0 ml of medium, and allowed to recover for 24 hr. Then
10 ul of a solution of BaP in acetone (0.2% acetone in the medium) was
added to the culture for three days. Acetone at this concentration
had no effect on the cloning efficiency of NMuLi. At the end of BaP
treatment, the medium was aspirated off, the cells were gently washed
one time with 2 ml of isotonic Tris buffer, and fresh medium was
added. At day 9 to 16 post-plating, as the colonies became visible
to the eye, the medium was removed and the colonies were fixed and
stained for 1 min with a solution of 1% crystal violet (Matheson,
Coleman, and Bell, Norwood, Ohio) in 25% ethanol-water. The plates
were then gently rinsed three times in tap water and the colonies
counted.

Growth curves of cells in BaP constituted the second type of
experiment in order to determine the time dependence of the toxicity.
In these assays, cells were seeded and treated exactly as in the cell
counting kinetics assay above, with the following modifications: cells
were counted each day and BaP was always present. Media was not
renewed in these arrays.

4. Chemicals

Acetone Regent grade (Matheson, Coleman, and Bell, Norwood, Ohio),
was redistilled. Benzo(a)pyrene (Aldrich, San Leandro, Calif.) was

purified by column chromatography on neutral alumina (Woelm, Eschewege, Germany) with chromatoquality (Aldrich) benzene as eluant. It was recrystallized from benzene-isopropanol, and its purity was verified by thin-layer chromatography on 6060 silica gel plates (Eastman Kodak, Rochester, N.Y.) with 19/1 (v/v) benzene-ethanol as developing solvent. 7,8 benzoflavone (Aldrich chemicals, San Leandro, Calif.), was used without further purification. $\pm$ -7$_\alpha$, 8$_\beta$ -dihydroxy - 9$_\beta$, 10B -epoxy -7, 8, 9, 10 -tetrahydrobenzo(a)pyrene was synthesized by K. Straub, this laboratory.

5. Aryl Hydrocarbon Hydroxylase Induction and Assay

After an 11 hour treatment of cultures with 1 ug/ml of BaP, which was found to be maximal for induction (J. Landolph, J. Becker, and H. Gamper, manuscript in preparation), cell sonicates were prepared, and AHH activity measured essentially as described previously (1). The sample was kept in ice until addition to the incubation mixture. For blanks, the enzyme was denatured by the addition of acetone to the incubation mixture at the beginning of the assay. This was found necessary, since in some cases sufficient BaP remained from the induction period and the reaction proceeded in the absence of additional substrate. These blanks corrected for the carry-over of fluorescent hydroxylated derivatives formed during the induction period, which in some cases was substantial. These blank values were in all cases higher than the no-enzyme controls. The assay was linear up to 1.4 mg of protein (total cellular protein) in the 30 min incubation, and for up to 90 min with 1.4 mg of cellular protein.

The inhibition of AHH by BF was tested by adding BF in acetone to

the incubation mixture (1 ml), followed by sub-strate and cell

homogenate.

Protein concentration was measured by the method of Lowry, with

crystalline bovine serum albumin as a standard (30).

D. Results

1. Time Dependence of the Toxicity Expression

Growth curves of NMuLi in the presence of benzo(a)pyrene (BaP)

(Chart 1) show that BaP depresses the growth and saturation density

of NMuLi.

This data can be analyzed to show the effect of time on the

expression of the toxicity more clearly. For cells in logarithmic

growth phase, $N = N_0 \times \exp(\alpha t)$ where α is the fractional growth rate,

N is the number of cells at time t and N_0 is the number at time 0.

For log phase cells growing in BaP, a death term due to the effect of

the carcinogen must be added, $N_b = N_0 \exp(\alpha' t) \times \exp(-\beta t)$ (if death is

one-hit), where β is some function of carcinogen concentration and α is

the growth rate of cells in BaP. Taking the ratio of a BaP-treated

culture to a mock-treated culture, $\log(N_b/N) = (\alpha - \alpha - \beta)t$, and a

plot of $\log(N_b/N)$ vs. t will be linear as long as the cells are growing

exponentially and the carcinogen concentration is held constant. These

plots are shown in Chart 2 and indicate that the toxicity increases

after one day of BaP treatment, i.e., the slope of the survival curve

becomes more negative.

After one day of treatment, the survival curves appear approx-

imately exponential until a plateau value is approached. The curve

at the highest concentration of BaP employed, 5 ug/ml indicates that
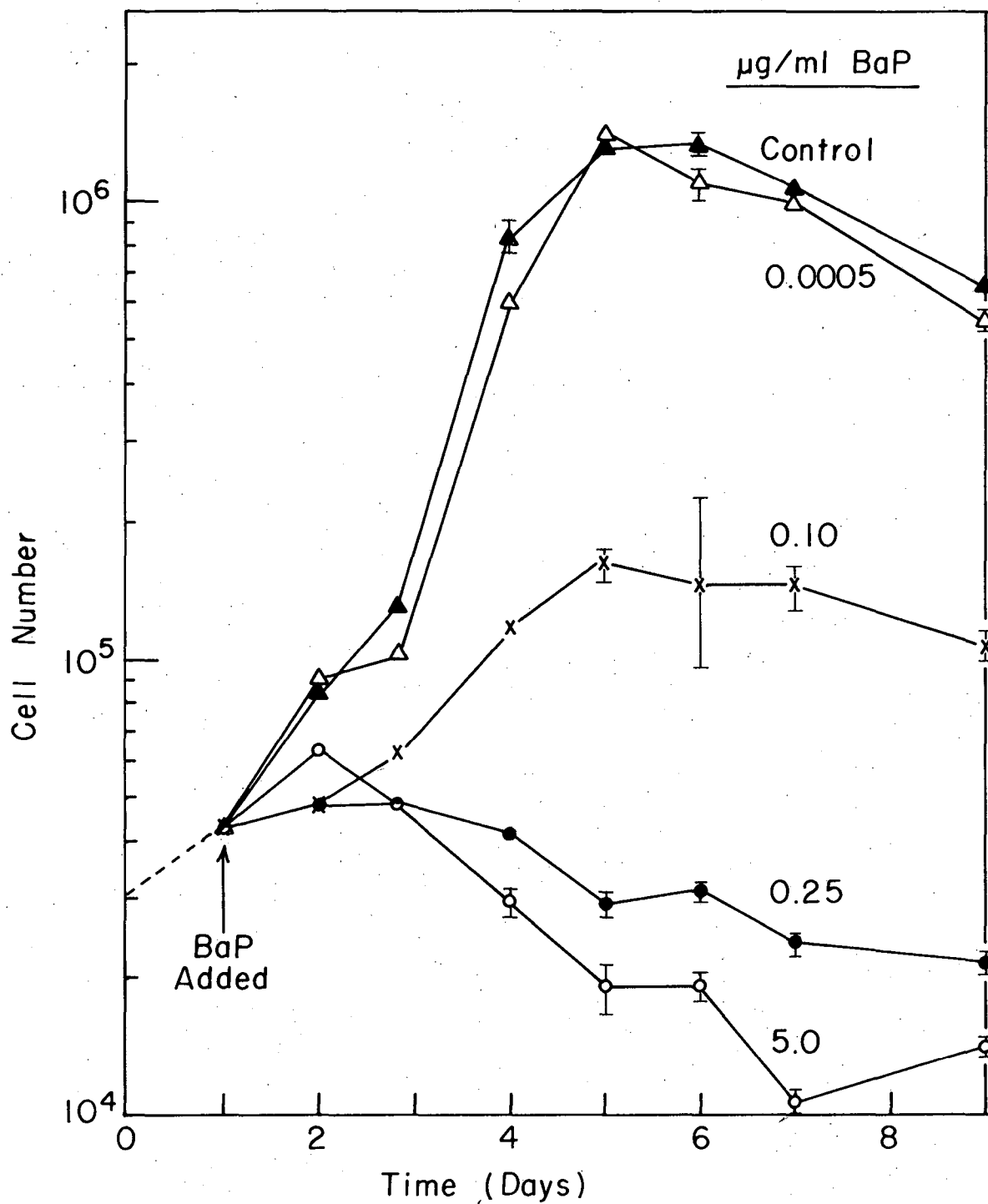
XBL757-5358

Chart 1
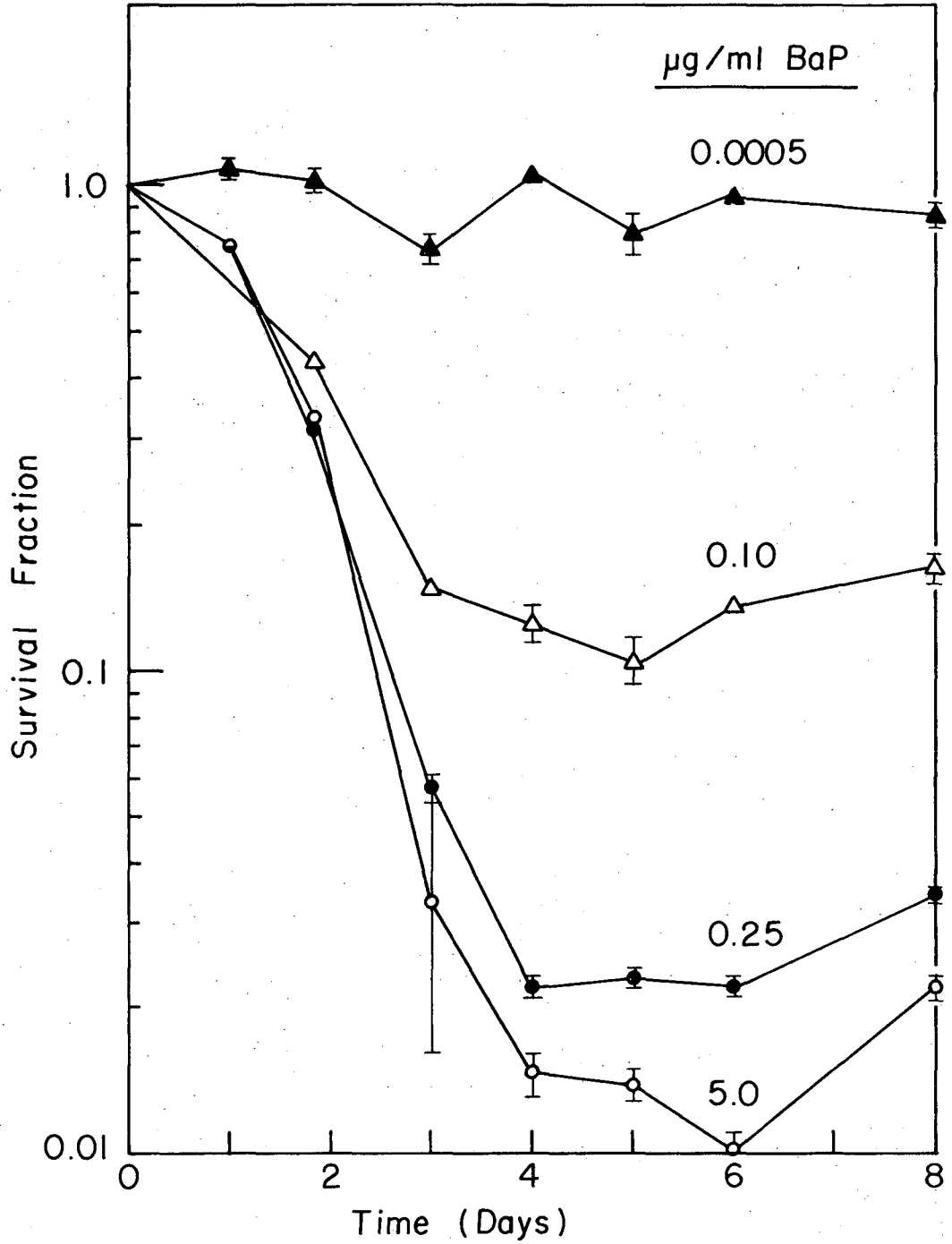
XBL757-5359

Chart 2

99 ± 1% of the cells are killed by 6 days of treatment. The plateau

values are a function of the concentration of BaP in the medium.

If the growth rate is the same for cells in the presence of BaP

and in the control medium, then the plot will show the effects of

carcinogen-induced death directly. However, if the carcinogen changes

the cycling parameters of the cells that it does not kill, i.e., if

$\alpha \neq \alpha'$, then this analysis will not distinguish between the two cases,

although the limit of greatly increased cell cycle times be opera-

tionally treated as cell death. However, visual inspection of the BaP-

treated plates did show massive release of the cells from the plates

into the medium, as well as necrosis of the cell layer, vacuolation of

the cells, and cellular debris, implying that true cell death is a

major contributor to these curves. At high concentrations of carcin-

ogen (20 ug/ml), colony size was smaller in a clone sensitive to BaP,

indicating that growth depressive effects also contribute to these

curves.

2. Concentration Dependence of the Toxicity

The effect of BaP concentration on exponentially growing NMuLi was

studied by the cell counting assay. The curves (Chart 3) appear

initially exponential, and then gradually approach a constant value.

This plateau appeared to be an exposure (concentration × time) limited

value, since the concentration dependence curves show lower plateau

values as the time of exposure increases. All survival curves extra-

polate to a survival fraction of 1.0.

Because the dead cells might stick to the plates and be released

by trypsin in the cell counting assay, leading to an underestimate of

-13-
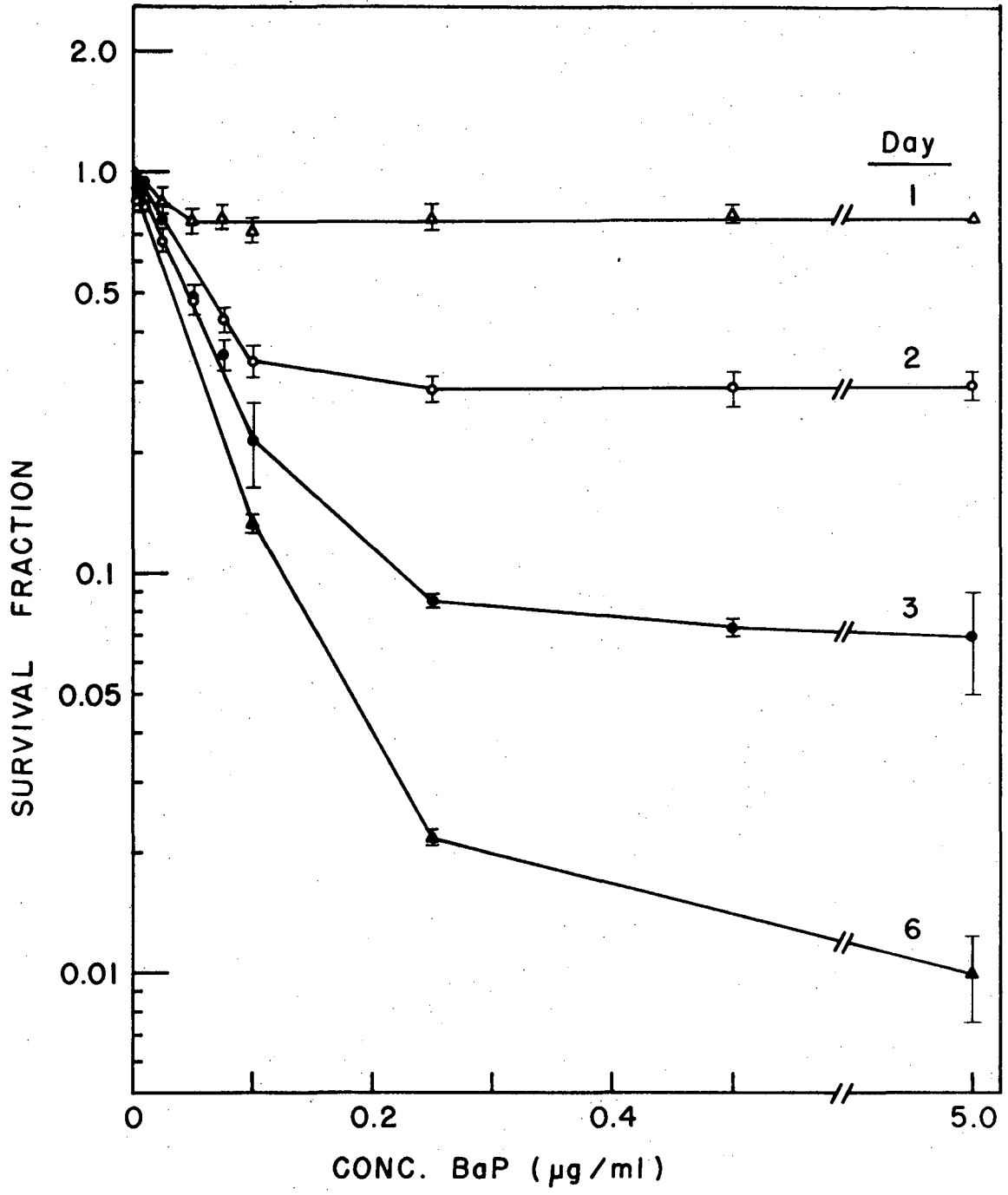
XBL 763-5797

Chart 3

the toxicity, the death clones of NMuLi was also investigated to confirm

the cell counting assay. Three day exposures were used in each assay,

since the cells would still be growing logarithmically. The results of

clonal killing experiments paralleled the cell counting assays in

qualitative shape (Chart 4), and the LD_{50} values for NMuLi were not

significantly different in the two assays, 0.06 ug/ml in each assay.

In addition, both assays yielded the same exposure-limited plateau

values (Table 1), and both extrapolated to a survival fraction of 1.0.

The three-day plateau values are constant over a number of passages

(Table 1).

The solubility of BaP in growth medium without cells was checked

by incubating various concentrations of BaP in medium for 2 hr at 37°,

taking the absorbance spectra of these solutions, filtering these

solutions through a 0.28 um Nalgene filter, and then rerunning the

absorbance spectra. These results showed that up to 1.5 ± 0.5 ug/ml

of BaP in the medium (2 experiments averaged) the absorbance values

were the same in filtered and unfiltered solutions, indicating that no

insoluble BaP had been filtered off. Above this value, the absorbance

of BaP in the filtered solutions decreased, indicating loss of

insoluble BaP. Since the killing curves presented here indicate that

99% of the cell death is complete by 0.5 ug/ml of BaP in the dose-

dependent experiments (Chart 3), the insolubility of BaP at high

concentrations is not contributing to the plateau in these curves.

3. Inhibition of the Toxicity by 7,8 Benzoflavone

The addition of 1.42 ug/ml benzoflavone (BF), (a competitive

inhibitor of AHF (2) to NMuLi increases the plateau value of surviving

a) Cell counting assay

b) Clonal assay

SURVIVAL FRACTION

(CELLS)

(CLONES)

CONC. BaP (μg / ml)
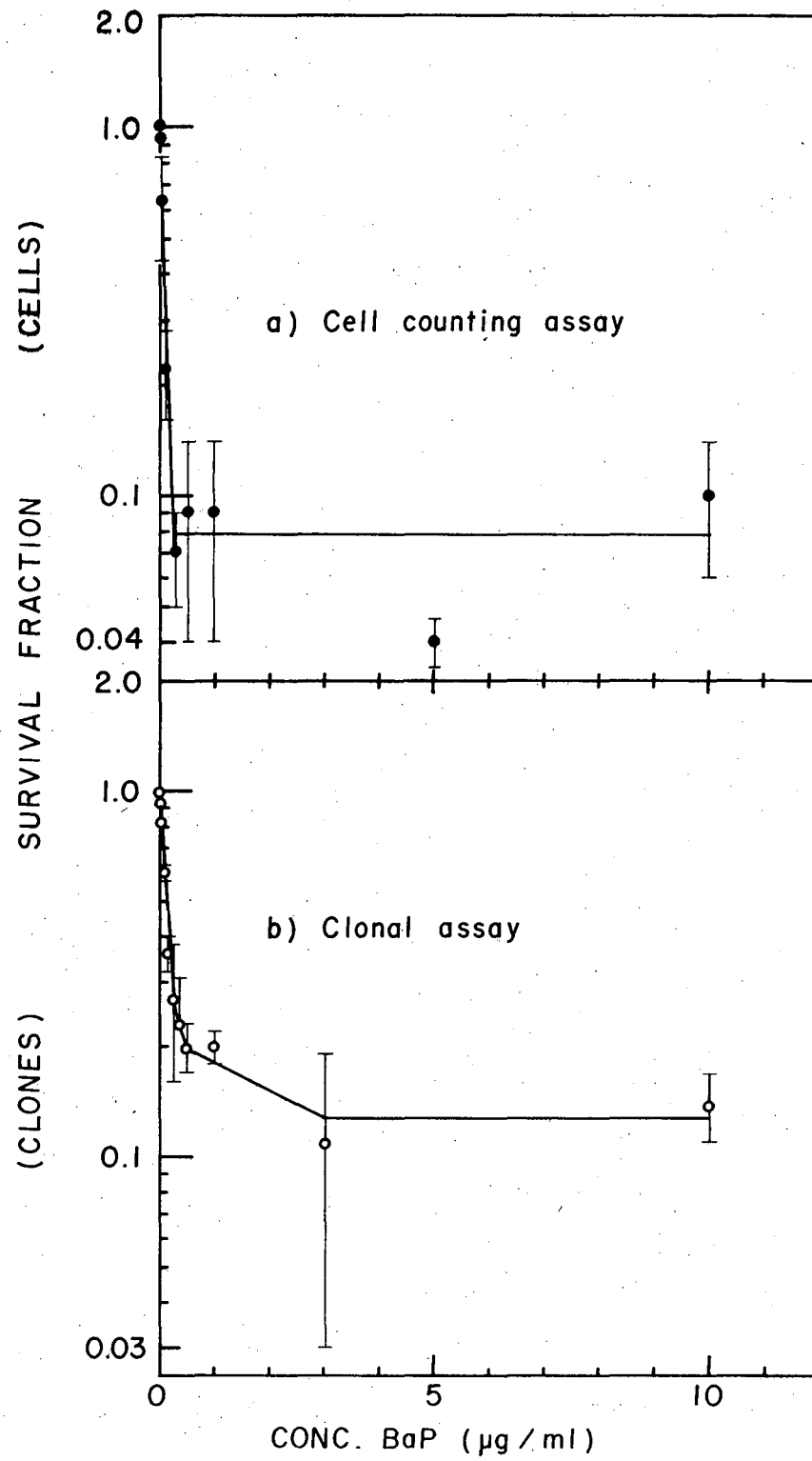
XBL 763-5757

Chart 4

Table I

a. Constancy of the fraction of cells resistant to the cytotoxic effects of BaP in the NMuLi population as a function of passage number: cell counting assay, BaP treatment for 3 days

% resistant cells	Passage number
NMuLi	
12	27
4	29
4	30
7	33
12	34
5	35
NET 7±4	

b. Clonal assay, BaP treatment for 3 days, passage 30 and 31:

% resistant cells	Passage number
5±2	30
14+5	31
NET 10±5	

cells from 10 to 40% in the three day assay (Chart 5). This concen-
tration of BF was chosen because it is the highest one effective
without exerting marked toxic effects on the cells (Chart 6).

The effects of BF in preventing the toxicity of BaP are dose-
dependent until the inhibitor itself becomes toxic (Chart 7). BF also
inhibits AHH in vitro from whole cells, cell homogenates, and microsomes
obtained from NMuLi in approximately the same dose-dependent manner
(Chart 7). Below 1 ug/ml of BF, it may require slightly more BF to
inhibit AHH in vitro than it does to prevent cell killing. The con-
centration of BF giving 50% inhibition in these experiments was
approximately 1.8 µM, while the BaP concentration was 4.0 µM, indicating
fairly specific inhibition.

4. The Necessity for Cell Division in the Toxicity

The effects of BaP on confluent populations of NMuLi was also
studied by the cell counting assay. The slope of the confluent killing
curve is 130 times less than that of the exponential death curves, and
the estimated LD_{50} would be 16.6 ug/ml vs. 0.06 ug/ml respectively
(Chart 8). Since the number of cell divisions is 50 times less in the
confluent than in the exponential assays, the decreased toxicity at
confluence is consistent with a requirement for cell division and/or
growth in the expression of toxicity.

It is conceivable that the AHH levels would be higher in expo-
nentially growing cells than in confluent cells, leading to a higher
toxicity in the former. Therefore, the inducibility of AHH in cells
was measured as a function of the growth curve, and it is seen that
maximal AHH levels in growing cells are only 2.4 ± 1.1 times those from

XBL761-5601

Chart 5

Chart 6

XBL761-5600

Chart 7

XBL762-5684

CONC. BaP (μg / ml)

SURVIVAL FRACTION
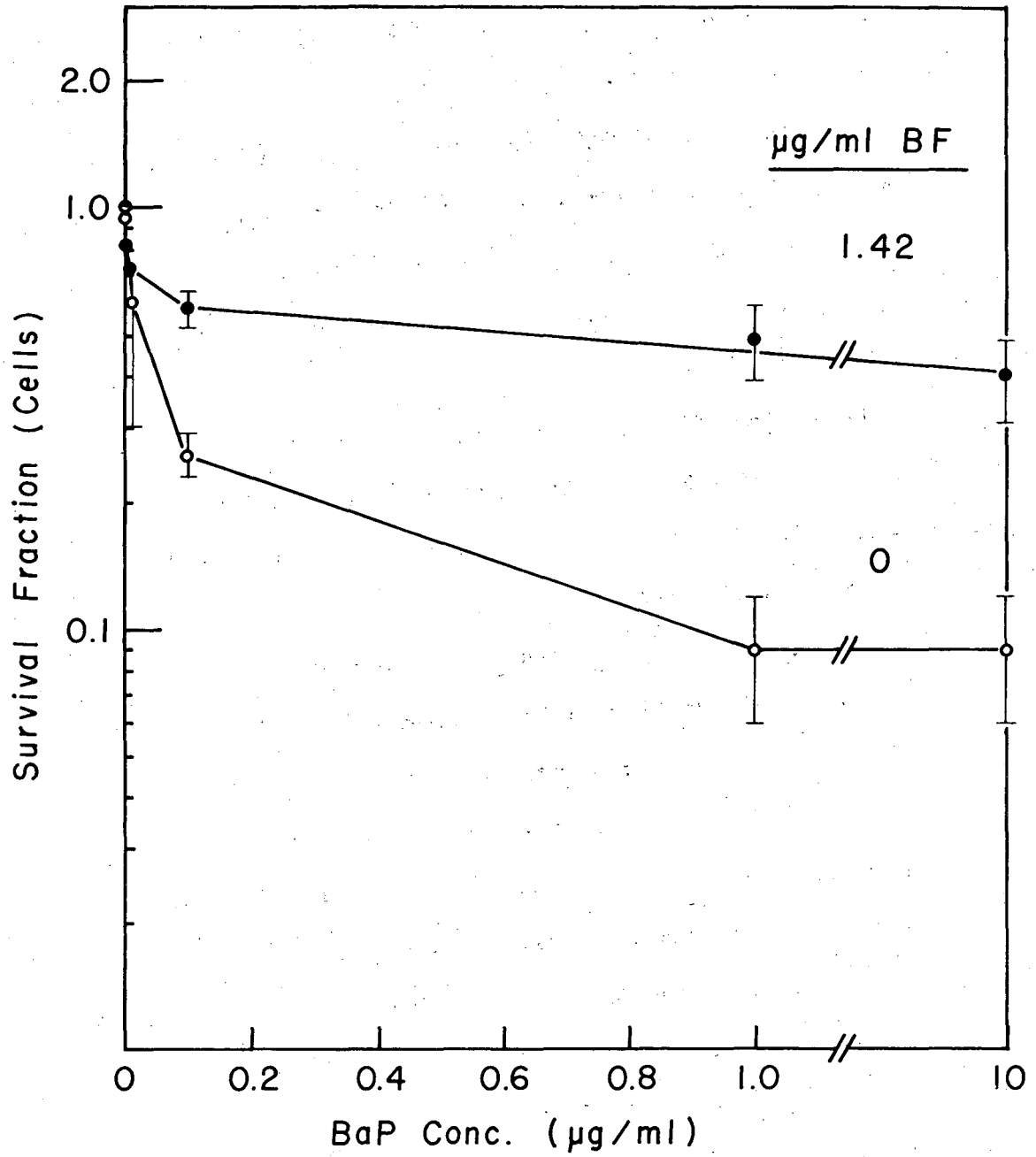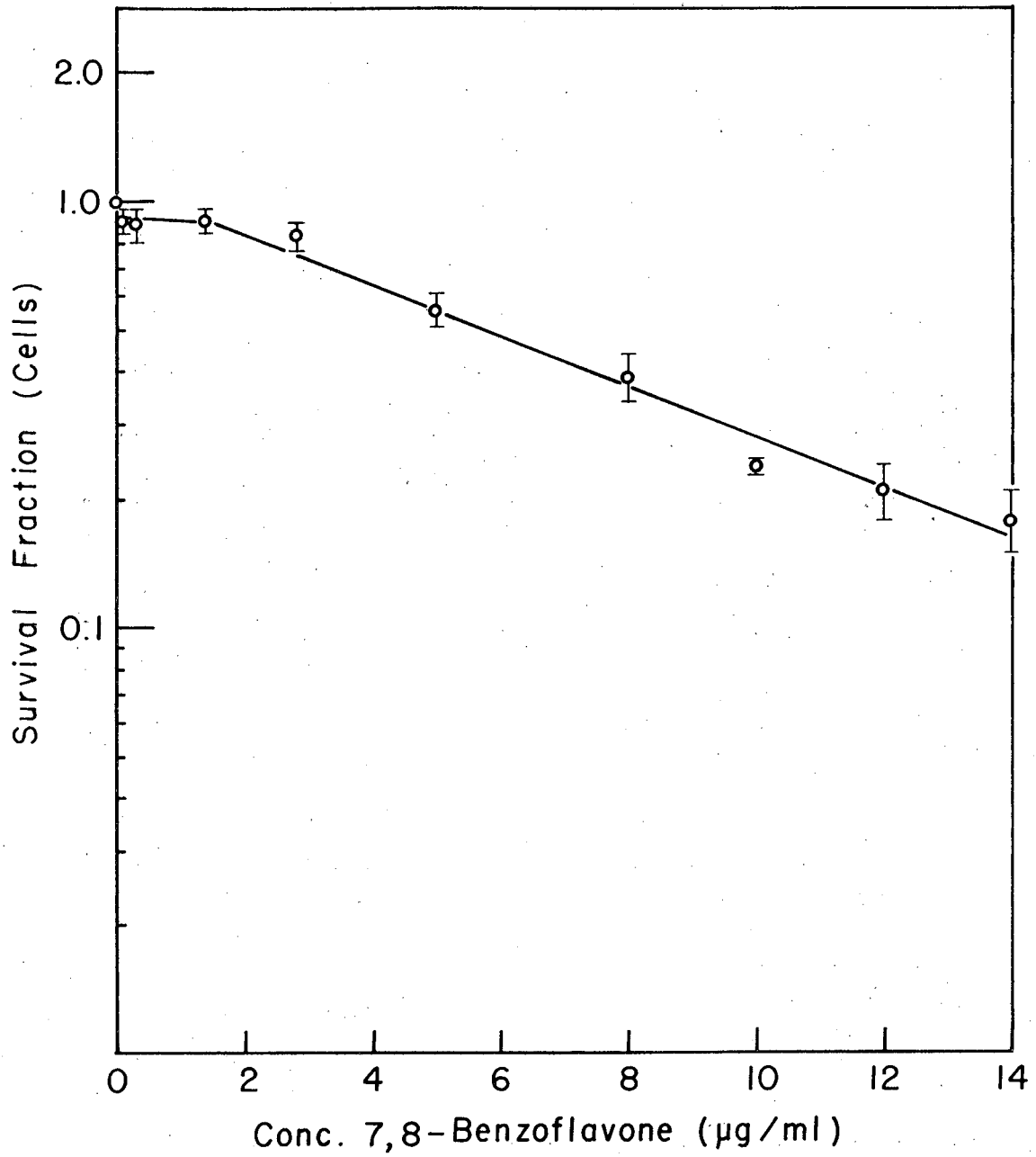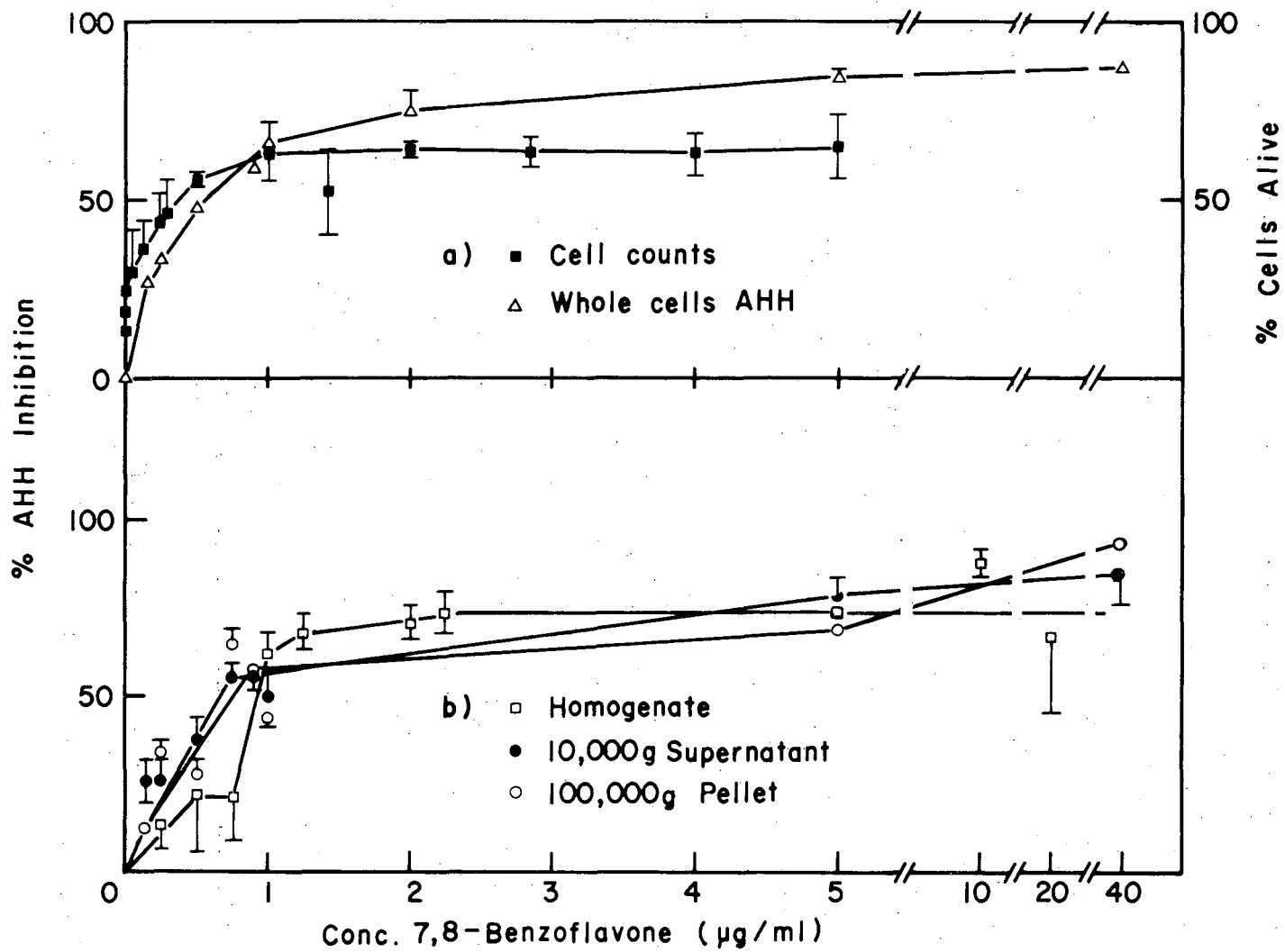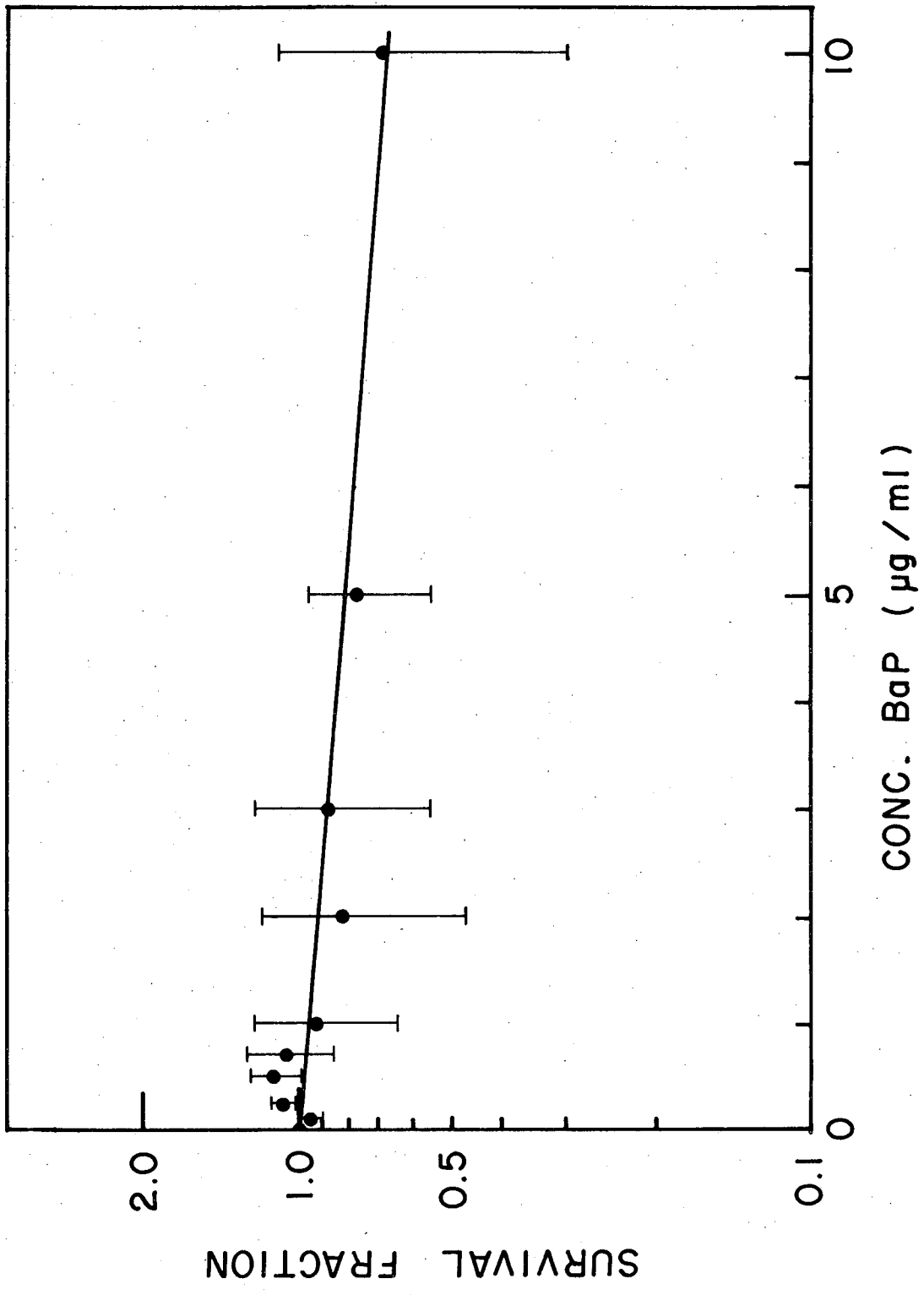
XBL 763-5796

Chart 8

confluent cells (Table 2). Integrating the total picomoles of toxic

3-hydroxy-BaP in growing and confluent cells under the conditions of

the toxicity assay by cutting and weighing appropriate portions of the

AHH vs. time curves yielded exactly the same ratio 2.4 ± 1.1. Protein

content/cell increased by a factor of three during the course of these

assays. Plotting picomoles of 3-hydroxy-BaP/cell-30 min and integrating

the curves showed that growing cells produced 1.7 ± 0.7 times as much

toxic metabolites as did confluent cells. This assay was conducted

a number of times because of the variability in the shape of the

induction curves and the absolute levels of the induced enzyme.

The cell division dependence of the toxicity was studied explicitly

by varying the seeding density of the cells while holding the time of

treatment and the concentration of BaP constant. This generated killing

curves in which the main variable was the number of population doublings.

As shown in Chart 9a, the killing curve appeared to decrease exponen-

tially with an increase in the number of population doublings, until

it reached the exposure-limited plateau value.

To determine the varying ratios of BaP to cells affected the killing

curves, an additional set of experiments were performed. The cell number

was held constant at 3×10^4 per 100 mm plate, and the killing curves

were conducted by varying the serum concentration. This procedure varies

the number of cell divisions by lowering the growth rate (Chart 10).

Again, the plot of survival fraction vs. the number of population

doublings appear roughly exponential, until it reaches an exposure-

limited plateau value (Chart 9b).

Finally, the question of enzyme induction vs. cell division or growth in

Table II

Maximal Inducible Levels of AHH Activity in Growing

and Confluent Cultures of NMuLi[*]

Highest Specific Activity of AHH, pmoles of 3-OH-BaP/mg cells
homogenate/30 min.

Experiment Number[†]	Growing Cells	Confluent Cells	Ratio, Growing/Confluent
1	188 ± 10	186 ± 23	1.01 ± 0.09
2	410 ± 31	159 ± 02	2.58 ± 0.13
3	161 ± 05	N.D.	--
4	341 ± 16	156 ± 01	2.18 ± 0.07
5	275 ± 25	N.D.	--
6	167 ± 06	45.5 ± 0.6	3.67 ± 0.01
		Average	2.4 ± 1.1

[*]For each point, cultures were induced with 1 ug/ml of BaP for 11 hours before the measurement. N.D. = not determined. The same ratios were obtained if BaP was left on the cultures for 3 days during log phase and for 3 days during confluence, and measurements made.

[†]The first two measurements were conducted on 100 mm plates. The other four experiments were conducted in roller bottles in order to obtain more protein.

a)

expt. 1
expt. 2
expt. 3

b)

NO. POPULATION DOUBLINGS (N/N₀)

XBL 763-5799

Chart 9

% Serum

10.0

5.0

1.0

0.5

0.2

0.1

0

CELL NUMBER

10^6

10^5

10^4

0

5

10

DAYS POST–SEEDING

XBL 763-5798

Chart 10
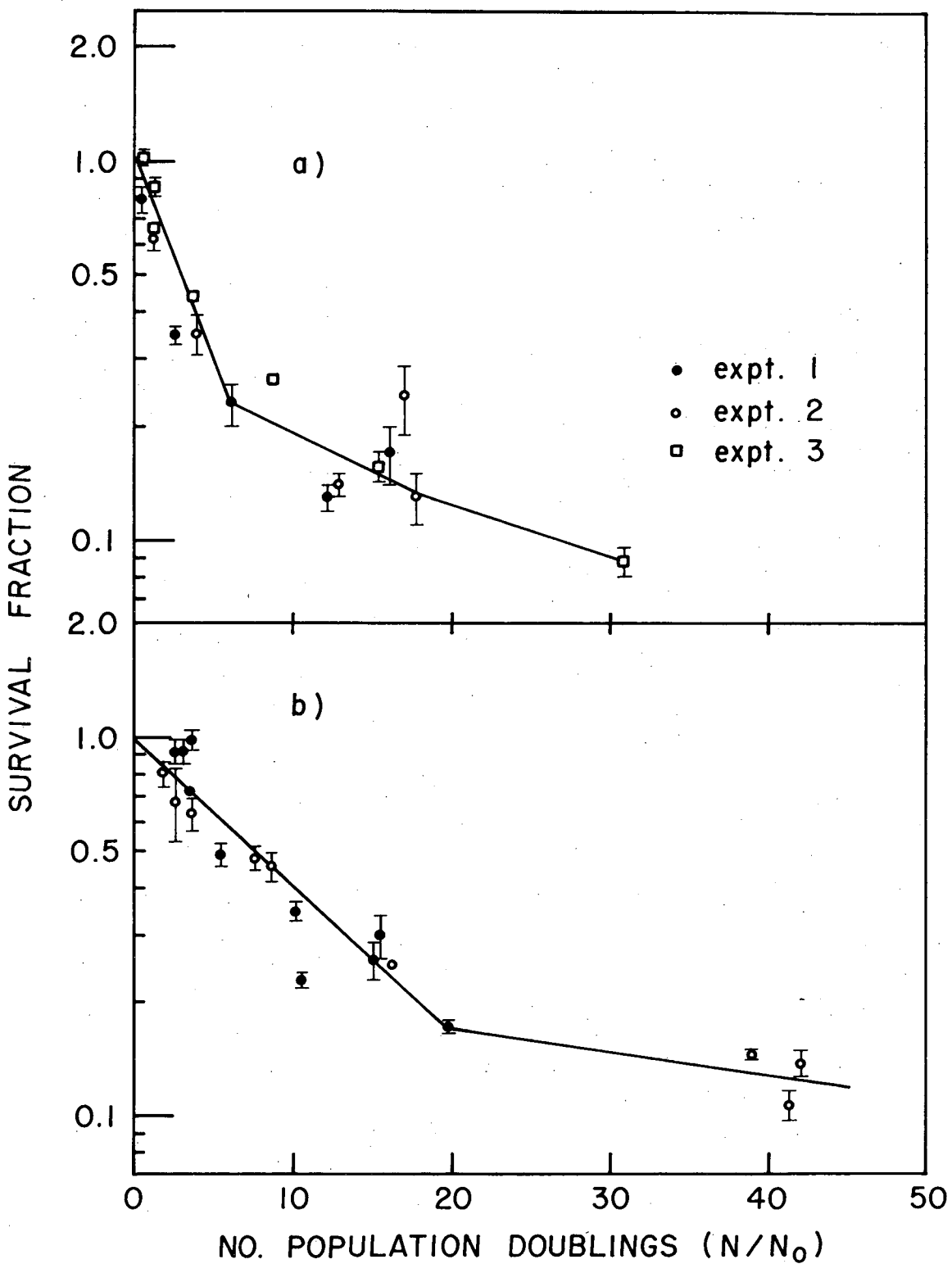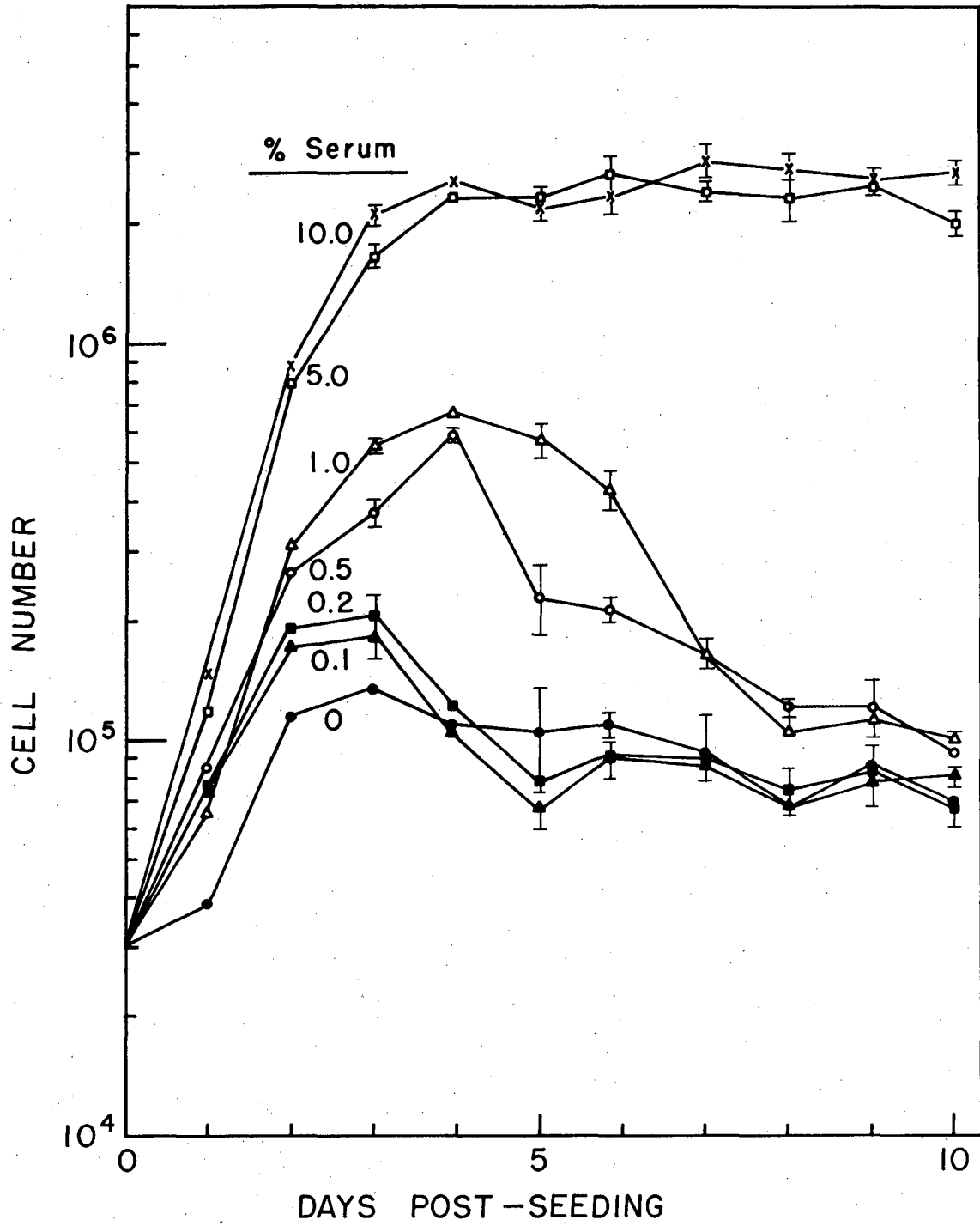
contributing to the relative slopes of the confluent vs. the exponential killing curves was assessed by use of a proximate toxic derivative of BaP, $\pm 7\alpha$, 8β- dihydroxy-9β, 10β-epoxy-7,8,9,10-tetrahydrobenzo(a)pyrene (diol-epoxide). The toxicity of this compound to an early passage sensitive clone derived from NMuLi is much greater to exponentially growing cells than to confluent cells (Chart 11). The ratio of the slope of the linear portion of the exponential killing curve to that of the confluent curve is 40, and the ratio of the number of divisions in the exponential cells to those of the confluent cells is 24, during the course of the assay.

In nine-day clonal killing assays, there were still variants resistant to BaP in this same early passage sensitive clone derived from NMuLi (Chart 12). However, use of the diol-epoxide in the clonal killing assay produced a survival curve that was exactly exponential with no resistant fraction (Chart 12).

E. Discussion

We have shown that a strain of mouse liver epithelial cells is extremely susceptible to the toxic effects of BaP, 99% of the cells being killed after a six-day exposure to 5 ug/ml of BaP. Increases in the toxicity of BaP to NMuLi was found after one day of BaP treatment, and these are most likely explained by higher levels of AHH due to induction followed by cell division. Results from this laboratory indicate that 4 hours are sufficient for the induction of AHH to be measurable (J. Landolph, J. Becker, and H. Gamper, manuscript in preparation).
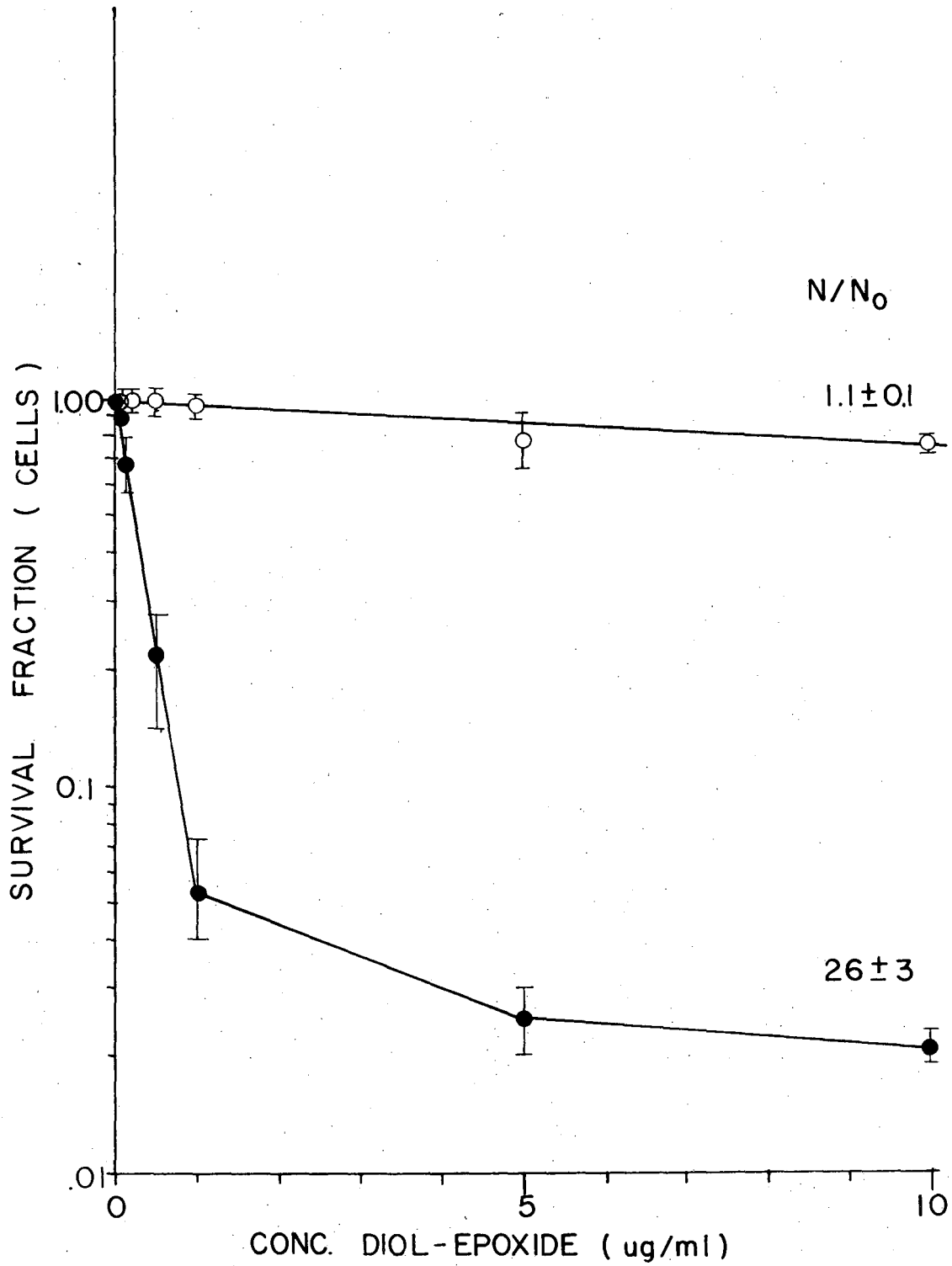
XBL 767-6042

Chart 11

XBL 767-6043 **A**

Chart 12
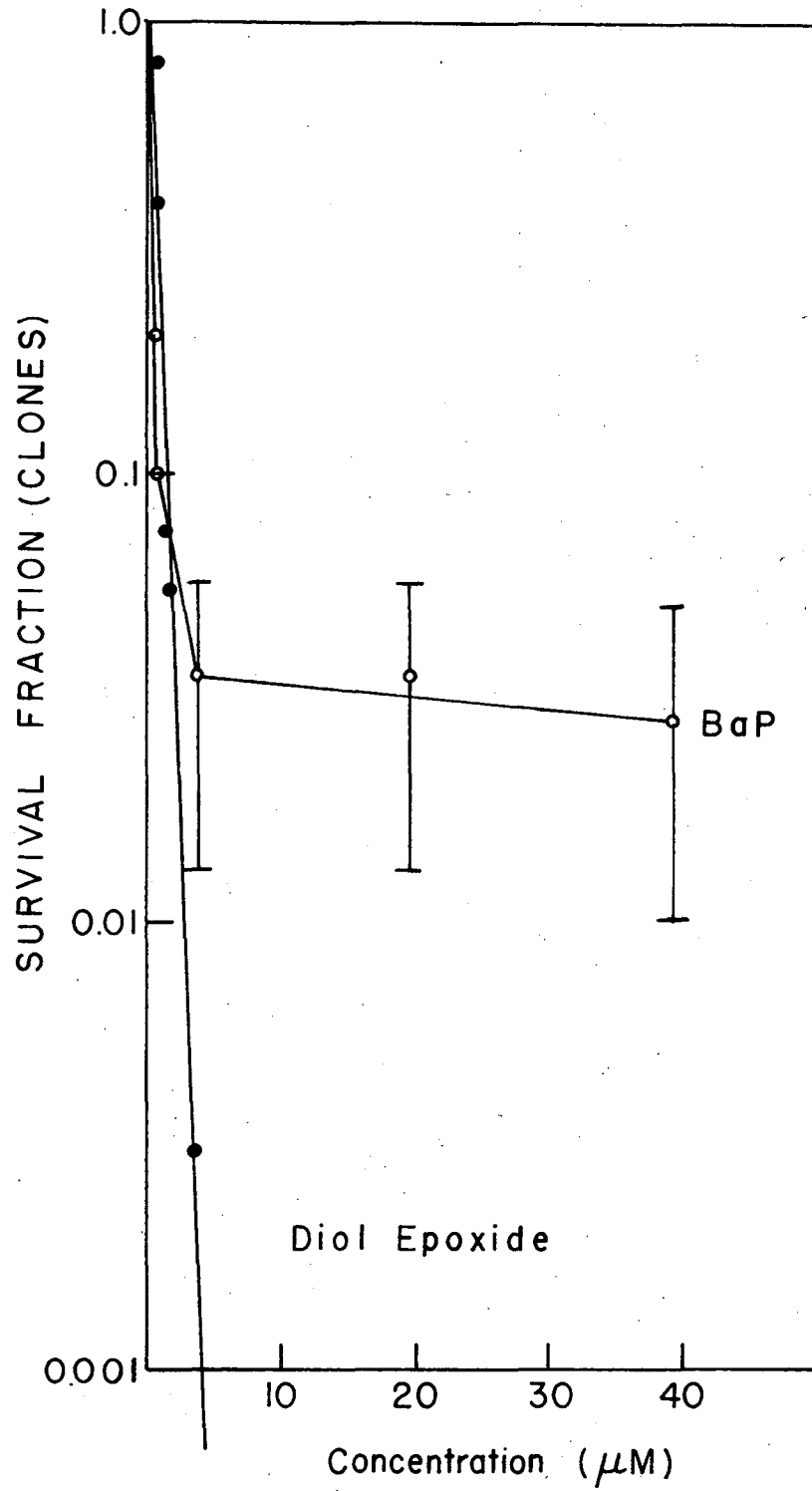
The concentration, time, and cell division dependence of the toxicity are all initially exponential, but then curve toward plateau values. These plateau values decrease as a function of time, but eventually a 1% level of resistant variants remains. Subtraction of the plateau values and replotting yields exponential plots for the time, concentration, and division dependence of the toxicity (data not shown). Unfortuantely, of 4 sensitive clones from NMuLi that were tested, all rapidly became 100% resistant in both the cell-killing and the clonal assays within 6 passages from isolation (data not shown). Hence, we have worked with the parent line. An expression for toxicity consistent with experimental data would be: $N_b/N = A \exp(-\beta ct) + B \exp(-\varepsilon ct)$, where N_b is the number of cells (clones) in the BF-treated dishes, N is the number in the control dishes, c is the concentration of BaP, t is the time of exposure to BaP, and β and ε are factors including the cell division dependence. The first and second terms in the expression are due to the death of sensitive and more resistant cells, respectively, and A and B are weighting factors for the fraction of sensitive and resistent variants in the population respectively. In nine-day clonal killing experiments with the acti-vated diol-epoxide of BaP, we were able to obtain exponential killing curves with no curvature and no resistant plateau values, suggesting that the curvature is due to resistant variants that have lost the ability to metabolize BaP to toxic derivatives. Huberman et al. have shown this diol-epoxide to be a metabolite of BaP in a rat liver microsomal incubation system and one of the most mutagenic derivatives of BaP yet isolated, and have suggested it as the possible ultimate

carcinogenic form of BaP (26).

The concentration dependence plots extrapolate to a survival fraction of 1.0 in both the clonal and the cell-killing assays. This most likely is because BaP can induce the necessary AHH, and can then be metabolized by the enzyme to cytotoxic derivatives. Hence, all BaP is involved in cell killing, and this would be expected to lead to one-hit kinetics. Our description of the concentration dependence of the toxicity of BaP to epithelial cells is qualitatively similar to the study of Gelboin et al. in a series of normal and transformed hamster and mouse cells. These investigators showed that treatment of the cells with BaP for 8 days resulted in one-hit kinetic curves with a certain fraction of resistant cells (16), and that 3-hydroxy-BaP, formed in the cells from BaP by AHH, kills even these resistant cells.

If one compares the figure for the induction of AHH in NMuLi from (1) with the dose dependence killing experiments in Chart 3, it is seen that they follow the same BaP dose-dependence. This implies that the induction of AHH to make cytotoxic metabolites from BaP kills the cells, as suggested by Gelboin et al. (16). Further support for the involvement of induced AHH in the toxicity process comes from the fact that BF increased the number of resistant cells in NMuLi exposed to BaP by a factor of 5, and this compound also inhibited induced AHH in these cells in vitro by 90%. These results for our epithelial cells are in qualitative agreement with those of Diamond and Gelboin, who showed that 1 ug/ml of BF reduced AHH levels in hamster embryo cells, decreased the metabolism of BaP in these cells by 90% and markedly inhibited the growth rate depressing effect of

7,12 dimethylbenz(a)anthracene in the cells (10).

In working with L5178Y lymphoblasts, Goldenberg et al. showed that log phase cells were 2.6 times as sensitive to nitrogen mustard-induced toxicity as were stationary phase cells and showed that this difference could be accounted for by a more efficient transport mechanism in log phase cells (18, 19). This is qualitatively similar to our case, except that in NMuLi the log phase cells are 130 times more susceptible to the toxicity of BaP, if we use the criterion of D_o (the concentration giving 37% survival) that Goldenberg used. Part of the enhanced sensitivity of the growing cells to the toxicity is undoubtedly due to the 2.4 fold higher levels of AHH in log phase cells, but this alone cannot account for the 130 fold difference. A proximate toxic BaP metabolite $\pm$ 7α8β-dihydroxy-9β, 10β-epoxy-7,8,9,10-tetra-hydrobenzo(a)pyrene dissociated the relative importance of metabolism of BaP from cellular division and growth in the toxicity, since this metabolite was forty times more toxic to growing than to confluent NMuLi. Therefore, cellular division is probably mostly responsible for the differential toxicity in growing vs. resting cells.

It was significant that the toxic effects of BaP also required cell division for expression, as does malignant transformation. This draws a parallel between the toxic and transforming process. In vivo, there are a number of situations that could lead to the requisite number of cell divisions for the expression of the transformed phenotype. This could occur in the rapidly growing tissues of young animals, adult tissues, such as the crypts of the intestine, where cellular renewal rates are high, or in regenerating tissues, such as those

responding to the toxic effects of a chemical. Hence, by invoking

cellular division, the toxic effects of a chemical could complement its

transforming ability.

In conclusion, the liver epithelial cells used in this study respond

to the toxicity of BaP in qualitatively the same way that fibroblasts

and mixed systems do: the toxicity is prevented by an inhibitor of AHH,

is correlated with the induction of AHH, and is expressed during cell

division. The marked cytotoxicity of carcinogens to epithelial cells

could be due to the high levels of AHH in epithelial cells. Such

considerations make the study of the toxicity of carcinogens to

epithelial cells particularly relevant.

-33-

F. References

1. Bartholomew, J. C., Salmon, A. G., Gamper, H. B., and Calvin, M.
    Benzo(a)pyrene Effects on Mouse Epithelial Cells in Culture.
    Cancer Res., 35: 851-856, 1975.

2. Benedict, W. F., Gielen, J. E., and Nebert, D. W. Polycyclic
    Hydrocarbon-Produced Toxicity, Transformation, and Chromosomal
    Aberrations as a Function of Aryl Hydrocarbon Hydroxylase Activity
    in Cell Cultures. Int. J. Cancer, 9: 435-451, 1972.

3. Brown, A. M. In Vitro Transformation of Submandibular Gland
    Epithelial Cells and Fibroblasts of Adult Rats by 3-Methylcholan-
    threne. Cancer Res., 33: 2779-2789, 1973.

4. Cairns, J. Mutation Selection and the Natural History of Cancer.
    Nature, 255: 197-200, 1975.

5. Chen, T. T., and Heidelberger, C. Quantitative Studies on the
    Malignant Transformation of Mouse Prostate Cells by Carcinogenic
    Hydrocarbons In Vitro. Int. J. Cancer, 4: 166-178, 1969.

6. Culp, L. A., and Black, P. H. Release of Macromolecules from
    Balb/c Mouse Cell Lines Treated with Chelating Agents. Biochemistry,
    11: 2161-2172, 1972.

7. Diamond, L. The Effect of Carcinogenic Hydrocarbons on Rodent and
    Primate Cells In Vitro. J. Cell. Comp. Physiol., 66: 183-198, 1965.

8. Diamond, L. Metabolism of Polycyclic Hydrocarbons in Mammalian
    Cell Cultures. Int. J. Cancer, 8: 451-462, 1971.

9. Diamond, L., Defendi, V., and Brookes, P. The Interaction of
    7,12-Dimethylbenz(a)anthracene with Cells Sensitive and Resistant
    to Toxicity Induced by this Carcinogen. Cancer Res, 27: 890-896,1967.

10. Diamond, L., and Gelboin, H. V. Alpha-Naphthoflavone: An Inhibitor of Hydrocarbon Cytotoxicity and Microsomal Hydroxylase. Science, 166: 1023-1025, 1969.

11. DiPaolo, J. A., Donovan, P. J., and Nelson, R. L. Transformation of Hamster Cells In Vitro by Polycyclic Hydrocarbons Without Cytotoxicity. Proc. Natl. Acad. Sci. USA, 68: 2958-2961, 1971.

12. DiPaolo, J. A., Donovan, P. J., and Nelson, R. L. In Vitro Transformation of Hamster Cells by Polycyclic Hydrocarbons: Factors Influencing the Number of Cells Transformed. Nature New Biology, 230, 240-242, 1971.

13. Eagle, H. Amino Acid Metabolism in Mammalian Cell Cultures. Science, 130: 432, 1969.

14. Evans, V. J., Price, F. M., Kerr, H. A., and de Oca, H. M. Effect of 7,12-Dimethylbenz(a)anthracene on Non-Neoplastic Rodent Cells in Culture. J. Nat. Cancer Inst., 45: 429-441, 1970.

15. Fox, C. H., Selkirk, Price, F. M., Croy, R. G., Sanfork, K. K., and Cottler-Fox, M. Metabolism of Benzo(a)pyrene by Human Epithelial Cells In Vitro. Cancer Res., 35: 0117-0123, 1975.

16. Gelboin, H. V., Huberman, E., and Sachs, L. Enzymatic Hydroxylation of Benzopyrene and Its Relationship to Cytotoxicity. Proc. Natl. Acad. Sci. USA, 64: 1188-1194, 1969.

17. Gelboin, H. V., and Wiebel, F. J. Studies on the Mechanisms of Aryl Hydrocarbon Hydroxylase Induction and Its Role in Cytotoxicity and Tumorigenicity. Ann. N. Y. Acad. Sci., 179: 529-547, 1971.

18. Goldenberg, G. J. Properties of L5178Y Lymphoblasts Highly
    Resistant to Nitrogen Mustard. Symposium on Biological Effects
    of Alkylating Agents. Ann. N. Y. Acad. Sci., 163: 936-953, 1969.

19. Goldenberg, G. J., Lyons, R. M., Lepp, J. A., and Vanston, C. L.
    Sensitivity to Nitrogen Mustard as a Function of Transport Activity
    and Prolfierative Rate in L5178Y Lymphoblasts. Cancer Res., 31:
    1616-1619, 1971.

20. Grover, P. L., Sims, P., Huberman, E., Marquardt, H., Kuroki, T.,
    and Heidelberger, C. In Vitro Transformation of Rodent Cells by
    K-Region Derivatives of Polycyclic Hydrocarbons. Proc. Natl. Acad.
    Sci. USA, 68: 1098, 1101, 1971.

21. Heidelberger, C. Chemical Carcinogenesis. Ann. Reviews. Biochem.
    44: 79-121, 1975.

22. Huberman, E., and Sachs, L. Metabolism of the Carcinogenic Hydro-
    carbon Benzo(a)pyrene in Human Fibroblast and Epithelial Cells.
    Int. J. Cancer, 11: 412-418, 1973.

23. Huberman, E., and Sachs, L. Susceptibility of Cells Transformed by
    Polyoma Virus and Simian Virus 40 to the Cytotoxic Effect of the
    Carcinogenic Hydrocarbon Benzo(a)pyrene. J. Natl. Cancer Inst.,
    40: 329-336, 1968.

24. Huberman, E., Yamasaki, H., and Sachs, L. Genetic Control of the
    Regulation of Cell Susceptibility to Carcinogenic Polycyclic Hydro-
    carbons by Cyclic AMP. Int. J. Cancer, 14: 789-798, 1974.

25. Huberman, E., and Sachs, L. Cell Susceptibility to Transformation
    and Cyctotxicity by the Carcinogenic Hydrocarbon Benzo(a)pyrene.
    Proc. Natl. Acad. Sci. USA, 60: 300-304, 1968.

26. Huberman, E., Sachs, L., Yang, S. K., and Gelboin, J. V. Identification of Mutagenic Metabolites of Benzo(a)pyrene in Mammalian Cells. Proc. of Natl. Acad. Sc. USA, 73: 607-611, 1961.

27. Kakanaga, T. The Role of Cell Division in the Malignant Transformation of Mouse Cells Treated with 3-Methylcholanthrene. Cancer Res., 35: 1637-1643, 1975.

28. Kakanaga, T. Requirement for Cell Division in the Fixation and Expression of the Transformed State in Mouse Cells Treated with 4-Nitroquinoline-1-Oxide. Int. J. Cancer, 14: 736-742, 1974.

29. Kinoshita, N., and Gelboin, H. V. Aryl Hydrocarbon Hydroxylase and Polycyclic Hydrocarbon Tumorigenesis: Effect of the Enzyme Inhibitor 7,8 Benzoflavone. Proc. Natl. Acad. Sci. USA, 69: 824-828, 1972.

30. Lowry, O. H., Rosebrough, N. J., Farr, A. L., and Randall, P. J. Protein Measurement with the Folin Phenol Reagent. J. Biol. Chem., 193, 265-275, 1951.

31. MacPherson, I. Agar Suspension Culture for Quantitation of Transformed Cells. In Fundamental Techniques in Virology. Eds. K. Habel and N. P. Salzman. 1969 Acad. Press, N. Y., pp. 214-219,1969.

32. Marquardt, H. Cell Cycle Dependence of Chemically Induced Malignant Transformation In Vitro. Cancer Res., 34: 1612-1615, 1974.

33. Marquardt, H., Sapozink, M. D., and Zedeck, M. S. Inhibition by Cystiamine of Oncogenesis Induced by 7,12-Dimethylbenz(a)anthracene Without Affecting Toxicity. Cancer Res., 34: 3387-3390, 1974.

34. Owens, I., and Nebert, D. W. Aryl Hydrocarbon Hydroxylase Induction
in Mammalian Liver-Derived Cell Cultures. Mol. Pharmacol., 11:
94-101, 1974.

35. Owens, R. B., Smith, H. S., and Hacket, A. J. Epithelial Cells
from Normal Glandular Tissue of Mice. J. Natl. Cancer Inst.,
53: 261-269, 1974.

36. Owens, R. B. Glandular Epithelial Cells from Mice: A Method for
Selective Cultivation. J. Natl. Cancer Inst., 52: 1375-1378,1974.

37. Peterson, A. R., Bertram, J. S., and Heidelberger, C. Cell Cycle
Dependency of DNA Damage and Repair in Transformable Mouse Fibro-
blasts Treated with N-Methyl-N'-Nitro-N-Nitrosoguanidine. Cancer
Res., 34: 1600-1606, 1974.

38. Puck, T. T., Marcus, P. I., and Cieciura, S. J. Clonal Growth of
Mammalian Cells In Vitro. Growth Characteristics of Colonies from
Single HeLa Cells With and Without "Feeder" Layer. J. Exp. Med.,
103: 273-283, 1956.

39. Renznikoff, C. A., Bertram, J. S., Brankow, D. W., and Heidelberger,
C. Quantitative and Qualitative Studies of Chemical Transformation
of Cloned C3H Mouse Embryo Cells Sensitive to Postconfluence of
Cell Division. Cancer Res., 33: 3239-3249, 1973.

40. Schwartz, A. G. The Protective Effect of Estradiol-17b Against
Polycyclic Hydrocarbon Cytotoxicity. Cancer Res., 2431-2436, 1973.

41. Silber, D., Checinsha, E., Rabczynska, J., and Kochman, M.
Isozyme Pattern of Fructose Diphosphate Aldolase During Hepa-
tocarcinogenesis Induced by 2-Acetylaminofluorene in Rat Liver.
Int. J. Cancer, 16, 675-681, 1975.

42. Starikova, V. B., and Vasiliev, J. M. Action of 7,12-Dimethyl-benz(alpha)anthracene on the Mitotic Activity of Normal and Malignant Rat Fibroblasts In Vitro. Nature (London), 195: 42-43, 1962.

43. Warren, P. M., and Stich, H. F. Reduced DNA Repair Capacity and Increased Cytotoxicity Following Split Doses of the Mutagen 4-Nitroquinoline-1-oxide. Mutation Research, 28: 284-293, 1975.

44. Watanabe, M., and Horikawa, M. Analyses of Differential Sensitivities of Hela S_3 Cells to Radiations and Chemical Carcinogens During the Cell Cycle. Mutat. Res., 28: 295-304, 1975.

45. Whitlock, J. P., and Gelboin, H. V. Induction of Aryl Hydrocarbon (Benzo(a)pyrene) Hydroxylase in Liver Cell Culture by Temporary Inhibition of Protein Synthesis. J. Biol. Chem., 248: 6114-6121, 1973.

46. Whitlock, J. P., and Gelboin, H. V. Aryl Hydrocarbon (Benzo[a]-pyrene) Hydroxylase Induction in Rat Liver Cells in Culture. J. Biol. Chem., 8: 2616-2623, 1974.

47. Yamaguchi, N., and Weinstein, I. B. Temperature-Sensitive Mutuants of Chemically Transformed Epithelial Cells. Proc. Natl. Acad. Sci. USA, 72: 214-218, 1975.

Chart Legends — Chapter I

Chart 1. Growth curves of NMuLi, passage 30, in the presence of BaP. Cells were seeded at 3×10^4 and allowed to grow for one day before treatment with BaP in acetone.

Chart 2. Normalized growth curves of NMuLi in the presence of BaP. Curves from Chart 1 were all divided by the acetone controls and replotted as survival curves. Note that day 0 on this figure is that day on which BaP was added to the medium, i.e., it corresponds to day 1 on Chart 1, and the cells are growing exponentially at this time.

Chart 3. The kinetics of toxicity to BaP to exponentially growing NMuLi as measured in the cell counting assay at passage 30. Cells were seeded at 3×10^4/plate, allowed to recover for one day, and then treated with BaP in acetone for the indicated time.

Chart 4. Comparison of the concentration dependence of the toxicity of BaP to NMuLi a) in the cell counting assay (average of 6 experiments) (passages 26-40) and b) in the clonal death assay (average of 2 experiments). Cells and clones were exposed to BaP for three days.

Chart 5. Inhibition of BaP cytotoxicity by 7,8-benzoflavone. The kinetics of toxicity of BaP to NMuLi was measured in the absence of (●----●) and in the presence of (o----o) of 5.2×10^{-6} M (1.4 ug/ml) 7,8 benzoflavone by the cell counting assay after three days of exposure to BaP.

Chart 6. The toxicity of 7,8-benzoflavone to NMuLi was measured in the

cell counting kinetics assay. Each point represents the aver-

age of two experiments. For each experiment, four plates were

averaged per point. Cells were exposed to BaP for 3 days.

Chart 7. a) Dose dependence of the inhibition of BaP-induced cellular

toxicity by 7,8-benzoflavone. Cells were treated with

1.0 ug/ml of BaP for 3 days along with varying concentra-

tions of 7,8-benzoflavone and then counted (□----□).

Each point represents the average of four separate

experiments. The inhibition of AHH from whole cells was

determined in one experiment, with duplicate determina-

tions at each point (▲----▲).

b) The concentration profile of the inhibition of AHH from

crude cell homogenates (□----□, 1 experiment), the

10,000 g supernatant (o----o, 2 experiments), and the

microsomal pellet (100,000 g pellet, 1 experiment, o----o).

In each experiment, each point is the average of duplicate

determinations. The protein contents were: 2.0 mg for

the whole cells, 1.6 and 1.5 mg for the 10,000 g super-

natant, 1.5 mg for the microsomal pellet, and 2.5 mg for

the cell sonicate experiment, in each assay flask. AHH

activity was 257, 142 and 130, 244, and 194 picomoles

30 H-BaP/30 min.

Chart 8. The concentration dependence of the toxicity of BaP to con-fluent NMuLi. Cells were seeded at 1.5×10^5 per 35 mm plate, and allowed to recover and divide for one day. BaP in acetone was then added (10 ul), and the cells were counted 3 days later. Each point represents the average of six separate experiments, with 4 plates being counted for each point in each experiment.

Chart 9. The division dependence of the toxicity. Cells were treated with 1 ug/ml of BaP for 3 days, and then counted. a) The seeding density was varied from 1×10^4 to 1.5×10^6 cells per plate, and the survival fraction counted on day three. b) In this experiment, the percentage of serum added to the medium was varied from 0.05% to 10% in order to vary the num-ber of cell divisions. The seeding density was 3×10^4 cells per plate. For the repeat experiments, (o----o), BaP was added upon plating the cells rather than allowing them to recover one day.

Chart 10. Growth cruves of NMuLi in varying amounts of serum. Cells were seeded at 3×10^4 in different levels of serum, and growth curves were determined each day.

Chart 11. The toxicity of the activated diol-epoxide of BaP to an

early passage sensitive clone derived from NMuLi was tested

in the three-day cell-killing assay. Each point is an

average of the results from four plates. N/N_o represents

the ratio of the number of cells per 35 mm plate present at

the end of the assay in the control (solvent only)-treated

plates to that present at the beginning of the assay. Cells

were seeded at 3.0×10^4 (●-----●) and at 1.5×10^6 (o-----o)

35 mm dish.

Chart 12. An early passage sensitive clone derived from NMuLi was

exposed to BaP (o-----o) and to the activated diol-epoxide of

BaP (●-----●) for 9 days in the clonal killing assay. Each

point is the average of 2 experiments, four plates being

averaged for each point per experiment. The last point on

the BaP killing curve, 40 um, is 10 ug/ml of BaP, for com-

parison with the other experiments.

II. BIOLOGICAL CHARACTERIZATION OF RESISTANCE TO BaP IN

TUMORIGENIC CLONES DERIVED FROM NMuLi

A. Summary

Tumorigenic clones isolated from the epithelial lever cell line NMuLi at passage 40 became rapidly resistant to the toxicity of the carcinogen benzo(a)pyrene (BaP) as a function of passage. This was shown in both subcloning experiments and by monitoring the clones for their resistant fraction as a function of passage. Even immediately upon cloning, two sensitive clones showed high levels of resistant variants (10^{-2}), as demonstrated by measuring the concentration dependence of the toxicity in clonal survival analyses. The addition of 10 ug/ml of insulin to resistant populations generated from sensitive clones did not restore these populations to sensitivity.

Among four clones studied, resistance to BaP did not correlate with chromosome loss, cloning efficiency, saturation density, or population doubling times. Two of these clones went to almost total resistance as a function of passage. In these cases, the late passage, resistant populations derived from the clones had higher saturation densities, cloning efficiencies, and growth rates than the initially sensitive parent clones. Hence, it appeared that production of resistant variants and their outgrowing the cloned parent populations led to the resistant populations in these clones.

Both sensitive and resistant clones produced tumors, so no correlation was evident between the tumorigenic and resistant states. Additionally, tumor explants derived from tumors produced by the injection of resistant clones were initially sensitive, but then became

resistant as a function of passage. The ability of the tumor explants
to grow in soft agar appeared to correlate with the levels of reverse
transcriptase that the explants possessed.

B. Introduction

In studying the toxicity of benzo(a)pyrene to a mouse lever
epithelial cell line (NMuLi), we noticed a rapid appearance of high
levels of resistant subpopulations in sensitive clones derived from
this line (Chart 3, Chapter 1). These resistant cells made the inter-
pretation of survival curves of these clones difficult, and mandated a
study of the origin of resistant variants.

Studies characterizing the phenotype of cells resistant to the
cytotoxicity of BaP are important for four reasons. Firstly, many
investigators have shown that treatment of mammalian cells in vitro
with activated forms of chemical carcinogens elicits the production of
variants resistant 8-azaguanine (16-19, 32, 33). This suggests that the
production of variant resistant 8-azaguanine and the production of
malignantly transformed cells could be analogous processes. We would
like to develop resistance to BaP as a new marker, since transformation
and cytotoxicity resistance are two processes occurring in the presence
of the same chemical carcinogen without applying another selective
process. It would be extremely useful if analogies could be demon-
strated between resistance and transformation, since resistance is
relatively easy to study.

Secondly, the mechanism by which variants resistant to BaP arise
in epithelial cells is also important, since these cells are in areas
such as skin, lung, and liver which receive initial or high exposure to

toxic chemicals:

A study of resistance to BaP might establish a marker that is analogous to resistance to purine and pyrimidine derivatives. Investigations of bromodeoxyuridine resistance in frog cells (22) and resistance to 8-azaguanine in Chinese hamster cells (12, 29) showed that the variant frequency was not a strong function of the ploidy level of the cells, leading to doubts as to whether the variants arose by simple nuclear genetic mutations. Epigenetic processes or extranuclear mutations have been suggested as explanations for these anomalous results (12). Alternatively, nondisjunction and X-chromosome inactivation would be other possibilities. The resistance of mammalian cells to base analogues has recently been reviewed by de Mars (4). In addition to analogies with the base analogue literature, a study of BaP resistance might lead to a better understanding of the process of de novo variation of cells in culture, which is vital if cell culture results are to be extrapolated with any confidence to in vivo situations.

Finally, since these clones are all tumorigenic, it is reasonable to use them to evaluate published correlations between tumorigenicity and resistance to polycyclic aromatic hydrocarbons that are carcinogenic (5, 9, 13, 27).

C. Materials and Methods

All cell culture techniques and toxicity studies were conducted as per Chapter I. For freezing cells, 10^6 cells were resuspended in 1.0 ml of minimal Eagle's medium fortified with 20% fetal calf serum, 10% dimethyl sulfoxide (Matheson, Coleman, and Bell, Cincinnati, Ohio), 50 ug/ml of streptomycin sulfate (Mann Research Labs., New York,

New York), and 250 units/ml of penicillin G (Grand Island Biological Col, Grand Island, New York). Freezing sensitive or resistant clones of NMuLi at liquid nitrogen temperature for one year did not markedly affect the level of variants resistant to BaP in the clones.

Tumor injection experiments were conducted as follows: Ten 100 mm confluent plates of cells (3 to 4. × 10^7 cells) were resuspended in 1.0 ml of isotonic Tris buffer (Chapter I). Then, 0.1 ml of this cell suspension was injected intrascapularly into two to three day old Namru mice. Mice were examined each week for tumor appearance.

Tumor explants were prepared by excising a representative portion of each tumor, washing it in isotonic Tris buffer, mincing the portion with sterile scissors, and trypsinizing it three times for 15 minutes each time with 0.01% trypsin (Difco, 1:250, Detroit, Mich). The decanted supernatants were diluted with minimal Eagle's medium containing 10% fetal calf serum, and 10^6 cells were plated per dish. Medium was changed on days one, three, and six post-plating, and the cells were then passaged and tested for cytotoxicity resistance as per Chapter I.

Reverse transcriptase assays were performed on the tumor explants by removing 5 ml of medium off the cells, centrifuging this medium at 1750 × g for 10 minutes, discarding the pellet, and then centrifuging the supernatant at 140,000 × g for one hour. The pellet was then resuspended in 50 ul of virus disruption buffer (50 mM Tris-HCl, 500 mM KCl, 0.1 mM EDTA, 0.25% Triton X-100, 10 mM dithiothreitol, 100 ug/ml methylated bovine serum albumin, and 10% glycerol, all at pH 8.0). Assay of reverse transcriptase was performed by the usual methods (1, 29) using poly-rA, oligo-dT as template.

Fluctuation analysis was performed according to the original method of Luria and Delbruck (20) with the modifications for mammalian cells as per Harris (12). Briefly, a sensitive clone from NMuLi was recloned, grown until it reached approximately 200 cells, and then distributed into fifteen 60 mm dishes to initiate sublines. A second 1/10 dilution of the first innoculum was prepared, and this was also seeded to initiate another fifteen sublines. The dilution yielding ten or less visible colonies by day ten post-plating was used to continue the sublines. Minimal Eagle's medium containing 10% fetal calf serum, 100 units/ml of mycostatin, 50 units/ml of streptomycin sulfate, and 250 units/ml of penicillin G was used in this experiment. Medium was changed every three days after day 10 post-plating until the plates were confluent (saturation density of about 2×10^6 cells/plate). Then, cells from each subline were trypsinized and seeded at 10^2, 10^3, 10^4, 10^5, and 10^6 cells per 60 mm dish, with 10 plates at 10^2 cells/plate and six plates at all other densities. One day post-plating, 10 ug/ml of BaP was added to the medium in acetone to five plates at 10^2 cells/plate and to four plates at the other cell densities. The rest of the plates received 0.2% acetone. Medium was changed on days 4, 8, and 12 post-plating, and new BaP and acetone were added to the plates at this time. By day 14 post-plating, the colonies were visible, and the medium was removed, the colonies rinsed once in isotonic Tris buffer, and then they were stained with 1% crystal violet in 25% ethanol.

D. Results

1. Clonal Characteristics of the NMuLi Population

At passage 40 NMuLi was cloned, and twenty isolated clones were

tested for their sensitivity to the cytotoxic effects of BaP. The

screening test consisted of exposing 300 cells from each clone to

5 ug/ml of BaP for three days, media changing, and then scoring for

viable clones on day 10 post-plating. This treatment reduces the

survival fraction of NMuLi to about 8% (Chapter I), and will distinguish

between very sensitive and fairly resistant clones.

There are 2 resistant clones out of 19 isolated from NMuLi (11%)

at passage 40, and this value agrees with those obtained for resistant

cells and for resistant clones in the NMuLi population (7±4% and 11±8%,

respectively, Chapter I). There are also very sensitive clones in the

population, defined as those whose survival is reduced to less than

10% by BaP treatment (Chart 1).

In addition, there were 50% sensitive clones. When three out of

nine of these were subcloned, they gave resistant, sensitive, and inter-

mediately sensitive subclones (Chart 2). These epithelial cells are

very prone to aggregation, and the 50% resistant clones could be

aggregates of sensitive and resistant cells in equal numbers. Micro-

scopic examination of the cell suspension used for plating the cells

after trypsinization showed some clusters of more than one cell, despite

vigorous pipetting and increasing the trypsinization time. However, as

results in later sections will show, we cannot rule out the existence

of 50% sensitive clones that are undergoing rapid segregation and

producing more sensitive and more resistant subclones.

2. Attempts to Obtain Stable Sensitive and Resistant Clones

We determined the concentration dependence of the toxicity of BaP

to two sensitive clones from NMuLi at very early passages in order to

a) NMuli

% Relative Clonal Survival (5 µg/ml BaP, 3 days)
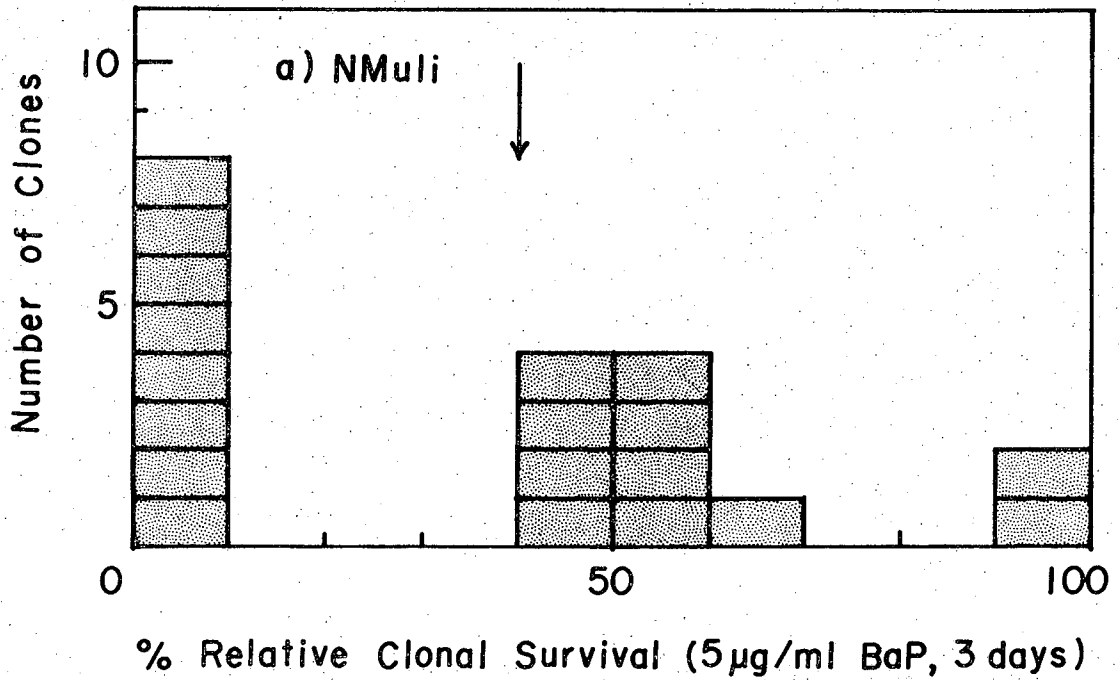
XBL757-5364 B

Chart 1

XBL75I2-8782
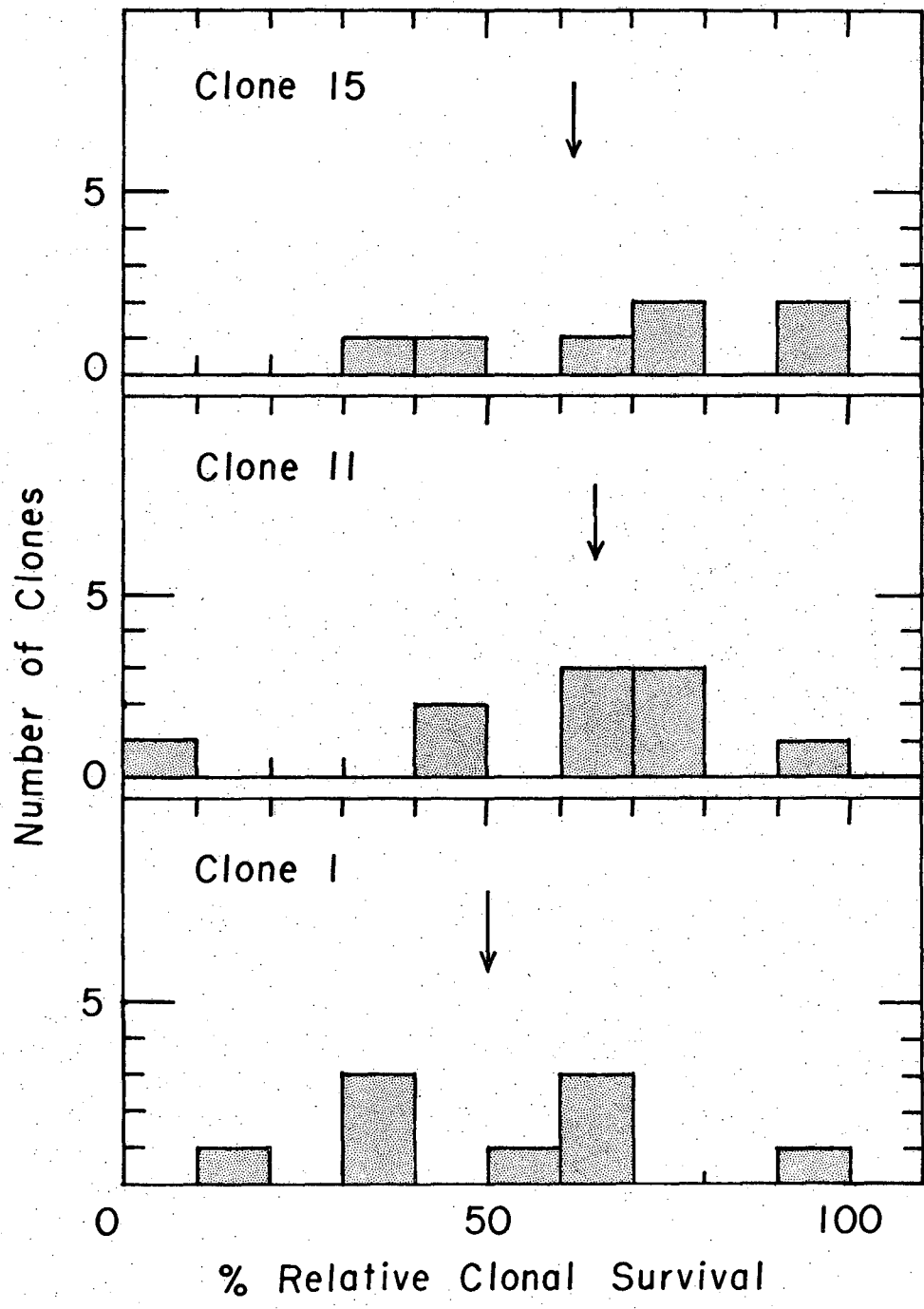
Chart 2

estimate the number of putative hits in the toxic process. Unfortu-
nately, the survival curves deviated from exponential relationships and
indicated a substantial fraction of resistant variants (Charts 3 and 4).
At later passages, the populations from these two clones were extremely
resistant.

To further examine the high levels of resistant variants, we
followed the resistant frequencies in four sensitive and in two resis-
tant clones as a function of passage. Three of the four sensitive
clones tested became greater than 10% resistant after six passages,
while the fourth one fluctuated wildly in its level of resistant variants
but in general stayed 99% sensitive (Chart 5). The progression of most
of the sensitive clones toward resistance was irreversible, and addition
of 10 ug/ml of insulin to two sensitive clones that became resistant
did not restore them to sensitivity. Insulin promotes attachment and
maintenance (13) and dome formation (14) in mouse mammary epithelial
cells at low fetal calf serum concentrations. Two resistant clones that
were examined remained resistant at least out to six passages. The rate
of approach to resistance varied among the sensitive clones.

We verified and extended these results by subcloning these clones
at passages post-isolation (passage 41 from isolation of NMuLi) to see
if their phenotypes bred true. As shown in Charts 6 and 7, the clones
do not breed true, since sensitive clones 8, 12, and 19 produced resis-
tant subclones. Sensitive clone 9 does not produce resistant subclones
at the small number of subclones tested. Resistant clones 7 and 17
bred both resistant and sensitive subclones. In most of the clones
tested, the fraction of subclones tested that were resistant agreed

9-DAY   CLONAL   ASSAY

Chart   3

XBL 767-8564

9-DAY CLONAL ASSAY

CLONE 9 PASSAGE 12

CLONE 9 PASSAGE 0

SURVIVAL FRACTION

CONC. BAP (ug/ml)

XBL 767-8565

Chart 4

$$\left(\frac{N_r}{N_r + N_s}\right)$$

PASSAGE NUMBER

Chart 5

XBL 767-8566

% RELATIVE CLONAL SURVIVAL

XBL 767-8573

Chart   6

% RELATIVE CLONAL SURVIVAL
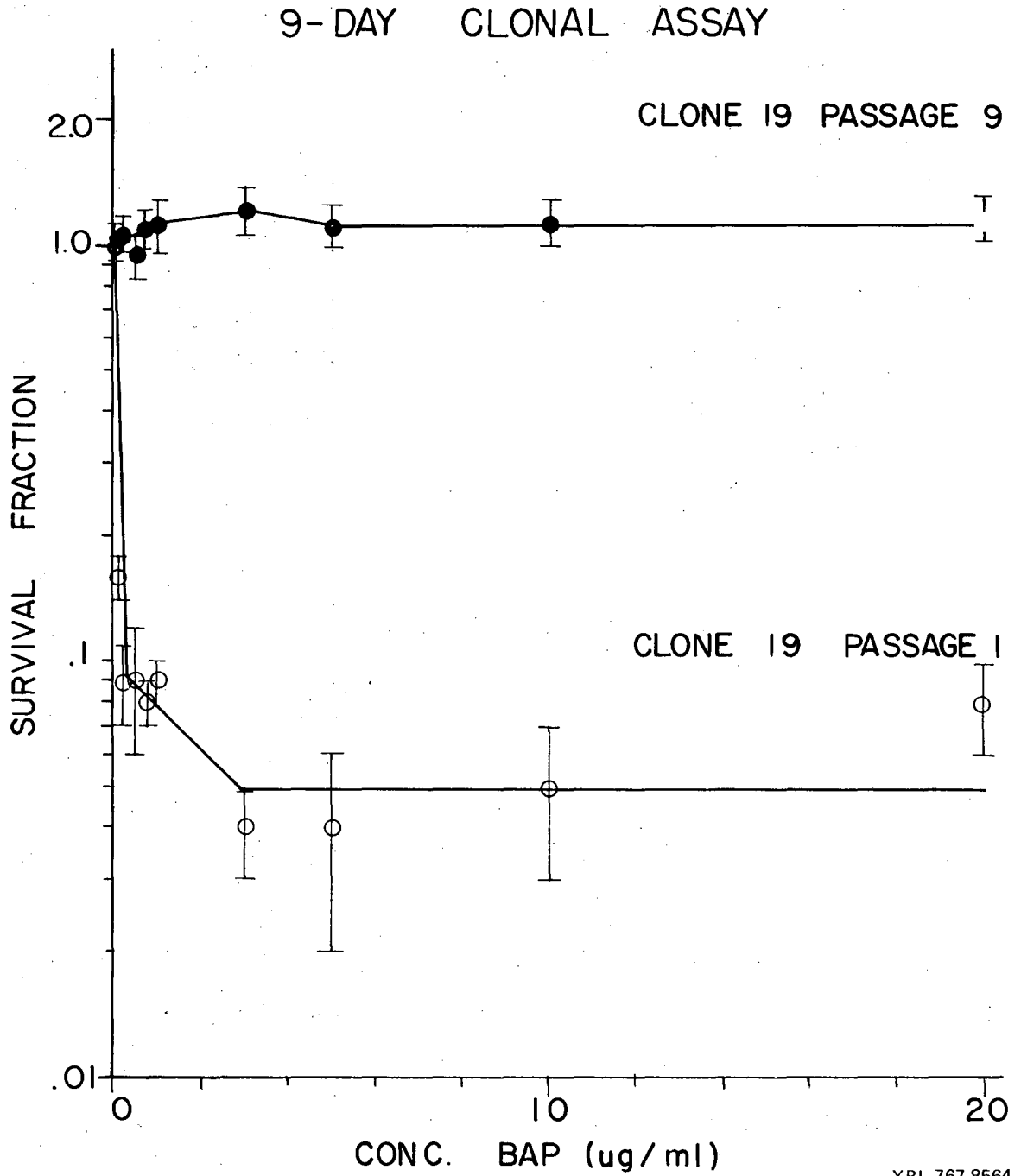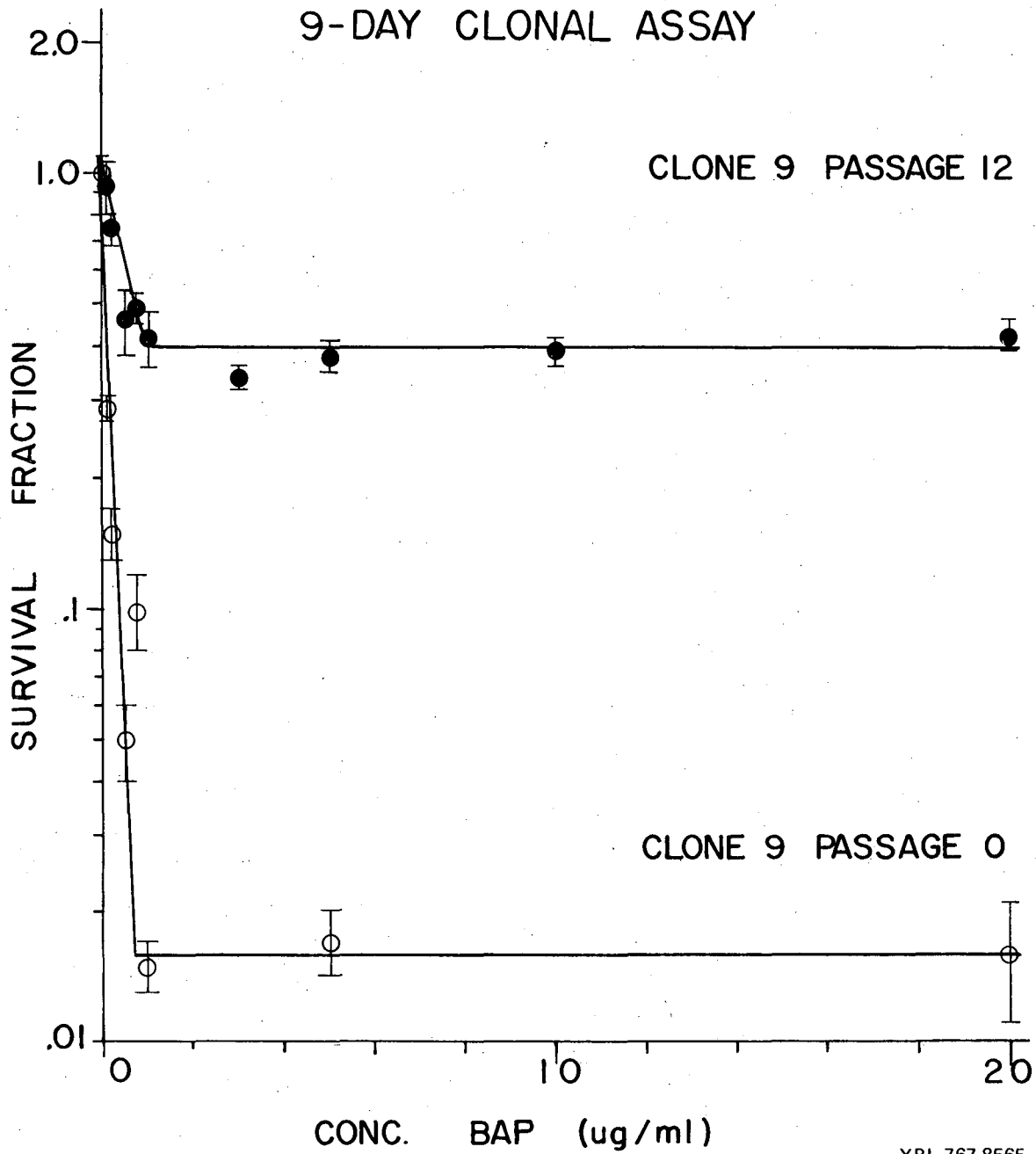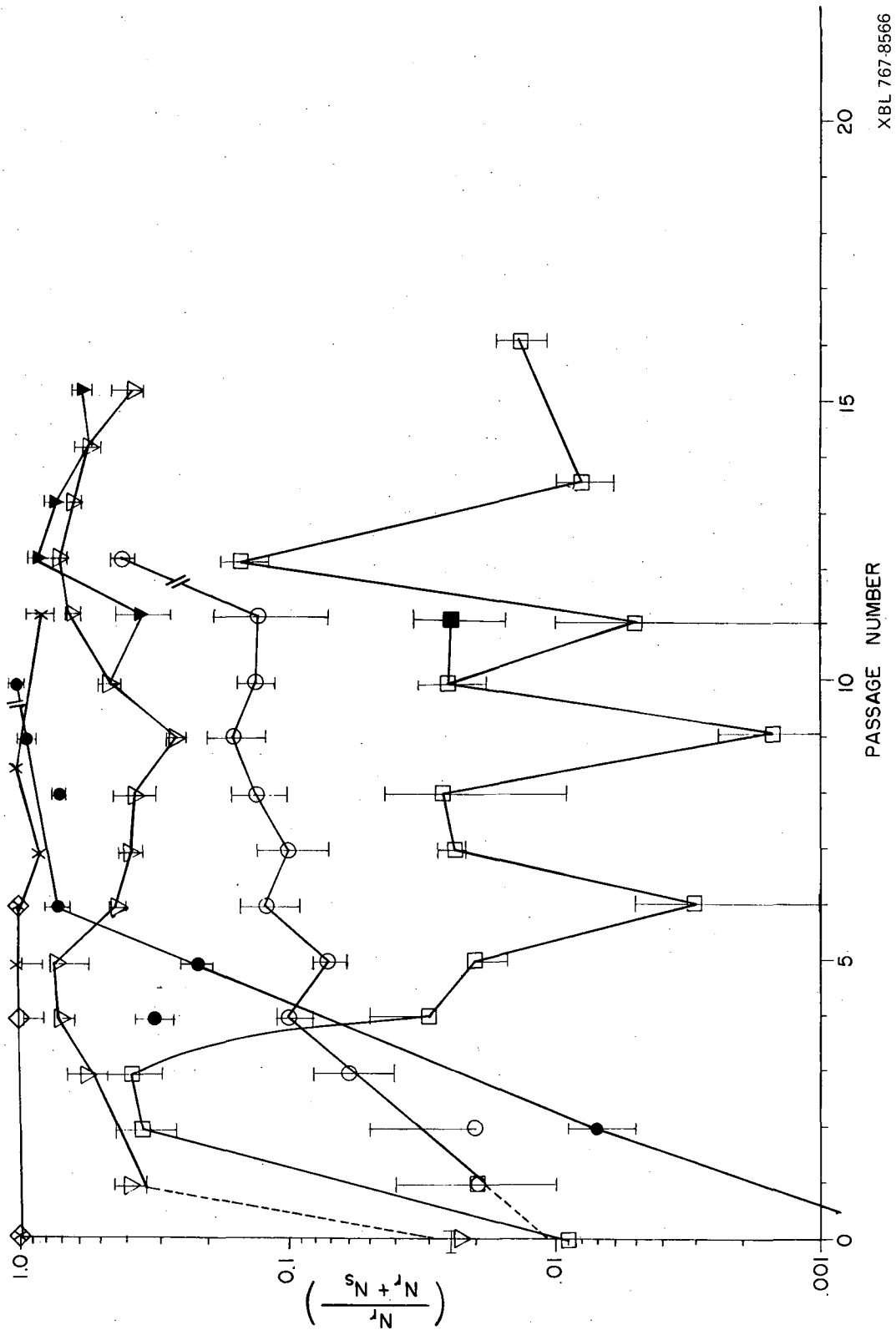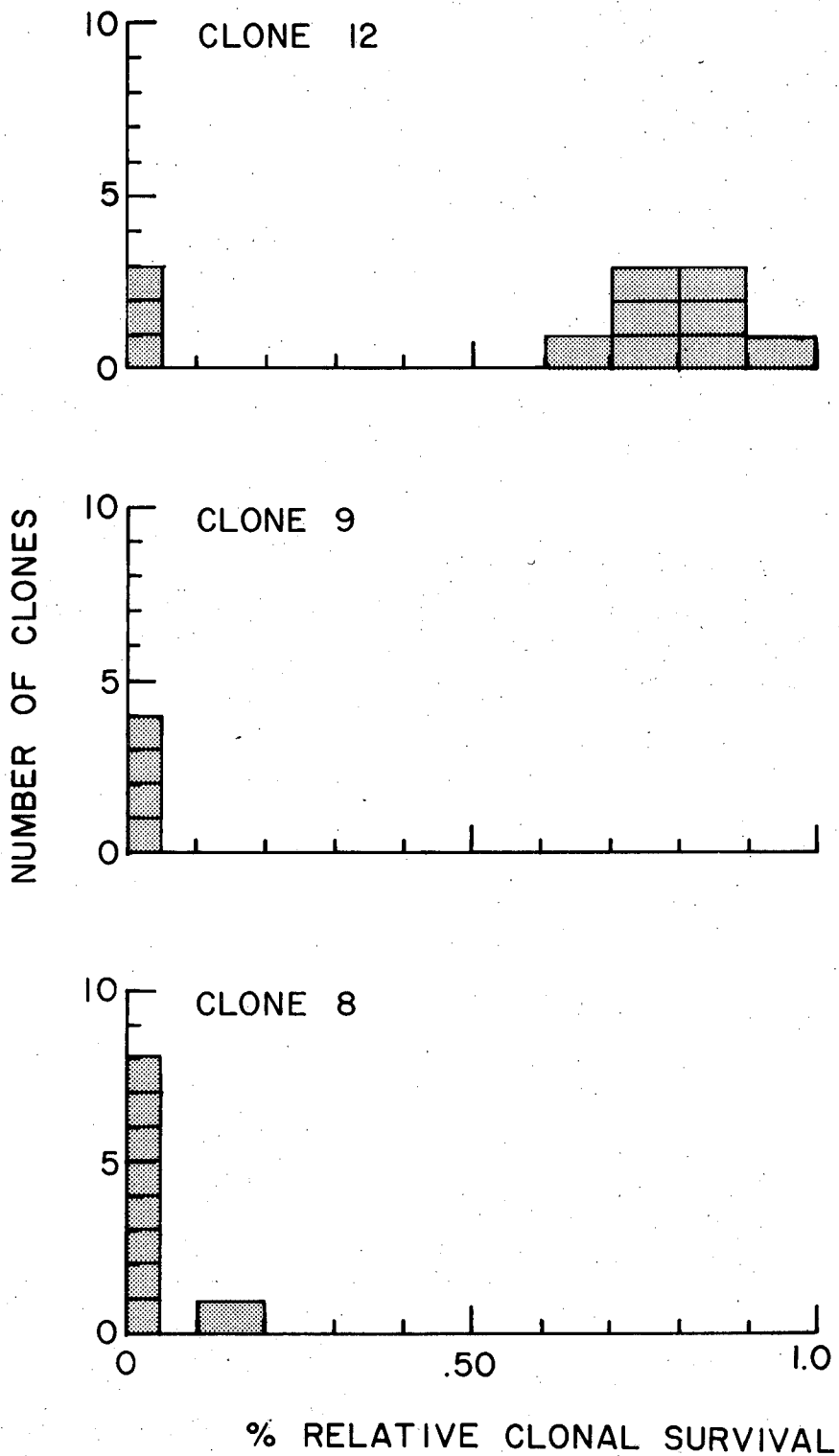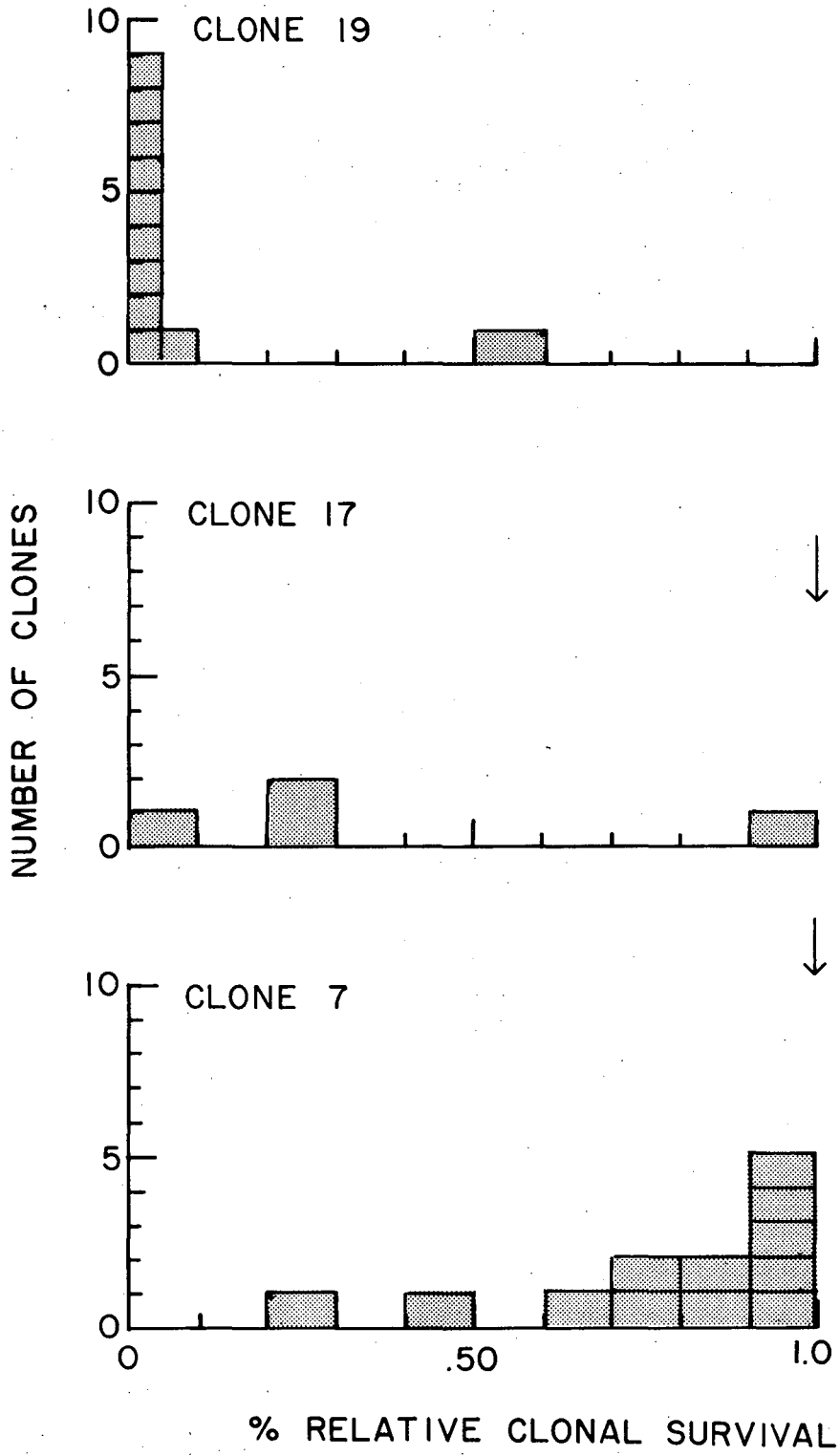
XBL 767-8574

Chart   7

with the fraction of resistant cells measured in the assay of Chart 5.
Clone 17 was anomalous, the sensitive frequency being too high, possibly
because of the small number of subclones tested.

Hence, neglecting aggregation affects, a comparison of the sub-
cloning and population assays shows that sensitive clones can breed
both sensitive and resistant subclones. Resistant subclones can breed
either type of subclone as well.

3. Effects of Growth Parameters on Resistance

Various growth parameters for the sensitive and resistant clones
are tabulated in Table I. There appears to be no correlation of the
sensitivity of a clone to the cytotoxicity of BaP with saturation
density or with mean generation time.

For the subclones of sensitive clones 8, 9, and 12 and those of
resistant clones 7 and 17, plots of resistance to BaP vs. cloning
efficiency were random collections of points (Chart 8). There were
huge variations in cloning efficiency for sensitive clone 8 as a
function of passage, and the cells became more resistant as a decrease
in cloning efficiency occurred (Chart 9). At passages 2, 3, 7, and 8
there were plateaus in both the cloning efficiency and the fraction of
resistant variants.

The same analysis of clone 19 (Chart 10) showed that the rapid
rise in the fraction of resistant variants here correlated with a large
increase in the cloning efficiency. In addition, the same plot for
clone 9 indicated a complete lack of correlation between the cloning
efficiency and the resistant fraction (data not shown). Therefore, it
appeared that these two properties were not related.

Table I. Growth and Resistance Parameters for Clones NMuLi

Clone No.	Resistant Variant Frequency	Saturation Density, Cells/35 mm Dish $\times\ 10^6$	Doubling Time, Hrs.	Passage No.
8	0.009 ± 0.003	1.7 ± 0.1	19 ± 3	41
9	0.02 (0/51)	0.5 ± 0.1	16 ± 2	41
12	0.03 (0/42)	1.4 ± 0.1	19 ± 3	441
7	1.000 ± 0.1	1.8 ± 0.1	19 ± 2	41
17	1.000 ± 0.1	1.0 ± 0.1	16 ± 1	41
19	0.900 ± 0.1	1.7 ± 0.3	18 ± 3	50
NMuLi*	0.900 ± 0.06	1.8 ± 0.4	16 ± 1	to 35
NMuLi-BaP**	0.600 ± 0.01	1.1 ± 0.6	20 ± 6	to 35

* NMuLi results are the average of four separate experiments.

** NMuLi-BaP results are the average of two separate experiments; all the other results are from one experiment only.

% CLONING EFFICIENCY
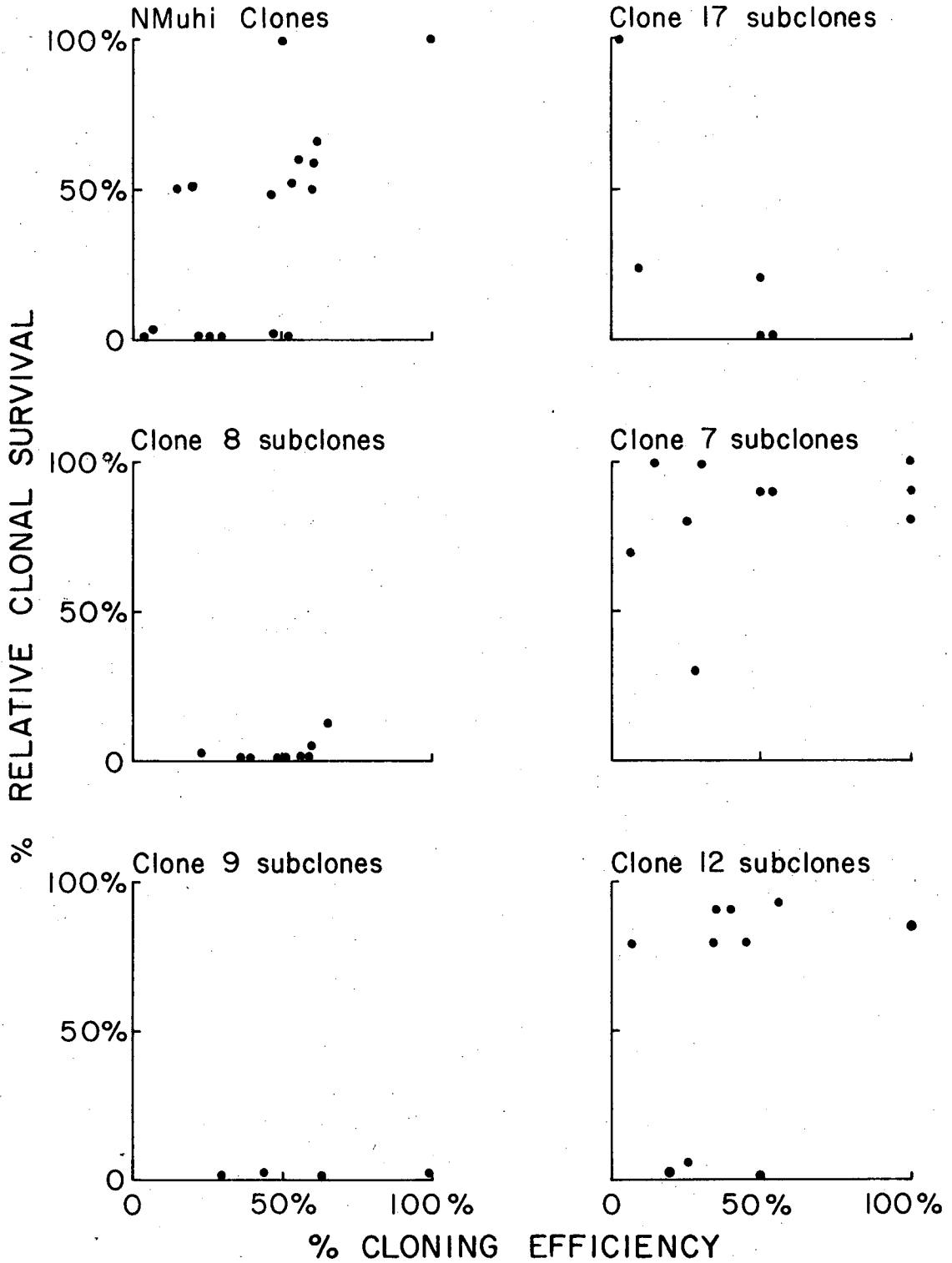
XBL 767-8563
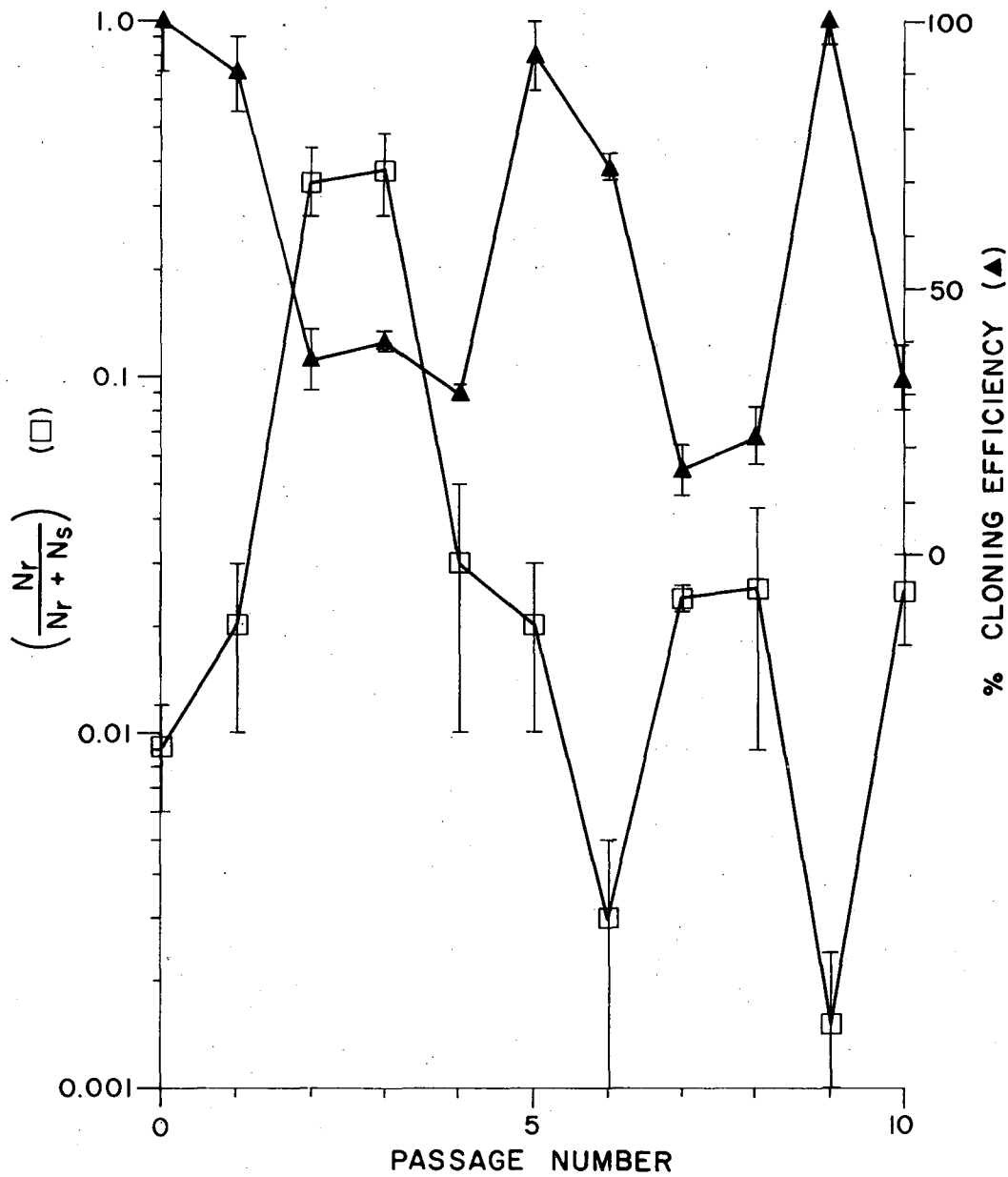
Chart 8

CLONE 8

XBL 767-8572

Chart 9

CLONE 19
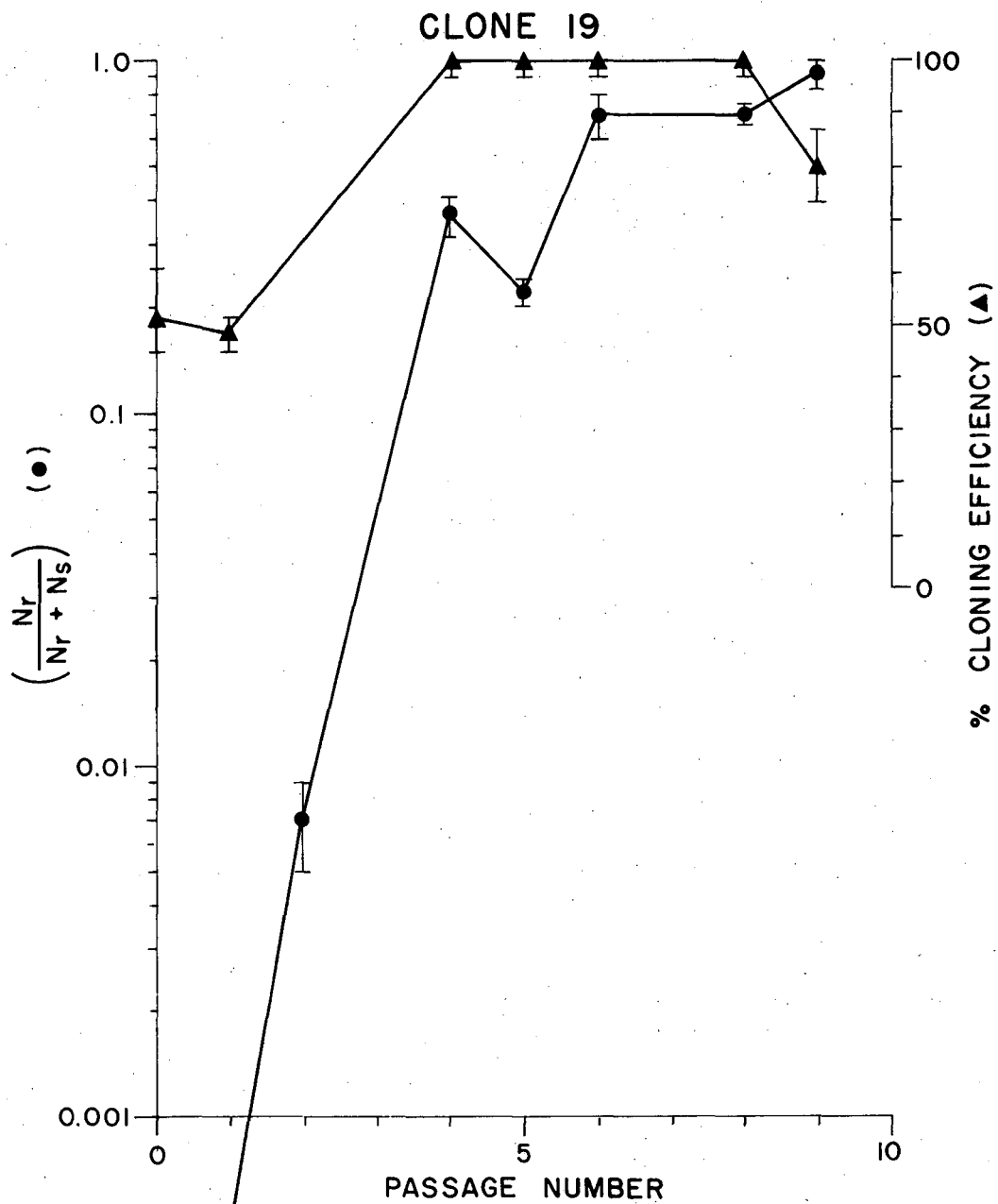
XBL 767-8571

Chart 10

4. Chromosome Numbers in Sensitive and Resistant Clones

The production of resistant variants from sensitive cells could be due to loss of one or more chromosomes. Specifically, a loss of the chromosome(s) coding for aryl hydrocarbon hydroxylase (AHH) could result in a loss of the cell's capacity to metabolize BaP to cytotoxic derivatives, especially epoxides and phenols. This might result in a resistant phenotype. In somatic cell hybrids between 3T3 mouse fibroblasts and BHK cells (which lack AHH), Benedict et al. found hydroxylase induction to be gene-dosage dependent in the only mouse-hamster clone having an excess of mouse chromosomes (3).

Since the chromosomes of the mouse are all telocentric, it would take considerable expertise to tell them apart. We therefore examined only the numbers of chromosomes in sensitive and resistant clones.

If chromosome loss is responsible for the acquisition of resistance, then 100% resistant lines should be 100% aneuploid. An unambiguous case was that of clone 19, which had less than 5% resistant variants and was 60% diploid at passage one (Chart 11). By passage nine the population was totally resistant but still 36% diploid. Although chromosome loss was occurring along with resistance, the numbers of anueploid and resistant cells were not equal.

For clone 9, there were also about 1% resistant variants when the population was 60% diploid at passage one (Chart 12). At passage 12, these cells were only 27% diploid and 40% resistant. There was also a large tetraploid and subtetraploid component to the population, and this accorded with the observation of multinucleated cells by light microscopy. The increase in the multinucleated cells by passage 12

NMuLi 19 PASS 9,   fr = 0.96

TOTAL = 61
Diploids = 36%

NMuLi 19 PASS 1,   .0002 ≤ fr ≤ .05

TOTAL = 43
Diploids = 60%

NUMBER OF CELLS

CHROMOSOMES / CELL

XBL 767-8569

Chart   11

NMuLi 9-PASS .12,   fr = 0.40

TOTAL = 56
Diploids = 27 %
Multinucleates= 30±10%
Hyperdiploids = 46 %

NMuLi 9 PASS .0,   fr = .013

TOTAL = 60
Diploids = 58 %

NUMBER OF CELLS

CHROMOSOMES / CELL
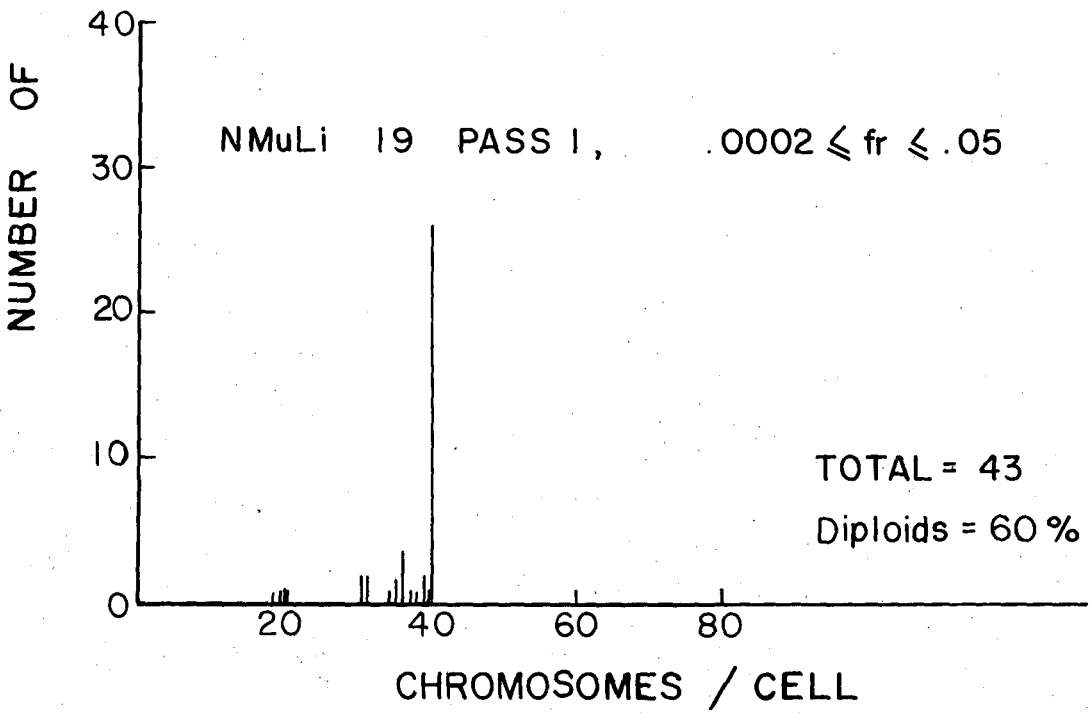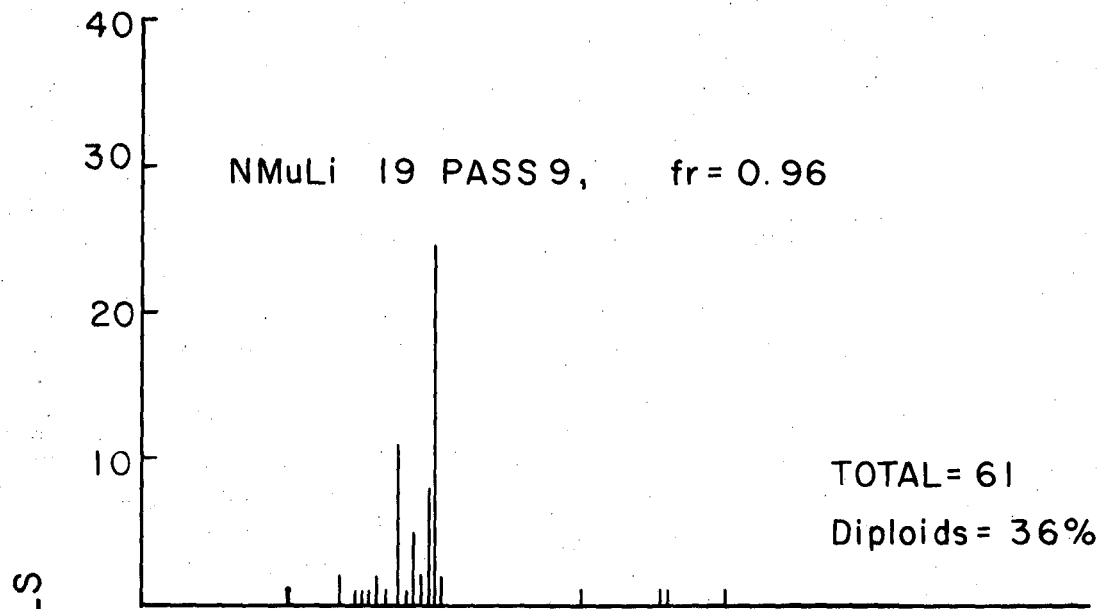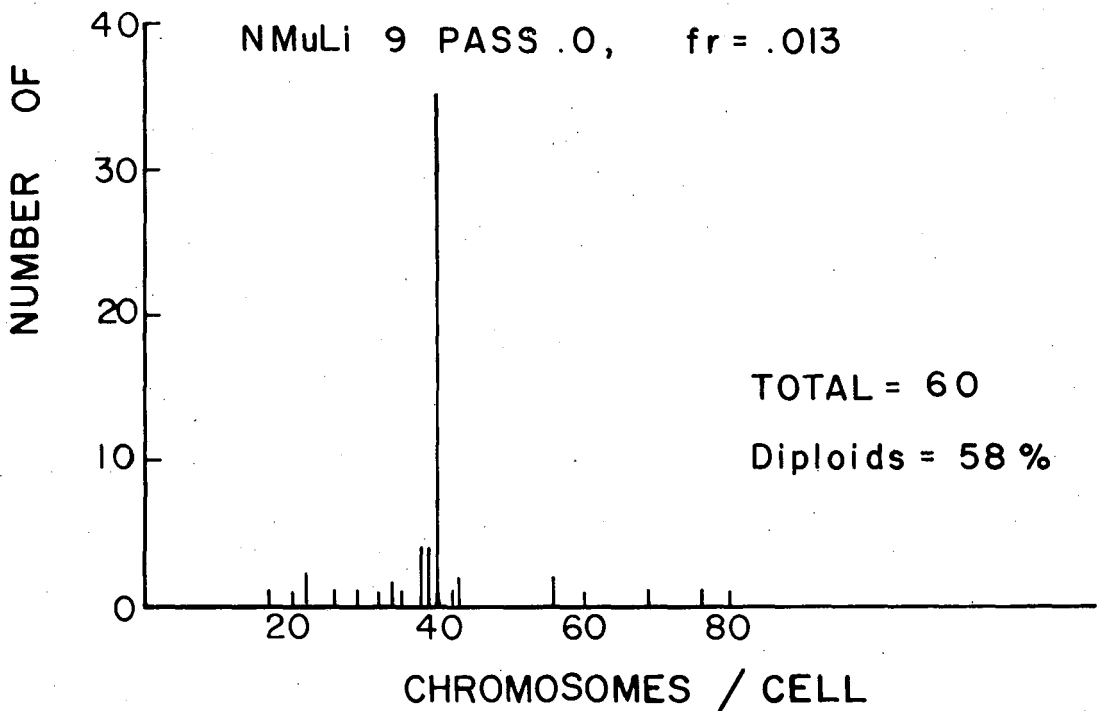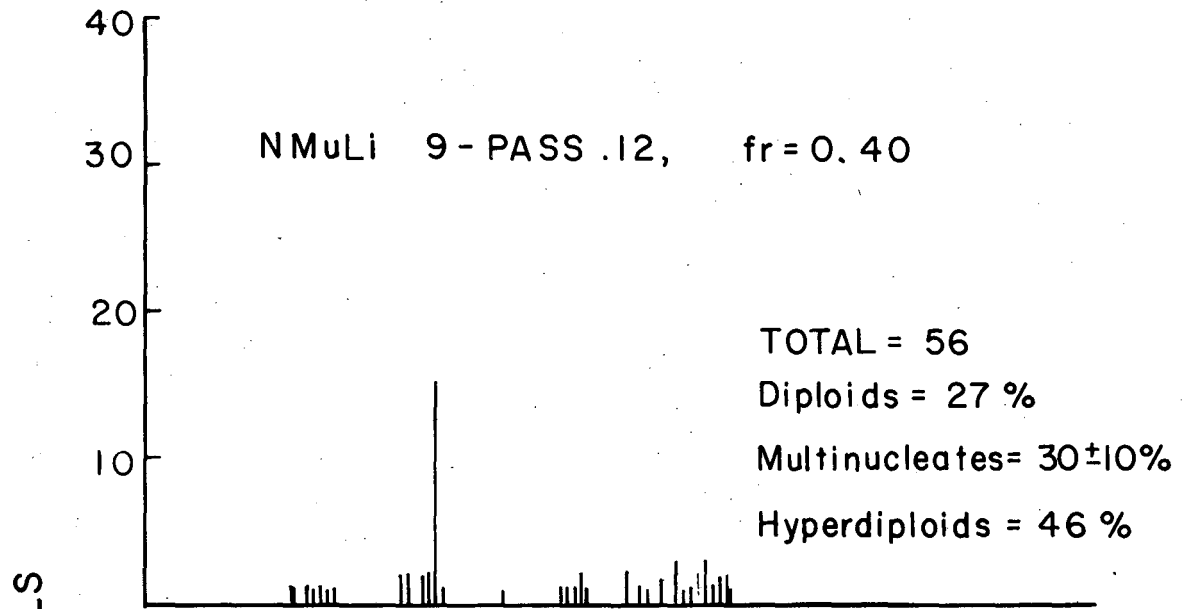
XBL 767-8570

Chart   12

of 20 ± 10% could have accounted for the decrease in the diploid popu-
lation of 31% and possibly the increase in the resistant variants.

Although clone 8 was 70% sensitive and 69% diploid at passage 2
(Chart 13), it actually became more sensitive at later passages
(Chart 5), when it probably would have lost chromosomes as did the
other clones. Finally, clone 7 was the most stably resistant clone
(Chart 5), and at passage three it was 100% resistant but still 44%
diploid.

5. Further Attempts to Understand the Instability of Sensitive Clones

We decided to examine some parameters that might contribute to the
variability in the resistance of these clones to BaP. Clones 9 and 19
were chosen, since they appeared to be going unambiguously resistant.

It was possible that the resistant variants had faster growth
rates than sensitive variants and rapidly took over the population. If
the fractional growth rate of the sensitive variants was a and that of
the resistant variants was a', then the equations for the growth rates
of the two subpopulations would be:

$$N_s = N_{os}e^{at} \quad \text{and} \quad N_r = N_{or}e^{a't} \tag{1}$$

Here, N_s and N_r are the numbers of sensitive and resistant variants at
time t and N_{os} and N_{or} are the numbers at time 0. The fraction of
resistant variants in the population at any time t will be:

$$N_r/(N_r + N_s) = N_{or}e^{a't}/(N_{or}e^{a't} + N_{os}e^{at}) \tag{2}$$

This treatment assumes that there is no conversion of sensitive to
resistant variants and vice versa during the growth of the population.
This is the easiest case to treat theoretically, although it is probably

NMuLi 7 PASS 3, fr = 1.00

TOTAL = 79
Diploids = 44 %

NMuLi 8 PASS 2, .001 ≤ fr ≤ .35

TOTAL = 49
Diploids = 69%

NUMBER OF CELLS

CHROMOSOMES / CELL

XBL 767-8568

Chart 13
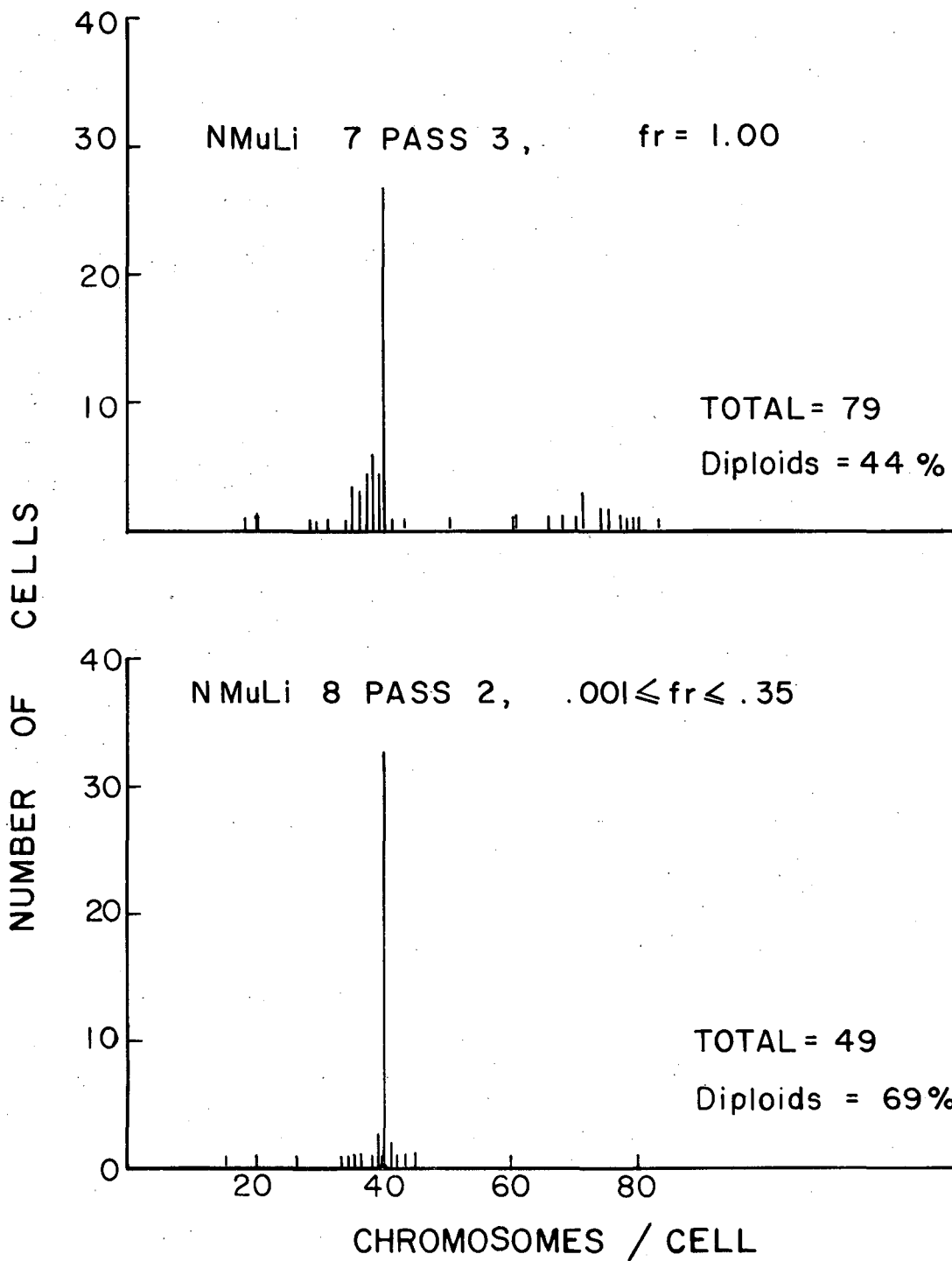
not true, and the more difficult case has been treated by Luria and Delbruck (18). This latter case, in which sensitive variants convert to resistant variants, has been shown by these investigators to yield the expression:

$$N_r/(N_r + N_s) = at, \tag{3}$$

in which a is the rate of mutation per cell per unit time. This predicts that the resistant fraction should increase linearly with time, assuming that the growth rates of the resistant and sensitive variants are the same.

Three cases now arise. If $\alpha' \gg \alpha$, then in the limit of long time, $N_r/(N_r + N_s)$ tends to 1 as a limit, and the resistant variants take over the population. If $\alpha' = \alpha$, then the population remains static in the proportion of original resistant variants, $N_r/(N_r + N_s)$ = $N_{r0}/(N_{r0} + N_{s0})$. Finally, if $\alpha' \ll \alpha$, then the sensitive variants take over the population, and the resistant fraction diminishes exponentially to zero as a function of time.

The experimental data for clones 9 and 19 are consistent with the spontaneous production of resistant cells according to the Luria-Delbruck model which then outgrow the sensitive cells. If the rate of production of resistant cells is smaller than the difference in growth rates of resistant and sensitive cells, case one might apply. By inverting equation 2, we arrive at:

$$1/F_r = 1 + (N_{0s}/N_{0r})\exp(\alpha-\alpha')t. \tag{4}$$

Here, F_r is the fraction of resistant variants in the population at time t. Further manipulation of this equation leads to:

$$\ln F_r/(1 - F_r) = \ln (N_{0r}/N_{0s}) + (\alpha' - \alpha)t \qquad (5)$$

Here, a plot of $\ln F_r/(1 - F_r)$ vs. t should yield a straight line. This is essentially plotting $\ln (F_r/F_s)$ vs. time, and the slope should reflect the increased growth rate of the resistant variants over that of the sensitive variant.

The plots for clones 9 and 19 appear initially linear, and then to curve away from linearity (Chart 14). The deviation is puzzling, unless there is a feedback mechanism modulating the permissible level of resistant variants in each population. All these experiments were performed with the same lot of fetal calf serum, and so this variable does not contribute to the curves in the plots. The linear portions of the plots were analyzed with a linear least squares computer fit, and the putative growth rate difference a' - a was determined from the slopes (Table IIb).

Growth curves of the two clones at passages when they were sensitive and when they were resistant obtained at the same time by thawing frozen clones. The curves were analyzed, and the data shows that for both clones the later passage resistant cells have markedly higher growth rates (Table IIa) and saturation densities and cloning efficiencies (Table III) than the early passage sensitive cells. For clone 9, the difference in growth rates of the sensitive and resistant cells would more than account for the slope of the resistance vs. time plot (Table IIb). For clone 19, the growth rate difference is about half of the slope of the resistance vs. time plot.

The ratio of the saturation densities of the early passage cells to the late passage cells for both clones is about 0.3 for both clones.

Chart   14
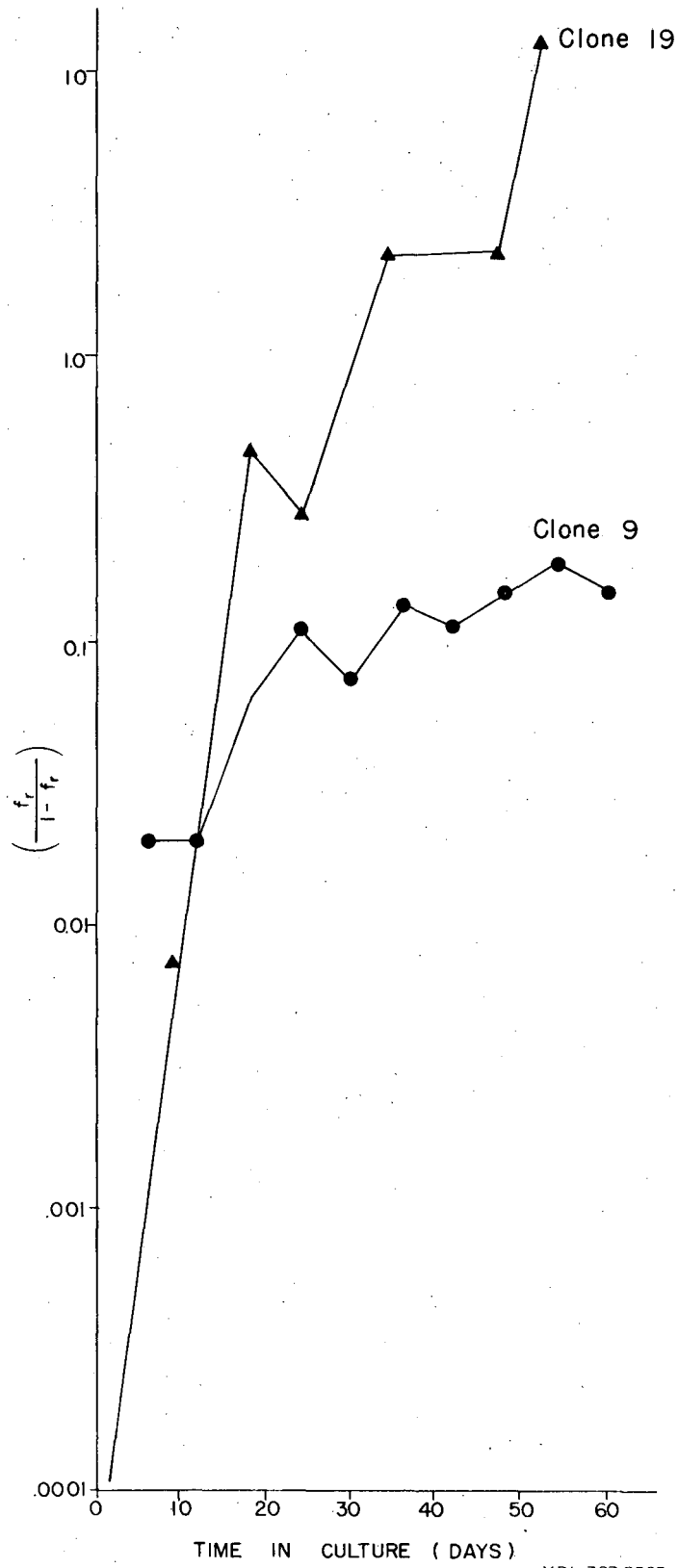
Table II.   Correlation of Resistance and Growth Rates

For Clones 9 and 19

a.   Growth Curve Data

Clone No.	a, per day	Doubling Time, Hours	a' − a, per day
9 Passage 0	0.34 ± 0.01	49 ± 2	
9 Passage 12	0.95 ± 0.14	18 ± 4	0.60 ± 0.07
19 Passage 1	0.70 ± 0.15	24 ± 3	
19 Passage 9	9.90 ± 0.10	19 ± 4	0.23 ± 0.10

b.   Plot of N_r vs. Passage Number

Clone No.	Slope of Plot (=a' − a)
9	0.10 ± 0.02
19	0.52 ± 0.04

Table III. Growth Parameters for Sensitive
and Resistant Clones*

Clone No.	Cloning Efficiency, %	Saturation Density, Cells/100 mm Dish $\times$ 10^6
9 Passage 0	52 ± 4	0.34 ± 0.05
9 Passage 12	83 ± 3	1.00 ± 0.05
19 Passage 1	36 ± 4	0.84 ± 0.40
19 Passage 9	49 ± 7	3.40 ± 0.40

* These clones had all been in the -70° freezer for one year. This
treatment did not appreciably affect the level of resistant variants.
The clones were all thawed together and the growth assays conducted
at the same time.

After four passages, this would result in both populations becoming 99%

resistant $(0.3^4 = 0.0081$ sensitive fraction). Assuming an initial

conversion of a few sensitive cells to resistant variants, this differ-

ence in saturation densities could allow the resistant variants to take

over the population in itself.

After six passages the cloning efficiency differences between the

early and late passage populations would reduce the sensitive fraction

to 0.06 in clone 9 and to 0.16 in clone 19. This factor is also more

than sufficient to account for the overgrowth of a resistant subpopu-

lation in the two clones.

Clone 19 appears morphologically the same at early and late

passages. Clone 9 possessed a few multimucleated cells at passage

one and a high proportion at passage nine. It is possible that clone 9

was heterogeneous upon cloning, although its sensitivity upon isolation

does not seem to indicate this. For clone 19 the extremely low level

of resistant variants indicates that it was probably derived from a

single cell.

6. The Tumorigenicity of Sensitive and Resistant Clones Derived From

   NMuLi and Resistance to BaP in Tumor Explants Derived From These

   Clones

As reported by Owens et al.(25), NMuLi produced tumors when

injected into newborn isogeneic mice at passage 10. Most of these

tumors were differentiated cystademomas although one fibrosarcoma and

one adenocarcinoma were observed. These latter two also possessed

a cystic component.

Since the literature indicates that growth in soft agar is one

property that correlates with tumorigenicity (26), we tested the ability

of NMuLi to grow in agar by the method of MacPherson (21). After one

month in agar, an innoculum of 5×10^5 cells produced only small flecks

that we attributed to cell aggregation. At the same cell innoculum,

a positive control, Balb 373 A31 cells transformed by murine Moloney

sarcoma virus produced large colonies of greater than 2 mm diameter and

turned the medium acidic. The latter colonies were clearly visible by

day 21 post-seeding into the agar.

Four clones from NMuLi and two clones from a derivative of NMuLi

that was resistant to BaP (NMuLI-BaP) were injected intrascapularly

into Namru mice at passage 41. All clones produced large cystic tumors

with malignant components, and the pathology report indicated that all

the tumors contained bifrosarcomatous components. Both initially

sensitive and initially resistant clones produced tumors (Tables IV

and V).

One tumor from each group of animals that had been innoculated

with a different clone was explanted to test for its resistance to

BaP toxicity. In five out of six cases, the explants were more sensi-

tive than the parent clone immediately upon explantation, even for

injected resistant clones (Table V). The explants from the NMuLi-BaP

series were relatively more sensitive. By passage three post-explanting,

all of the tumor derivatives were resistant to clonal killing, but

susceptible to growth inhibition. This was because colony size was

reduced in The BaP-treated clones, as was seen for NMuLi (Chapter I),

and probably represents a cell-cycle lengthening effect.

The reverse transcriptase levels of the tumor explants were also

Table IV. Tumorigenicity of Clones Isolated from NMuLi at Passage 40.

Cell Innoculum/Animal

NMuLi	4×10^6	3×10^6	1×10^6	4×10^5	3×10^5	1×10^5	4×10^4
	Number of Animals With Tumors/Number of Animals Injected						
Clone #							
1	8/8			8/8			
3			9/9			7/7	
7		9/9			6/6		
17		6/6			6/6		
NMuLi-Bap							
Clone #							
3	12/14			0/8			0/9
7	7/11			3/9			

Note 1. Ann Hughes noted that most of the tumors have a latent period of one week, and that they are large cystic structures filled with fluid and occurred at the site of innoculation.

Note 2. The pathologist observed that all the NMuLi tumors were basically fibrosarcomas, but that NMuLi clone 7 had scattered tubular structures lined by epithelium. Histologically, he called it a malignant mixed tumor.

Note 3. Ann Hughes performed the injections, maintained the animals, and prepared the slides for pathology.

Table V.   Resistance to BaP in Tumors Derived From Clones of NMuLi and NMuLi-BaP[*]

NMuLi Clone #	Clonal Resistance Upon Innoculation	Clonal Resistance of Tumor Explants, Fraction of Control			Cellular Growth Resistance of Tumor Explants	
		Pass. 1	Pass. 2	Pass. 3	Pass. 2[**]	Pass. 3
1	0.5 ± 0.1	0.5^{***}	1.1 ± 0.1	0.5 ± 0.2	+++	0.23 ± 0.01
3	0.1 ± 0.01	0.5 ± 0.1	0.8 ± 0.1	0.6 ± 0.2	+++	0.16 ± 0.01
7	1.0 ± 0.1	0.3	0.6 ± 0.1	0.4 ± 0.1	+++	0.14 ± 0.01
17	1.0 ± 0.1	0.8	0.9 ± 0.1	0.7 ± 0.1	+++	0.36 ± 0.01

NMuLi-BaP Clone #						
3	0.9 ± 0.1	0.05 ± 0.04	0.6 ± 0.1	1.0 ± 0.1	$\pm$	0.21 ± 0.01
7	0.88 ± 0.04	0.13 ± 0.13	0.7 ± 0.1	0.6 ± 0.1	+++	0.17 ± 0.01

* Clonal killing and growth rate depressive effects were carried out exactly as described in Chapter 1, by exposure to 5 ug/ml of BaP for 3 days.

** The cells were not counted on this passage, but visual estimates of the growth rate depressive effects were made. +++ implies great toxicity, $\pm$ little or none.

***The passage one results are qualitative because the cloning efficiency of the cells at this point was so small that not enough survived to allow an accurate estimate of the resistant fraction.

measured, with Balb 3T3 A31 cells transformed by murine Moloney sarcoma virus serving as a positive control in the assay. There was a positive correlation between the ability of the explants to grow in agar and their levels of reverse transcriptase (Table VI). Other data from this lab indicated that NMuLi possessed varying levels of reverse transcriptase as a function of passage (J. Bartholomew and H. Hesser, unpublished results). The saturation densities and doubling times of the explants in liquid medium did not appear to correlate with the ability of the tumor explants to grow in agar.

E. Discussion

We have shown that cloned populations of sensitive epithelial cells become rapidly resistant to BaP. Resistant variants possessing higher cloning efficiencies, growth rates, and saturation densities than their sensitive progenitors appear to be spontaneously produced. Although these selective growth advantages allowed the resistant cells to take over the populations, there was no correlation between the resistant phenotype and growth rate parameters-saturation density, growth rate, or cloning efficiency- per se.

It seemed that chromosome loss and resistant variant production were not numerically equivalent. However, three points must be considered. Firstly, there is some subjective judgement in which squashes to select for counting chromosomes, so the process was not totally random, nor were a huge amount of samples counted. Secondly, even though a population has a diploid complement of chromosomes, the chromosome(s) coding for AHH could have a small deletion in this region, i.e., it might be a psuedodiploid population. Finally, although

Table VI. Growth Parameters and Reverse Transcriptase (RDP) Levels in Tumor Explants Derived From Clones of NMuLi and NMuLi-BaP

Explant	Saturation Density, Cells/35 mm plate × 10^6	Doubling Time, Hours	RDP Activity, ^{3}H dpm/ 5 ml medium/30 min. as acid insoluble polymer × 10^5 *	Growth in Soft Agar**
NMuLi Clones				
#1	2.7 ± 0.1	12.8 ± 0.6	1.7 ± 0.2	+++
#3	2.0 ± 0.1	15.5 ± 0.1	0.59 ± 0.04	+
#7	2.1 ± 0.1	14.0 ± 0.7	0.19 ± 0.02	+
#17	2.0 ± 0.1	15.0 ± 4	1.06 ± 0.03	+++
NMuLi-BaP Clones				
#3	2.4 ± 0.1	16.0 ± 3	0.04 ± 0.01	±
#7	1.4 ± 0.1	15.0 ± 1	0.05 ± 0.01	±
MSV Balb	---------	--------	-----------	
3T3 A31				

* This experiment was performed with the aid of Helen Hesser.

**Pluses and minuses are qualitative observations based on whether or not the cells produced 3 dimensional colonies in agar of 0.1 mm size by 30 days after seeding.

AHH is an autosomal dominant trait (23), and one might expect that tetraploid cells should be susceptible to BaP, there were tetraploid cells in clone 7, which was totally resistant.

It is not obvious why resistant variants generated from sensitive clones possessed a selective advantage over the sensitive cells. We cultured these cells in 10% fetal calf serum, because it has been known that this serum is less effective kinetically in inducing spontaneous malignant transformation in cultured cells than horse serum is (10, 26). Whitlock and Gelboin have noted that fetal calf serum induces AHH in epithelial cells cloned from Buffalo rat liver in a dose-dependent manner (30). This could conceivably result in a small but chronic toxic effect and hence a selection for cells that do not have the hydroxylase enzyme, i.e., resistant cells. We have noted that basal levels of AHH in NMuLi are of the order of 5 pmoles or less of 3-hydroxy-BaP/mg protein/30 minutes, while the induced levels are roughly 150 pmoles/mg protein/30 minutes (Chapter 1). We cannot conclusively rule out a small toxic effect of fetal calf serum, and hence a selective pressure, but we do not feel that this is responsible. Further, Evans et al. (9) note that mixed populations of freshly minced C3H/He mouse embryo cells became progressively susceptible to 7,12 dimethylbenz(a)anthracene (DMBA) toxicity when cultured in fetal calf serum, while the same cells cultured in horse serum became resistant. Although a mixed population of cells was used, the result for fetal calf serum is opposite to that which a small chronic toxicity would have.

Our results with tumor explants show that resistance to BaP-induced

toxicity does not correlate with the tumorigenic state, since both fully sensitive and fully resistant clones gave rise to malignant tumors. In addition, NMuLi-BaP resistant clones produced tumors which were sensitive immediately upon explantation. If these tumors were not derived from the host but from the injected clones (which is not certain), it may be that these cells can be reactivated in the host to recover higher levels of AHH, which then results in cell death upon exposure to BaP. This could be an example of gene derepression, as seen in somatic cell hybridization studies. Alternatively, it could also be that an endogenous virus is liberated from these clones upon injection and transforms neighboring cells that remain sensitive to BaP for some time.

Diamond has shown that neoplastic and non-neoplastic human cell lines are resistant to chemical carcinogens (5) and has noted that there was no strict correlation between resistance and malignancy in culture (8). Similarly, Huberman and Sachs showed that hamster cells transformed by polyoma virus acquired resistance at various times after transformation, and that both sensitive and resistant cells were susceptible to transformation (13). They also found that transformed clones that were sensitive at the time of transformation later became resistant.

On the other hand, Starikova and Vasiliev demonstrated that rat fibrosarcomas were resistant to the cytotoxicity of DMBA when cultured in vitro, whereas normal rat connective tissue from embryos and adults was very susceptible in vitro (27). Similarly, Evans et al. showed a good correlation between qualitative resistance to DMBA and the neoplastic state and between sensitivity to DMBA and the non-neoplastic state (9).

Our data is more consistent with the conclusions of Huberman and Sachs (13) and of Diamond (5, 8). Hence, it would appear that resistance and tumorigenicity are not necessarily mechanistically coupled. Subsequent to transformation numerous secondary changes can appear in cells, and the continuous dedifferentiation of the cells could result in a loss of the high levels of specific enzymes, among them AHH. This could explain a late acquisition of resistance. In addition, AHH levels have been shown to decline drastically with passage number in hamster fetus cells (21, 22).

This dedifferentiation could also allow the cell to devote more of its biosynthetic capacity to growth, and might explain the selective advantage that later passage resistant cells have over their earlier sensitive parent clones.

It also appears that resistance might be an artifact of culturing and might bear no relationship to in vivo results. Of course, levels of conjugating, detoxifying enzymes, such as epoxide hydrase and glutathione transferase are probably much higher in vivo and there is likely no large toxicity after small hydrocarbon exposures. In addition, it is possible that resistant cells might be altered antigenically and be selected out by the immune system. This question can only be answered by working in vivo and then for one passage in vitro, since in vitro resistance appears rapidly.

Attempts to use the phenotype, resistance to BaP, should be viewed with caution, since in one clone of these cells there are large fluctuations in resistance which correlate inversely with the cloning efficiency of the cells. Hence, there will be large variations in resistance

dependent upon how consistently the experimenter handles the cells. It should also be noted that the tendency of these epithelial cells to aggregate probably causes some error in the measured cloning efficiencies.

F. REFERENCES

1. Abrell, J. W., and Gallo, R. C. Purification, Characterization, and Comparison of the DNA Polymerases from Two Primate RNA Tumor Viruses.

2. Aviv, D., and Thompson, E. B. Variation in Tyrosine Aminotransferase Induction in HTC Cell Clones. Science 177: 1201-1203, 1972.

3. Benedict, W. F., Paul, B., and Nevert, D. W. Expression of Benz(a)-anthracene Inducible Aryl Hydrocarbon Hydroxylase Activity in Mouse-Hamster and Mouse-Human Somatic-Cell Hybrids. Biochem. Biophys. Res. Comm. 48: 293-298, 1972.

4. DeMars, R. Resistance of Cultured Human Fibroblasts and Other Cells to Purine and Pyrimidine Analogues in Relation to Mutagenesis Detection. Mut. Res. 24: 335-364, 1974.

5. Diamond, L. The Effect of Carcinogenic Hydrocarbons on Rodent and Primate Cells in Vitro. J. Cell. and Comp. Physiol. 66: 183-198, 1965.

6. Diamond, L., Defendi, V., and Brookes, P. The Interaction of 7,12-Dimethylbenz(a)anthracene with Cells Sensitive and Resistant to Toxicity Induced by this Carcinogen. Cancer Res. 27: 890-897, 1967.

7. Diamond, L. Metabolism of Polycyclic Hydrocarbons in Mammalian Cell Cultures. Int. J. Cancer 8: 451-462, 1971.

8. Diamond, L. The Interaction of Chemical Carcinogens and Cells in Vitro. Progr. Exp. Tumor Res. 11: 364-383, 1969.

9. Evans, V. J., Price, F. M., Kerr, J. A., and de Oca, H. M. Effect of 7,12-Dimethylbenz(a)anthracene on Non-Neoplastic and Neoplastic Rodent Cells in Culture. J. Nat. Cancer Inst. 45: 429-441, 1970.

10. Evans, V. J., Andresen, W. F. Effect of Serum on Spontaneous Neoplastic Transformation in Vitro. J. Nat. Cancer Inst. 37: 247-249, 1966.

11. Gelboin, H. V., Huberman, E., and Sachs, L. Enzymatic Hydroxylation of Benzopyrene and Its Relationship to Cytotoxicity. Proc. Nat. Acad. Sci. USA 64: 1188-1194, 1969.

12. Harris, M. Mutation Rates in Cells at Different Ploidy Levels. J. Cell Physiol. 78: 177-184, 1971.

13. Hosick, H. L., and Nandi, S. Plating and Maintenance of Epithelial Tumor Cells in Primary Culture: Interacting Roles of Serum and Insulin. Exp. Cell Res. 84: 419-425, 1974.

14. Hosick, H. L., and Nandi, S. Preliminary Survey of Hormonal Influences on Multicellular Architecture in Primary Cultures of Mammary Carcinoma Cells. J. Nat. Cancer Inst. 52: 897-902, 1974.

15. Huberman, E., and Sachs, L. Susceptibility of Cells Transformed by Polyoma Virus and Simian Virus 40 to the Cytotoxic Effect of the Carcinogenic Hydrocarbon Benzo(a)pyrene. J. Nat. Cancer Inst. 40: 329-336, 1968.

16. Huberman, E., Aspiras, L., Heidelberger, C., Gorver, P. L., and Sims, P. Mutagenicity to Mammalian Cells of Epoxides and Other Derivatives of Polycyclic Hydrocarbons. Proc. Nat. Acad. Sci. 68: 3195-3199, 1971.

17. Huberman, E., Donovan, P. J., and DiPaolo, J. A. Mutation and Transformation of Cultured Mammalian Cells by N-Acetoxy-N-2-Fluorenylacetamide. J. Nat. Cancer Inst. 48: 837-840, 1972.

18. Huberman, E., and Sachs, L. Cell-Mediated Mutagenesis of Mammalian

Cells with Chemical Carcinogens.   Int. J. Cancer 13: 326-333, 1974.

19.   Huberman, E., Sachs, L., Yang, S. K., and Gelboin, H. B.   Identi-
      fication of Mutagenic Metabolites of Benzo(a)pyrene in Mammalian
      Cells. Proc. Nat. Sci. USA 73: 606-611, 1976.

20.   Luria, S. E., and Delbruck, M.   Mutations of Bacteria from Virus
      Sensitivity to Virus Resistance.   Genetics 28: 491-511, 1943.

21.   MacPherson, I.   Agar Suspension Culture for Quantitation of
      Transformed Cells, In Fundamental Techniques in Virology. Eds.
      K. Habel and N. P. Salzman. 1969, Academic Press, New York,
      pp. 214-219.

22.   Mezger-Freed, L.   Effect of Ploidy and Mutagens on BUDR Resistance
      in Haploid and Diploid Frog Cells. Nature New Biology 235: 245-246,
      1972.

23.   Nebert, D. W., and Gelboin, H. B.   Substrate-Inducible Microsomal
      Aryl Hydroxylase in Mammalian Cell Culture. II. Cellular Responses
      During Enzyme Induction. J. Biol. Cheml. 243: 6250-6251, 1968.

24.   Nebert, D. W., and Gelboin, H. V.   The in Vivo and in Vitro
      Induction of Aryl Hydrocarbon Hydroxylase in Mammalian Cells of
      Different Species, Tissues, Strains, and Developmental and Hormonal
      States. Arch. Biochem. Biophys. 134: 76-89, 1969.

25.   Nebert, D. W., Gielen, J. E., and Goujon, F. M.   Genetic Expression
      of Aryl Hydroxylase Induction. III. Changes in the Binding of
      n-Octylamine to Cytochrome P-450. Mol. Pharmacol. 8: 651-666, 1972.

26.   Owens, R. B., Smith, H. S., and Hacket, A. J.   Epithelial Cells
      from Normal Glandular Tissue of Mice. J. Nat. Cancer Inst. 53:
      261-269, 1974.

-85-

27. Sanford, K. K.   Biologic Manifestations of Oncogenesis in Vitro:
     A Critique.   J. Nat. Cancer Inst. 53: 1481-1485, 1974.

28. Sanford, K. K. "Spontaneous" Neoplastic Transformation of Cells in
     Vitro: Some Facts and Theories.   Nat. Cancer Inst. Monogr. 26:
     387-418, 1967.

29. Starikova, V. B., and Vasiliev, J. M.   Action of 7,12-Dimethylbenz-
     (a)anthracene on the Mitotic Activity of Normal and Malignant Rat
     Fibroblasts in Vitro.   Nature (London) 195: 42-43, 1962.

30. Van Zeeland, A. A., and Simons, J. W. I. M.   Ploidy Level and Mutation
     to Hypoxanthine-Guanine-Phospho-Ribosyl-Transferase (HGPRT) Deficiency in
     Chinese Hamster Cells.   Mut. Res. 28: 239-250, 1975.

31. Waters, L. C., and Yang, W. I.   Comparative Biochemical Properties
     of RNA-Directed DNA Polymerases from Rauscher Murine Leukemia Virus
     and Avian Myeloblastosis Virus.   Cancer Res. 34: 2585-2593, 1974.

32. Whitlock, J. P. Jr., and Gelboin, H. V.   Aryl Hydrocarbon(benzo(a)-
     pyrene) Hydroxylase Induction in Rat Liver Cells in Culture.   J.
     Biol. Chem. 249: 2616-2623, 1974.

33. Wislocki, P. G., Wood, A. W., Chan, R. L., Levin, W., Yagi, H.,
     Hernandez, O., Jerina, D. M., and Conney, A. H.   High Mutagenicity
     and Toxicity of a Diol-Epoxide Derived from Benzo(a)pyrene.   Biochem.
     Biophys. Res. Comm. 68: 1006-1012, 1976.

34. Wood, A. W., Goode, R. L., Chang, R. L., Levin, W., Conney, A. H.,
     Yagi, H., Dansette, P. M., and Jerina, D. M.   Mutagenic and Cyto-
     toxic Activity of Benzo(a)pyrene 4,5-, 7,8-, and 9,10-Oxides and the
     Six Corresponding Phenols.   Proc. Nat. Acad. Sci. USA 72: 3176-3180,
     1975.

Chart Legends — Chapter II

Chart 1. NMuLi was clones at passage 40. Each clone was seeded at 300 cells/plate, allowed to recover for one day, and then treated with 5 ug/ml of BaP for three days. Viable colonies were scored on day ten post-plating.

Chart 2. Three of the 50% resistant clones from Chart 1 were subcloned and the subclones were tested for their ability to survive BaP in the same assay used in Chart 1.

Chart 3. The concentration dependence of the toxicity of BaP to NMuLi clone 19 was studied using a nine-day exposure in 1 the colony survival assay.

Chart 4. The concentration dependence of the toxicity of BaP to NMuLi clone 9 was studied using a nine-day exposure in the colony survival assay.

Chart 5. Six different clones from NMuLi were tested for their ability to survive BaP in the assay from Chart 1 as a function of passage. Clone 19 (●----●), clone 8 (□----□), clone 9 (0----0), clone 12 (∇----∇), clone 7 (◇----◇), and clone 17 (x----x). 10 ug/ml of insulin was added to some of the cultures from clone 8 (■----■) and from clone 12 (▼----▼) at passage 11, and these were then passaged as separate lines at this time. The symbol 11 indicates that the cells were frozen and thawed at this time.

Chart 6.   Sensitive clones 8, 9, and 12 were subcloned at passage one

post-isolation, and the subclones were tested for their

ability to survive BaP treatment in the assay of Chart 1.

Chart 7.   Clones 19, 17, and 7 were subcloned at passage one post-

isolation, and the subclones were tested for their ability

to survive BaP treatment in the assay of Chart 1.

Chart 8.   Various clones of NMuLi were subcloned, and the cloning

efficiency of the subclones was plotted against their ability

to survive BaP treatment in the assay of Chart 1.

Chart 9.   The ability of NMuLi clone 8 to survive BaP treatment in the

assay from Chart 1 and its cloning efficiency were monitored

as a function of passage.

Chart 10.   The ability of NMuLi clone 19 to survive BaP treatment in

the assay from Chart 1 and its cloning efficiency were

monitored as a function of passage.

Chart 11.   Chromosome histograms were constructed for NMuLi clone 19

at passages one and nine post-cloning. Total represents

the number of chromosome preparations counted. fr is the

fraction of the population that is resistant.

Chart 12.   Chromosome histograms were constructed for NMuLi clone 9

immediately upon isolation and at passage 12.

Chart 13. Chromosome histograms were constructed for NMuLi clones 7

and 8 at the indicated passages.

Chart 14. The ratio of the fraction of cells resistant to the assay

of Chart 1 (fr) to the fraction of cells sensitive to this

treatment (1-fr) was plotted as a function of passage

number for clones 9 (●----●) and 19 (▲----▲).

III. A MOLECULAR BASIS FOR THE ACQUISITION OF RESISTANCE TO BENZO(A)PYRENE IN CLONES DERIVED FROM NMuLi

A. Summary

Although clones derived from NMuLi rapidly built up a high level of variants resistant to benzo(a)pyrene (BaP), these clones were totally susceptible to the toxicity of $\pm 7\alpha$, 8β, dihydroxy-9, 10βepoxy-7,8,9,10 tetrahydro-BaP (diol-epoxide), a known in vitro metabolite of BaP. This suggested that loss of aryl hydrocarbon hydroxylase (AHH) activity was responsible for the loss of susceptibility to BaP-induced toxicity.

The time course of induction of AHH activity in NMuLi by BaP was shown to be the same in confluent and in growing cells, peaking at about 12 hours. In addition, the maximal levels and integrated values of induced AHH/cell in growing cells were roughly twice those in confluent cells. This induced AHH activity was inhibited 78% by gassing with carbon monoxide for 15 minutes or by addition of 4 ug/ml of 7,8 benzoflavone.

A radioactive assay for BaP metabolism was developed with rat liver microsomal material. This assay detected hydroxylated metabolites of BaP in the alkali extraction, which correlated with the production of fluorescent derivatives in the same layer (the classical AHH assay). In addition, it detected metabolites of BaP in the water-acetone layer, which were presumably detoxification products, such as gluthathione and cysteine conjugates of BaP-epoxides. It was also possible that RNA-BaP, DNA-BaP, and protein-BaP conjugates were in the water-acetone layer. The radioactive assay showed that the classical fluorescent assay was

sufficient for assessing BaP metabolizing activity.

A number of sensitive and resistant clones of NMuLi were assessed for their levels of AHH using the fluorescent assay, and it was seen that sensitive clones in general possessed higher AHH levels than resistant clones. This was true in sensitive clones that became resistant as a function of passage, suggesting that AHH loss was responsible for the acquisition of resistance to BaP toxicity.

<div align="center">B. <u>Introduction</u></div>

Studies of the relationship between drug resistance and the enzymology related to that resistance have been studied in mammalian cells in culture in many systems. Perhaps the best studied examples are those of 8-azaguanine, 6-thioguanine, and bromodeoxyuridine resistance. Kit <u>et al</u>. have shown that thymidine kinase is deleted in L cells resistant to bromodeoxyuridine (8). In haploid frog cells resistant to bromodeoxyuridine, Mezger-Freed found that an active transport function for this toxic agent was lost (9). Similarly, Van Zeeland and Simons showed that there was almost complete loss of hypoxanthine-guanine-phosphoribosyl transferase activity in variants resistant to 8-azaguanine, except that in tetraploid V79 cells 50 - 100% of the activity was retained (12).

The case of resistance to the toxicity of the carcinogen, benzo(a)pyrene (BaP), appears to be analogous to 8-azaguanine resistance, since there is an enzymological process associated with the toxicity. In a series of human, mouse, and hamster cells, Gelboin <u>et al</u>. have shown that the inducibility of aryl hydrocarbon hydroxylase (AHH), the enzyme system that metabolizes BaP, correlated with the sensitivity

of the cells to BaP-induced cytotoxicity (7). Diamond found that the

ability to metabolize BaP to alkali-soluble derivatives paralleled

sensitivity to the cytotoxicity of BaP in various primate and rodent

cell lines (5). Diamond et al. also found that 7,12 dimethylbenz(a)-

anthracene bound to nucleic acids and proteins of cells in proportion

to the amount of cytotoxicity that it exerted (4), and that normal

embryonic rodent cells were sensitive to the cytotoxic effects of

various carcinogenic hydrocarbons, whereas their transformed analogues

were not (3).

In many of the studies in the literature, it has been shown that

cell lines usually show high levels of variants resistant to BaP (3 - 7).

We have previously described the rapid acquisition of resistance to

BaP in isolated, sensitive epithelial clones derived from NMuLi on a

biological level, and now examine the molecular reasons for the

phenomenon. In particular, we ask whether the resistant variants that

arise have less AHH than the sensitive parent clones from which they

were derived.

C. Materials and Methods

1. AHH Assay

Aryl hydrocarbon hydroxylase (AHH) activity was measured fluori-

metrically as described previously by Nebert and Gelboin (10) with the

modifications of Nebert and Gielen (11). For the preparation of cell

sonicates, the procedure of Chapter I was modified by sonicating the

cells three times for 45 seconds each time at a power of 100 watts on a

model W185 Sonifier-Cell Disruptor (Heat Systems-Ultrasonics, Inc.,

Plainview, N.Y.). There was a 45 second period between each sonication

period to allow the dissipation of heat, and the sample was always

cooled to 0 degrees by a circulating water bath. Microsomes were

prepared from the crude cell sonicate first by homogenizing it with a

glass homogenizer in 50 mM Tris-HCl, pH 7.5, 0.25 M in sucrose. The

sample was then centrifuged at 600 × g for 10 minutes and then for

15 minutes at 7,000 g in a Sorvall RC2B centrifuge. Both pellets were

discarded. The final centrifugation was performed in a Beckmann/Spinco

at 75,000 × g for 90 minutes, and the pellet was resuspended in the

same solution used to suspend the crude cell sonicate.

2. Radioactive AHH Assay

A radioactive assay for benzo(a)pyrene (BaP) metabolism was

developed by a combination and modification of the fluorimetric assay

mentioned above and the radioactive that has been published (2). The

procedure was the same as the fluorimetric assay of Nebert and

Gelboin (10) and Nebert and Gielen (11), except that radioactive sub-

strate was used, and all of the extractions were aliquotted for liquid

scintillation counting. For this purpose, BaP labelled in the 7 and

10 positions with ^{14}C at a specific activity of 25 mc/mmole (Amersham-

Searle, Amersham, England) in benzene was extracted once with 1 N NaOH

and then once with water to remove impurities. The benzene was removed

with a stream of nitrogen, and cold BaP in dimethylsulfoxide was added

to give a final specific activity of 8.33 mc/mmole. Then 15 ul of this

solution (80 mM in BaP) was added to each incubation mixture.

After the incubation period (usually 30 minutes) and the extractions,

1 ml out of 2.0 ml of the hexane layer above the NaOH layer, 1 ml out

of 2.5 ml of the water-acetone layer, and 3 out of 4 ml of the NaOH

layer were aliquotted for liquid scintillation counting. Three ml of water and 12 ml of Aquasol II (New England Nuclear, Boston, Mass.) were added to the 3 ml of the NaOH layer. The 1 ml from the water-acetone layer was gelled by the addition of 12 ml of Aquasol II and 3 ml of water. Then 17 ml of Aquasol II was added to the 1 ml from the hexane layer to check for total recovery of the label. Sample volumes of from 13 to 18 ml give the same efficiency in this system.

All samples were counted in the green (C-D) channel of a Packard Tri-Carb Liquid Scintillation Spectrometer Model 3375. A standard automatic external standard (AES) vs. counting efficiency calibration curve was constructed with each experiment by the use of sealed ^{14}C toluene standards. Counting efficiencies were approximately 80% for the hexane samples and 55% for the water-acetone and NaOH samples. A few samples in each system were counted, 20 ul of a standardized ^{14}C toluene solution (636 dpm/ul) were added to them, and the samples were recounted to verify that each system counted correctly. No chemi-luminescence was noted in the NaOH or other samples when counted in the green channel (background was 32 dpm), and repeat counting of the samples 8 hours after the first count gave the same result. Blank values, in which enzyme was acetone-denatured at the beginning of the incubation, were high, around 4,000 dpm. They were kept this low in the water and NaOH layers by first removing the above hexane layers with a pipette before aliquotting.

3. Radioactive Binding Assay

For a measure of the binding of BaP metabolites to cells, the water-layer was extracted six times more than hexane, and then the water

layer was made 10% in trichloroacetic acid for 30 minutes in an ice-
bath to precipitate protein and nucleic acids. The water layer was
then filtered over a 2.4 cm glass fiber disc 934AH (Reeve Angel,
Whatman, Inc., Clifton, New Jersey) in a millipore apparatus to trap
the precipitated macromolecules. The filter was then washed five times
with 10% TCA, and the filtrates were counted in aquasol II as the
water soluble metabolites. The glass fiber disc containing the
precipitate was then transferred to a small flask and heated four times
for 10 minutes each time on a steam bath with 100% ethanol to remove
intercalated and trapped BaP. All ethanol extracts were then filtered
through another glass fiber disc and counted to insure that all
intercalated BaP had been removed. Then, both glass fiber discs were
counted in 15 ml of reagent grade toluene (Research Products Inter-
national Corporation, Elk Grove Village, Ill.) containing 2% Permafluor
(Packard Instrument Co., Downers Village Ill.). This value was desig-
nated as bound metabolites.

4. Chemicals

The 7,8 dihydrodiol of BaP, the ±7α, 8β, dihydroxy- 9β, 10β, epoxy-
7,8,9,10 tetra-hydro-BaP (diol epoxide), and the 7,8,9,10 tetra-hydro,
7,8,9,10 tetrahydroxy-BaP were all synthesized by K. Straub of this
laboratory.

D. Results

1. Clonal Killing Curves With Activated Derivatives of BaP

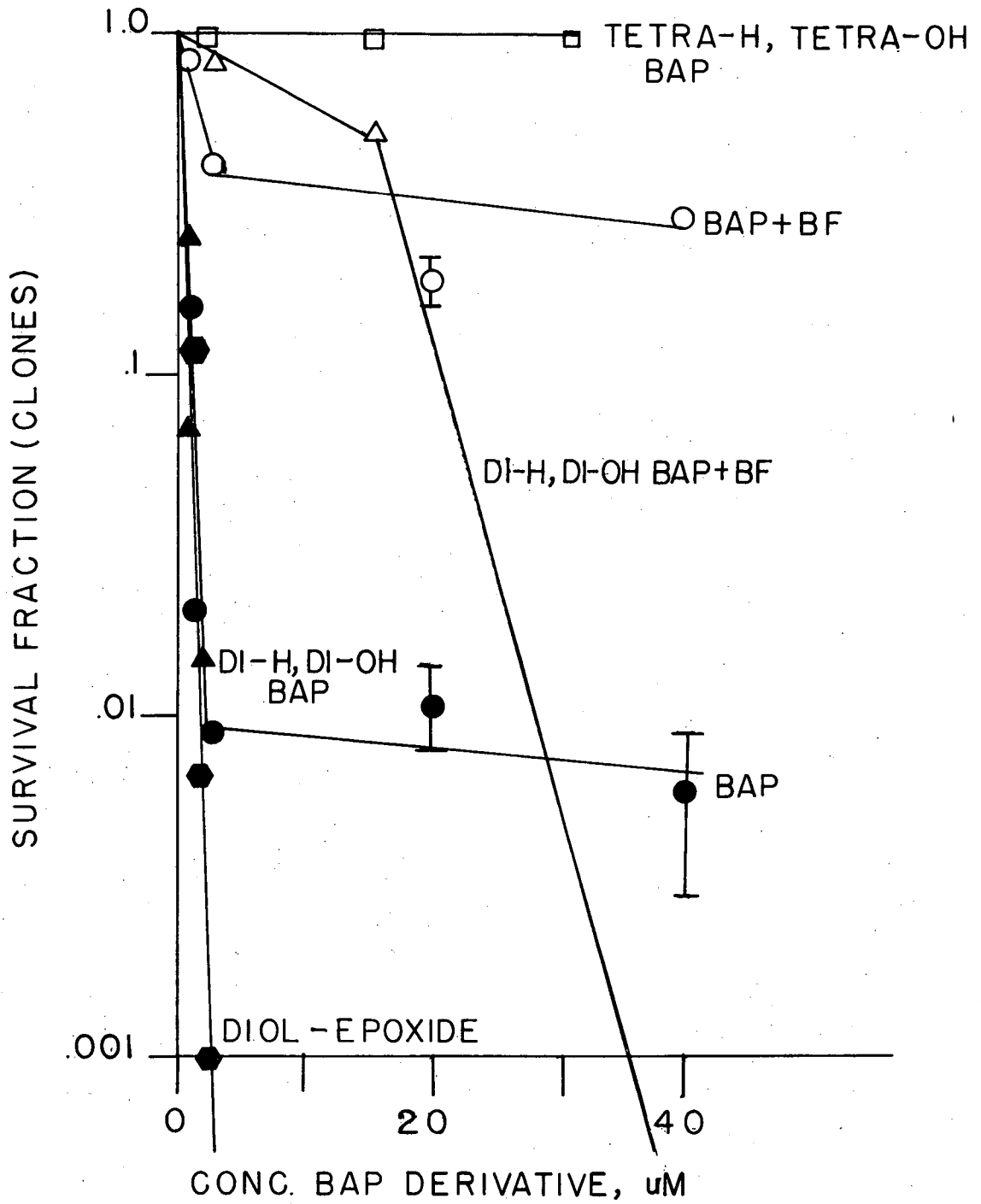The use of activated derivatives of BaP, such as the 7,8 dihydro-
diol of BaP and the ±7α, 8β, dihydroxy-9β, 10β epoxy- 7,8,9,10 tetra-
hydro-BaP (which does not require enzymic activation to a proximate

form) generated colony killing curves which were exponential and showed no plateau values at high concentrations of the toxic agent in an early passage sensitive clone (clone 8) derived from NMuLi (Chart 1). This occurred even though this clone possessed large numbers of cells resistant to the toxicity of BaP, and suggested that the block in the toxicity might be due to a loss in the initial hydroxylation of BaP to the 7,8 dihydrodiol. An inhibitor of AHH, 7,8 benzoflavone (BF), shut off the toxicity of BaP to a large extent and also largely mitigated the toxicity of the 7,8 dihydrodiol in this clone (Chart 1). The 7,8,9,10 tetra-hydro, tetra-hydroxy-BaP which would be generated in cells by the action of epoxide hydrase or by spontaneous attack of water on the diol-epoxide, was not toxic to this clone.

In the most resistant clone that we were able to isolate from untreated NMuLi, the diol-epoxide was as toxic as it was to the sensitive clone, and it appeared that there was a biphasic curve, suggesting heterogeneity in this clone. BaP was slightly toxic to this clone. In a second experiment, exactly the same trends were shown for the sensitive clone (data not shown), and it was found that BF shut off the slight toxicity that BaP exerted on the resistant clone (Chart 3). In addition, BF did not affect the toxicity of the 7,8 dihydrodiol to this resistant clone. Further, the killing of the sensitive clone by the dihydrodiol in the presence of BF resembled the killing curve for the resistant curve by the dihydrodiol (Charts 1 and 2). This suggested that this resistant clone has lost an enzyme activity that is BF-sensitive and capable of efficiently activating the dihydrodiol to the diol-epoxide.
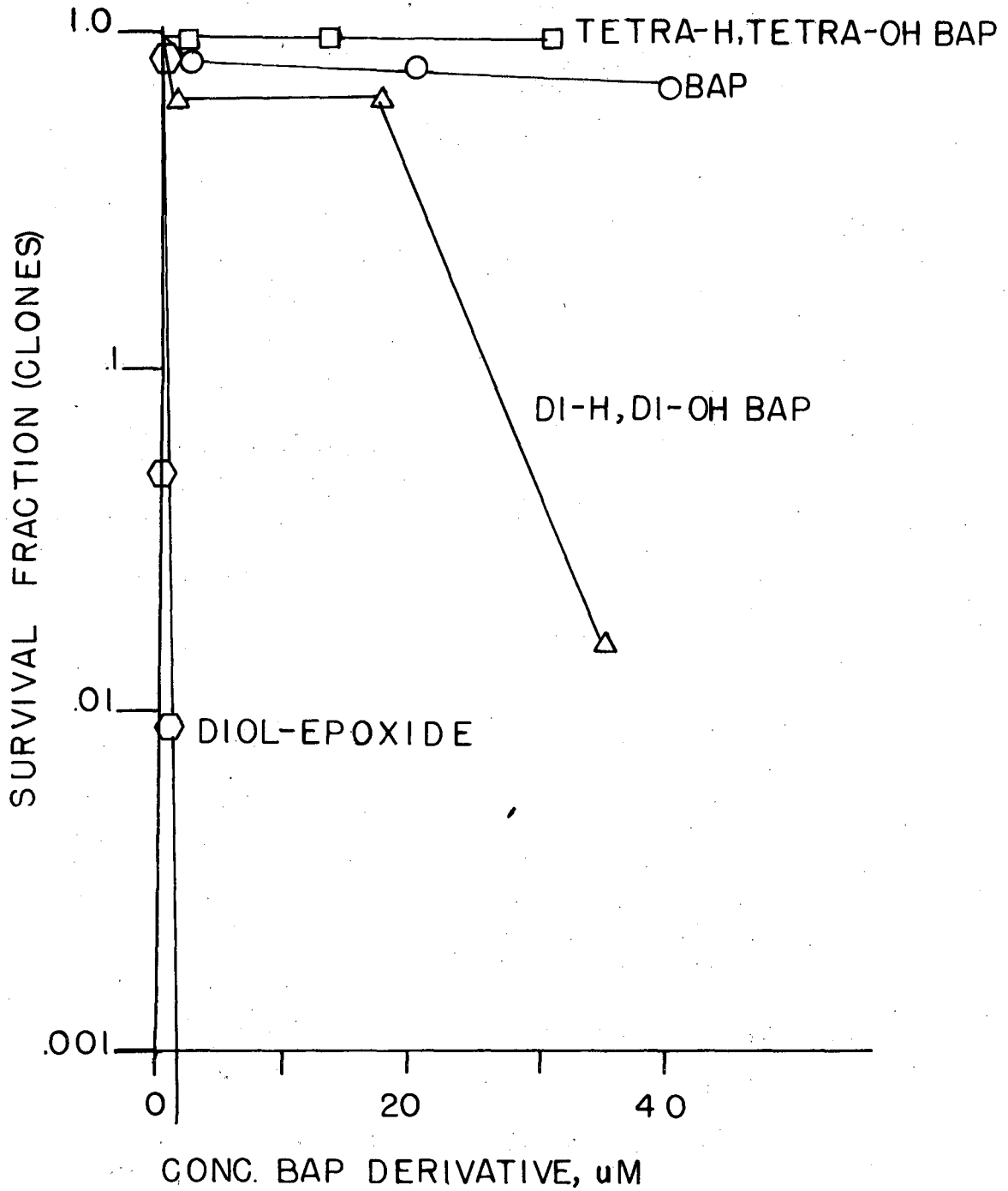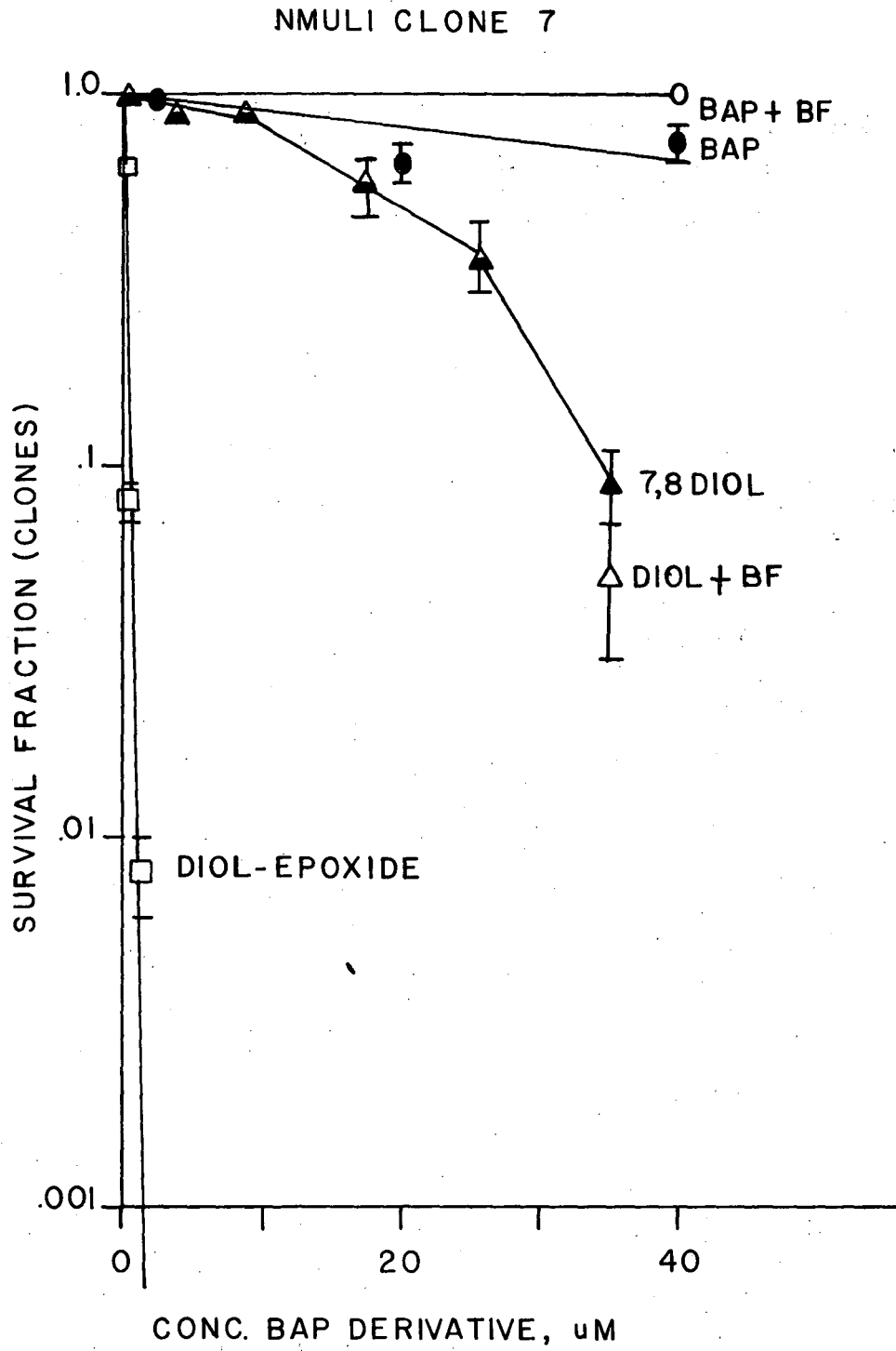
CLONE 8

CONC. BAP DERIVATIVE, uM

XBL 768-9516

Chart   1

00 0 4 6 0 1 8 8 4

CLONE 7

XBL 768 - 9513

Chart   2

NMULI CLONE 7

CONC. BAP DERIVATIVE, uM

XBL 768 − 9514

Chart   3

It was found that the first and second experiments on the toxicity of these derivatives to the sensitive clone could not be averaged and replotted as a single figure, since the frequency of variants resistant both to BaP and to the dihydrodiol increased as a function of passage (Chart 4).

The step-wise toxicity obtained with the activated derivatives of BaP in this system led us to believe that it had some relevance to the in vivo hydroxylation and toxicity of BaP to cells. They also suggested that it was a loss of a specific hydroxylase that could hydroxylate the dihydrodiol to the diol-epoxide that was responsible for the resistance to the toxicity. Consequently, we began to examine the levels of the hydroxylase in the cells.
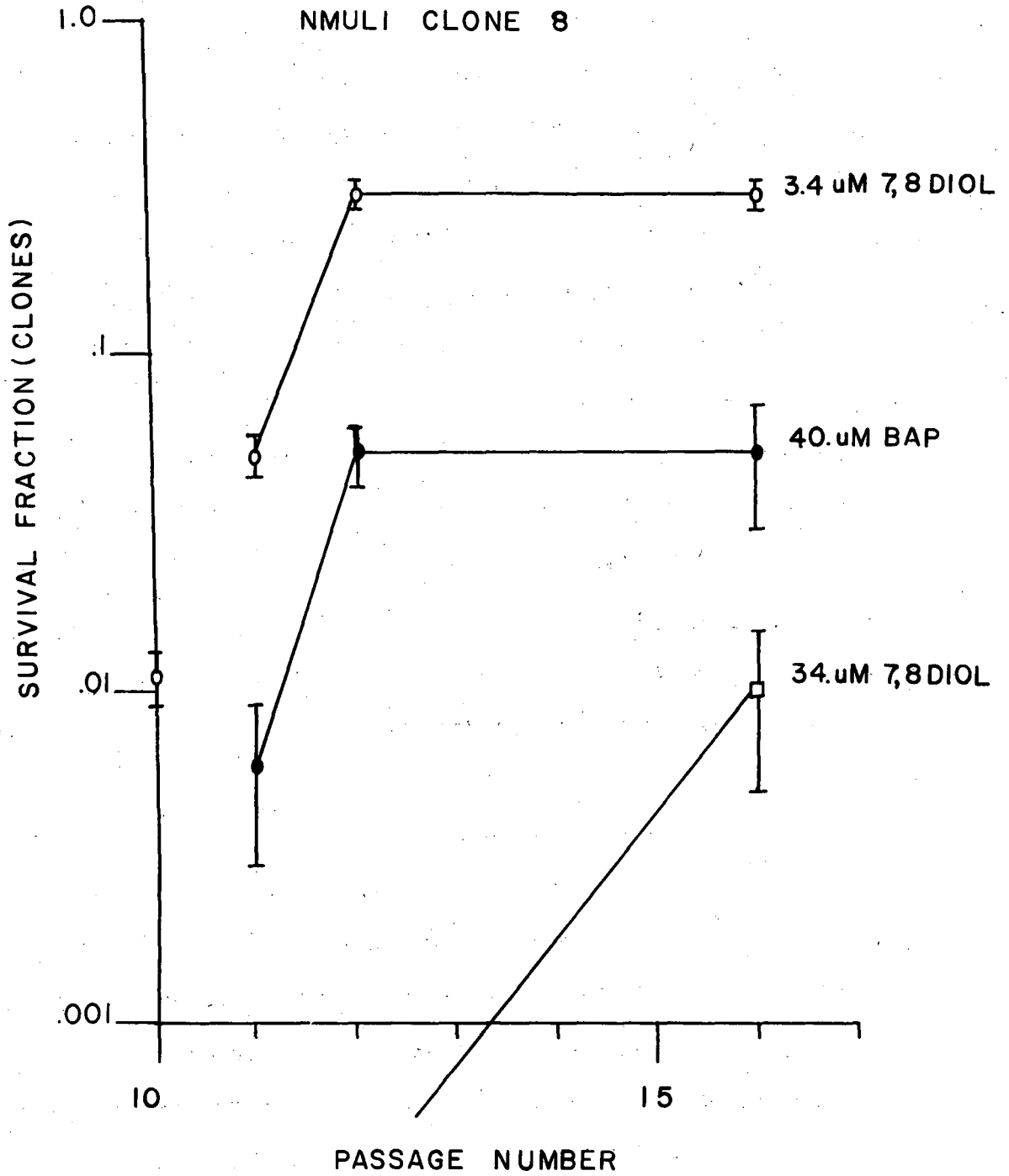
2. Characterization and Fractionation of AHH From Confluent NMuLi

In two separate experiments, AHH activity from whole cell preparations was not significantly altered by the sonication procedure (Table 1).

An attempt to fractionate the cells and concentrate the AHH by spinning out the mitochondria did not yield good results (Table II). Much of the activity spun out with the mitochondria, presumably due to inefficient sonication. Since the activities of this system are so low, and since sonication did not accomplish an increase in activity, it was decided to use whole cell suspensions in the following experiments.

The effect of carbon monoxide in inhibiting the enzyme activity from the microsomal pellet is shown below (Table III). Rat liver microsomes were run as a control to insure that the carbon monoxide inhibition was functioning.

Carbon monoxide inhibits the hydroxylation reaction in NMuLi

NMULI CLONE 8

SURVIVAL FRACTION (CLONES)

1.0

.1

.01

.001

3.4 uM 7,8 DIOL

40. uM BAP

34. uM 7,8 DIOL

10

15

PASSAGE NUMBER

XBL 768 − 9515

Chart 4

Table I. Effect of Sonication on the AHH Activity From Confluent NMuLi[*]

	AHH Activity	pmoles 3-hydroxy-BaP/ mg protein-30 minutes
	Experiment I	Experiment II
100 ul of cell suspension	81 ± 3	118 ± 1
100 ul of cell sonicate	72 ± 6	122 ± 1
Net increase after sonication	-11%	+3%
100 ul of cell sonicate, minus assay cocktail	21 ± 5 (26%)	47 ± 1 (40%)

*Cells were processed for AHH assay on day 4 post-seeding into roller bottles after an 11 hr incubation with 1 ug/ml of BaP.

Table II.   Attempts to Fractionate AHH Activity from NMuLi Cells

Fraction	AHH Activity*	AHH Specific Activity pmoles 3-OH-BaP/mg protein-30 min.
Crude Cell Homogenate	117	107
10,000 g Mitrochondrial Pellet	60	199
10,000 g Supernatant	83	137

*Each fraction was resuspended in equal volumes, so the values represent relative recovery yields.

Table III. Effect of Carbon Monoxide in Inhibiting AHH From

Microsomes Prepared From Confluent NMULI**

	Specific Activity of AHH, pmoles of 3-hydroxy-BaP/mg protein-30 minutes	% of complete
a. Microsomes from NMuLi		
Complete	167	
+ 15 minutes of CO	36	22
+ 15 minutes of N_2	145	87
+ 40 ug/ml of BF	12	7
b. Microsomes From Rat Liver		
Complete	12,100	
+ 15 minutes of CO	5,560	47
+ 15 minutes of N_2	10,600	87
+ 4.0 ug/ml of BF	4,000	33

**This experiment was performed in conjunction with Dr. Joseph Becker.

microsomes by 78%, and control, bubbling with N_2, only causes a 13%

inhibition. This specific inhibition implies that the enzyme activity

is associated with cytochrome P450. In the same experiment, 40 ug/ml

of 7,8 benzoflavone inhibited the enzyme activity by 93%. Note that

the specific activity of induced NMuLi microsomal AHH is roughly

100 times less than that from the analogous rat liver microsomal

preparation.

3. <u>Differential Inducibility of AHH in Growing vs. Resting Cells</u>

In conjunction with Drs. J. Becker and H. Gamper of this labora-

tory, the time course of induction of AHH in NMuLi was studied. A

typical experiment is shown in Chart 5, and a repeat experiment gave

qualitatively the same results. An average of the two experiments

indicated that the time required for maximal induction of AHH in both

growing and confluent NMuLi was essentially the same, 12 hours.

I used these conditions to determine if there was a differential

inducibility of AHH in growing vs. resting cells. This experiment was

repeated five times due to the variability among determinations. The

results (Table II of Chapter I and a typical experiment, Chart 6)

indicate that the inducibility of AHH is roughly 2 to 3 times higher in

growing vs. resting cells. Since resting cells have more protein than

growing cells, the pmoles of 3-hydroxy-BaP/30 min. -cell was roughly

1.7 times higher in growing cells. In all five experiments performed,

the high levels of AHH in growing cells decreased to almost basal

levels as the cells reached confluence, but then increased, peaked, and

decreased again. More frequent media changing did not alter the

qualitative shapes of these curves. Adding BaP for a three day period

a)

b) DAY (2)   c) DAY (6)

HOURS OF INDUCTION
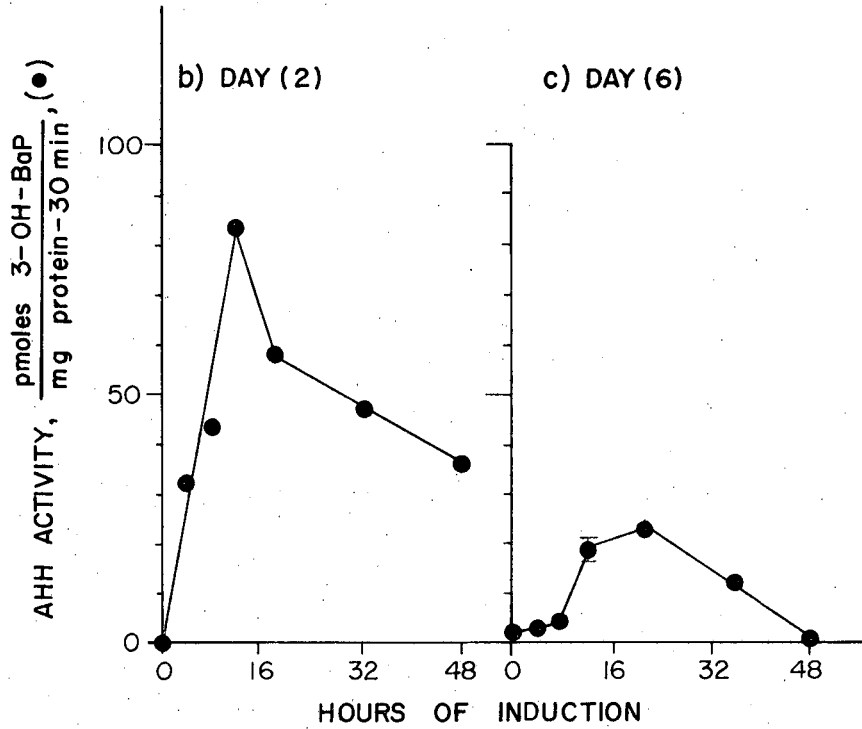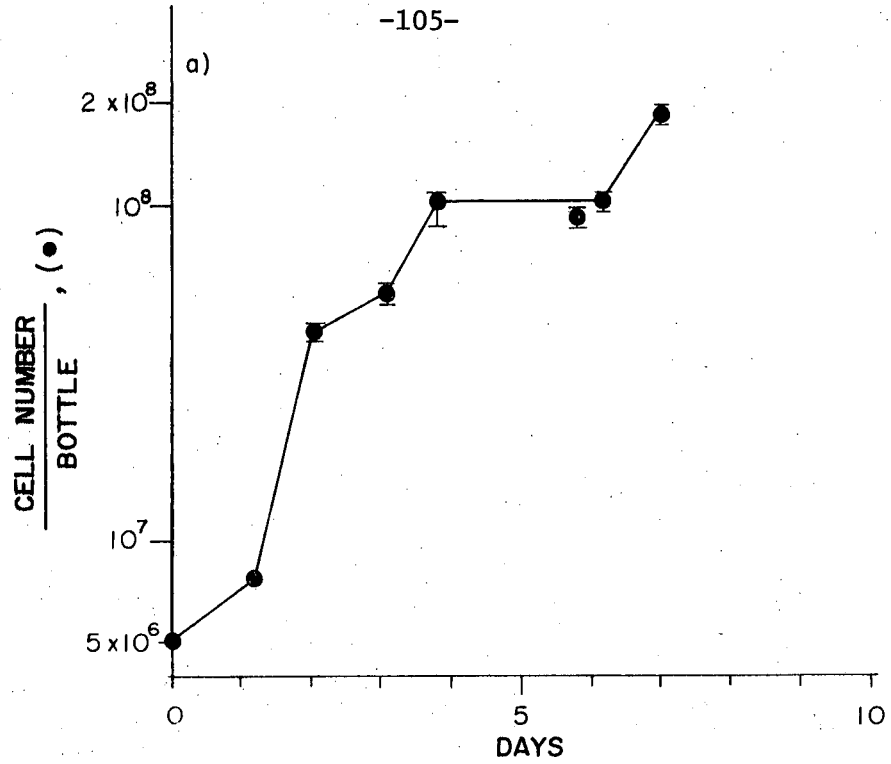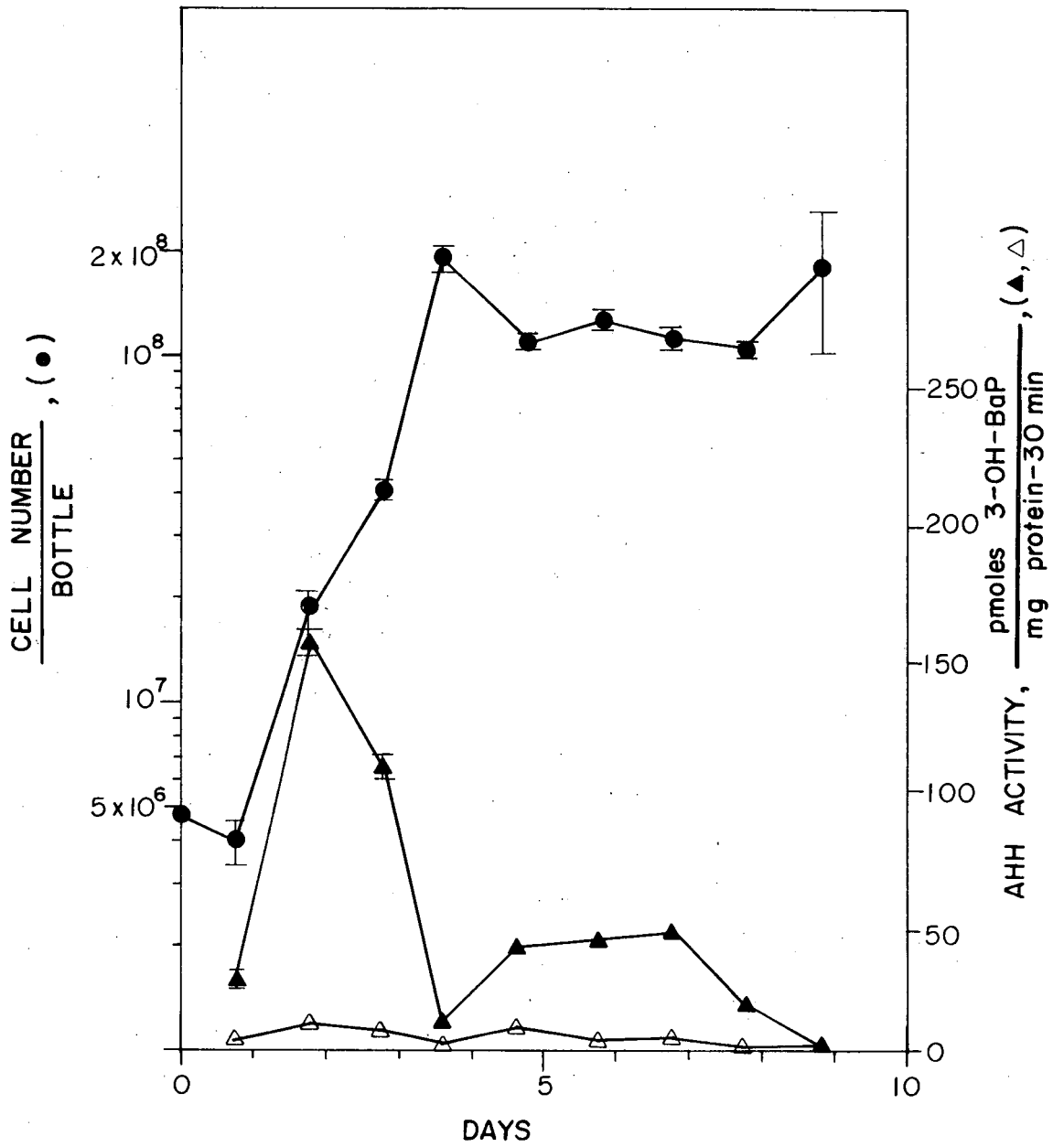
XBL 767-6019

Chart   5

Chart 6

during log phase and again for a three-day period during confluence gave a similar induction curve (Chart 7), so the curves reflect a physiological ability of the cells to induce and are not limited by BaP exposure times. Further, the ratio of the integrated AHH during the log phase exposure to that in the confluent exposure was 3.1, roughly the same as in the growth curve inducibility experiments (Chart 6).

The inhibition of AHH by 4 ug/ml of BF was essentially the same in growing and confluent cells, indicating that it was the same enzyme(s) that was induced in both situations (Table IV). Hence, it was decided to use a 12 hour induction with 1.0 ug/ml of BaP on day 1.8 post-seeding for induction of AHH in clones derived from NMuLi.

4. Development of a Radioactive Assay For AHH and Water-Soluble Metabolites of BaP With Rat Liver Microsomes

To develop a good assay, we decided to use the high AHH activity associated with rat liver microsomes. This would allow kinetic assessments of the levels of water-soluble metabolites vs. NaOH extractables to be made accurately. In the activity vs. protein plot, it is seen that the fluorescent products of reaction extracted into the NaOH layer, which are mono-hydroxy-BaP derivatives, correlate well with the radioactive products in the NaOH layer. Above 20 ug of protein, the hydroxylated metabolites of BaP show an apparent decrease in the rate of production. This is correlated with the appearance of the ^{14}C label in the water acetone layer, presumably due to the conjugation of BaP-epoxides to gluthathione, cysteine, protein, and nucleic acid conjugates. The water-acetone soluble products account for an
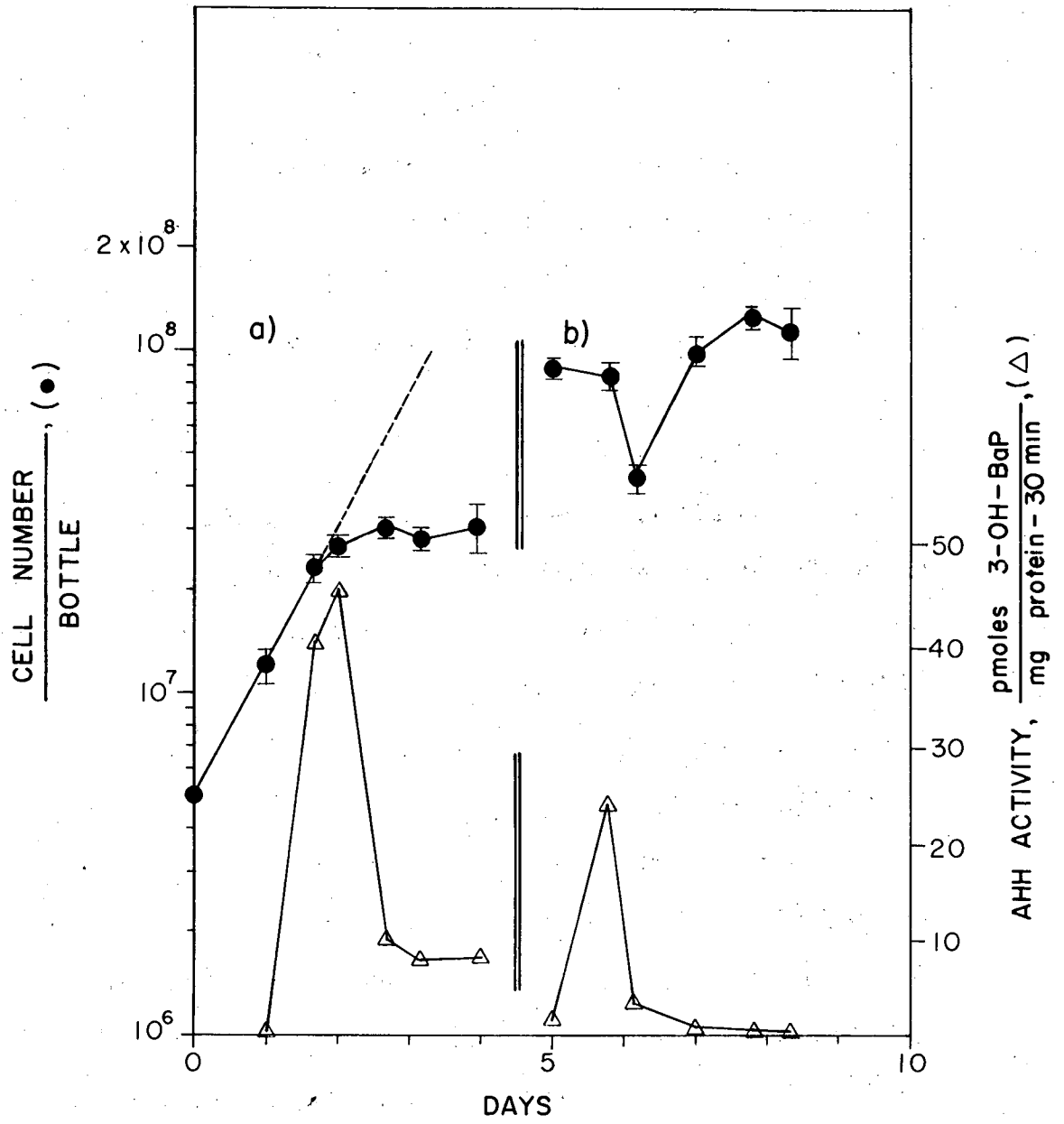
Chart   7

XBL 767-6016

Table IV. The Inhibition of AHH by 7,8 Benzoflavone in Growing and in Confluent NMuLi Cell Sonicates*

	AHH Activity, pmoles 3-hydroxy-BaP/mg protein- 30 minutes Growing Cells (Day 2)	Confluent Cells (Day 4)
Complete assay	87 ± 10	23 ± 2
Complete + 4 ug/ml BF	40 ± 5	7 ± 0.5
% Inhibition by BF	52 ± 6	69 ± 2

*1.24 mg of cellular protein was used in the growing cell assay and 0.67 mg was used in the confluent cells assay.

appreciable portion of the total metabolites (Chart 8).

Another experiment was conducted in which the protein was held constant at 10 ug per flask, and the time of incubation was varied. Again, the water soluble metabolites constitute a major fraction of the metabolites at longer times (Chart 9). This indicates that the production of water solubles is not an artifact due to high protein concentrations, but is presumably due to the action of such conjugating enzymes as epoxide hydrase and glutathione-S-epoxide transferase. The addition of BF to the assay inhibits water soluble products by 62% and the fluroescent hydroxylated products by 50%, indicating that the two product types are mechanistically linked. The plateau value in the activity vs. time plot could be due to endogenous peroxidation of microsomal lipids by the microsomes themselves. It is likely not due to cofactor limitations, since there is available 390 nmoles of NADH and 360 nmoles of NADPH, and metabolism of 4 nmoles of BaP was the highest value reached in the time plot. In addition, higher levels of metabolites were found in the AHH vs. protein plot, with no plateau effect.

In both time and protein plots, the production of water soluble metabolites lagged behind the production of NaOH extractable products. There are at least three possibilities for this. Firstly, amounts of such conjugating enzymes as glutathione-S-epoxide transferase could be in small amounts. Secondly, their K_m values could be large relative to those of the hydroxylase. Thirdly, they could be located on the outside of the microsomal membrane, and the primary products, such as phenols and epoxides, might have to diffuse out of the membrane to be conjugated.
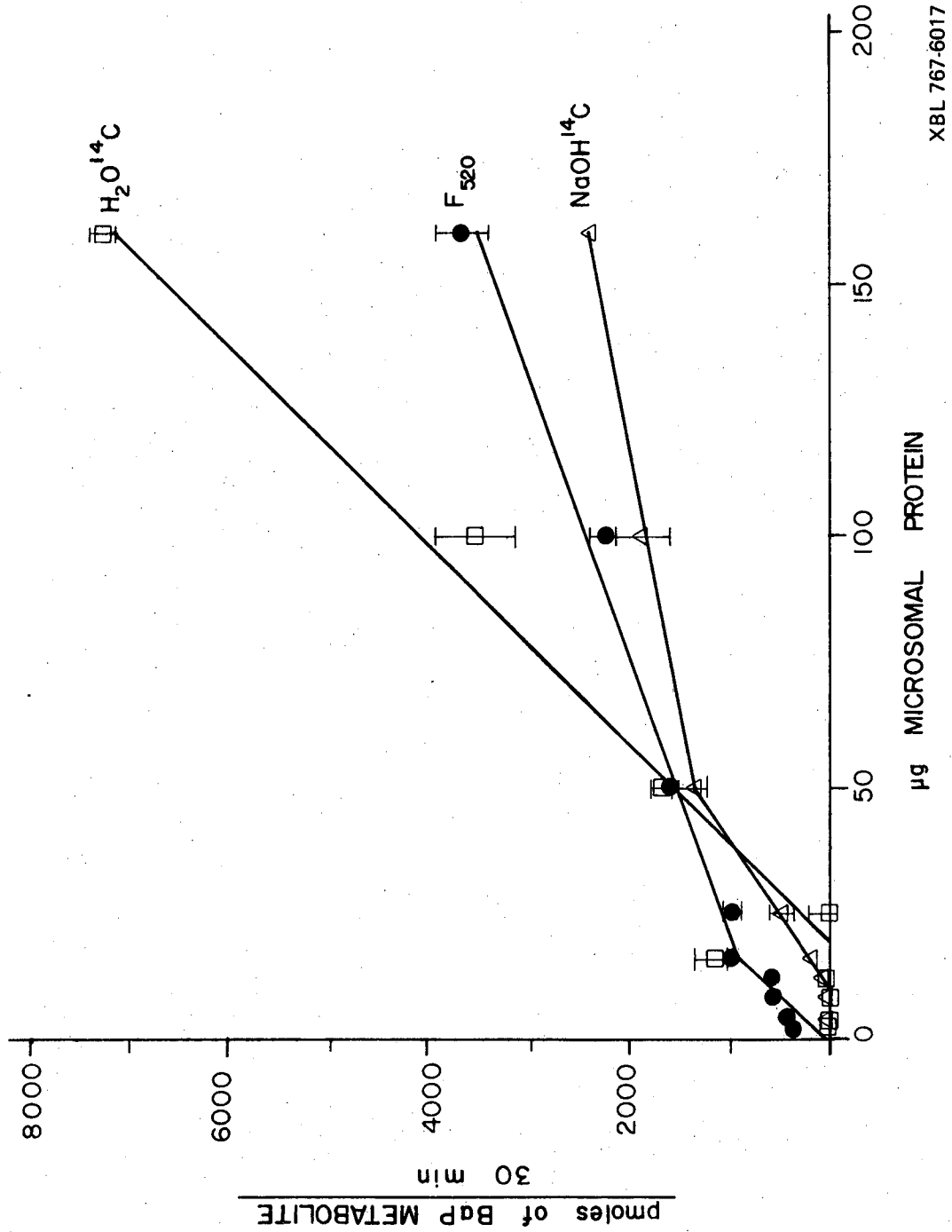
Chart 8

XBL 767-6017

Chart   9
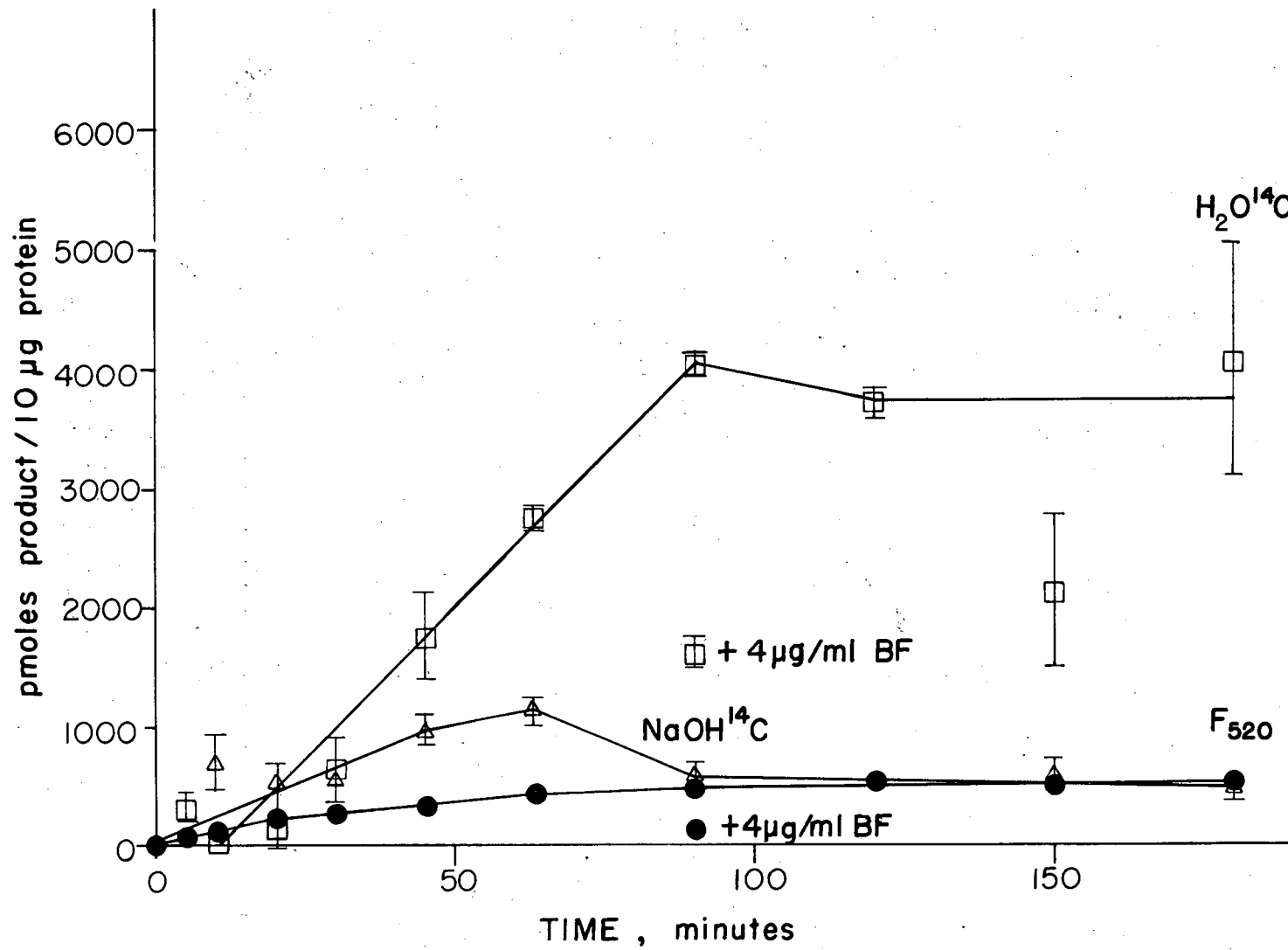
XBL 767-6018

The efficiency of extraction of the fluorescent products with hexane into the NaOH layer was 87% on the first extraction, 11% on the second, and 3% on the third. Hence, a measure of the first extraction of the fluorescent products (the classical AHH assay) should give a reasonable prediction of the metabolizing capability of the cells.

5. Attempts to Develop the Radioactive Assay with NMuLi: Substrate Carry-over During Induction

During the course of working with AHH from induced NMuLi cell sonicates, it was discovered that no-substrate blanks yielded appreciable AHH activity, indicating the presence of unmetabolized BaP from the induction period. Consequently, an experiment was performed to see whether exogenous radioactive substrate could compete with the endogenous BaP left over from the induction period. This was accomplished by inducing NMuLi cells with radioactive substrate and running the assay with unlabelled substrate, and vice versa.

A comparison of Tables V A and B shows that induction of the cells with cold (unlabelled) BaP does not interfere with the radioactive assay. Although use of radioactive BaP in the induction followed by an assay shows that left-over BaP will be used as substrate in the assay, this amount is small. In addition, cold BaP used in the assay will compete effectively with hot BaP left-over from the induction period. Hence, it can be concluded that unmetabolized, unlabelled BaP will not seriously interfere with the radioactive assay, and that equilibration of exogenous BaP with bound, leftover induction BaP is relatively fast.

The water-acetone layers from this assay were also counted, and the

results are presented in Tables VI A and B.

The cold induction does not cause a decrease in the amount of BaP metabolized to water soluble products. In addition, it appears that substantial amounts of BaP are bound to the cells in the form of water soluble products as a result of the hot induction. These are most likely covalent adducts of BaP with proteins and nucleic acids of the cell. Hence, we concluded that there was no problem associated with remaining induction BaP interfering with the radioactive for AHH and water-soluble metabolites.

6. Results of the Radioactive Assay Attempts on NMuLI Cells

Further experiments were attempted counting the ^{14}C label in the NaOH layers with NMuLi cells metabolizing BaP, but they were unsuccessful. With 2 mg of cell protein in a time course assay and with up to 4 mg of protein in the 30 minute incubation, the counts in the NaOH extraction were entirely random, and the background was too high. It was concluded that the activity was too low against a high background, and further attempts along this line were abandoned. Since the fluroescent assay with rat liver microsomes showed that the fluorescent assay and the radioactive assay provided essentially the same levels for alkali-extractable metabolites, this fluorescent assay was adopted for screening alkali-extractable metabolites.

Due to this failure with the alkali-extractable metabolites, the procedure was modified for the water-acetone metabolites as per materials and methods. In the activity vs. protein plot, it is seen that the levels of water soluble metabolites is less than that of the alkali extractables, and again there is a lag in their production (Chart 10),

Table V.   NaOH Extractions, Radioactive Assay

A.   Results From the Cold Induction, Hot BaP Assay Study*

Sample	Counts in NaOH Layer	Pmoles of 3-OH BaP, Fluorescence
Acetone at end, cold BaP at end of assay	0	5 ± 1
Acetone at start, cold BaP at start of assay	0	25 ± 3
Cold BaP in the entire assay	0	248 ± 4
Hot BaP in the entire assay	146,000 ± 4,000	331 ± 10

B.   Results From the Hot Induction, Cold BaP Assay*

Sample	Counts in NaOH Layer	Pmoles of 3-OH BaP, Fluroescence
Acetone at end, cold BaP at end of assay	9,000 ± 5,000	9 ± 4
Acetone at start, cold BaP at start of assay	2,600 ± 800	27 ± 2
Cold BaP in the Assay	2,200 ± 400	272 ± 2
Hot BaP in the Assay	111,000 ± 6,000	372 ± 2

*Each assay flask contained 0.30 mg of intact cells, harvested on day 3 post-plating. The usual 11 hr. induction with 1.0 ug/ml of BaP was used. Whole cells were used in the assay, not sonicates.
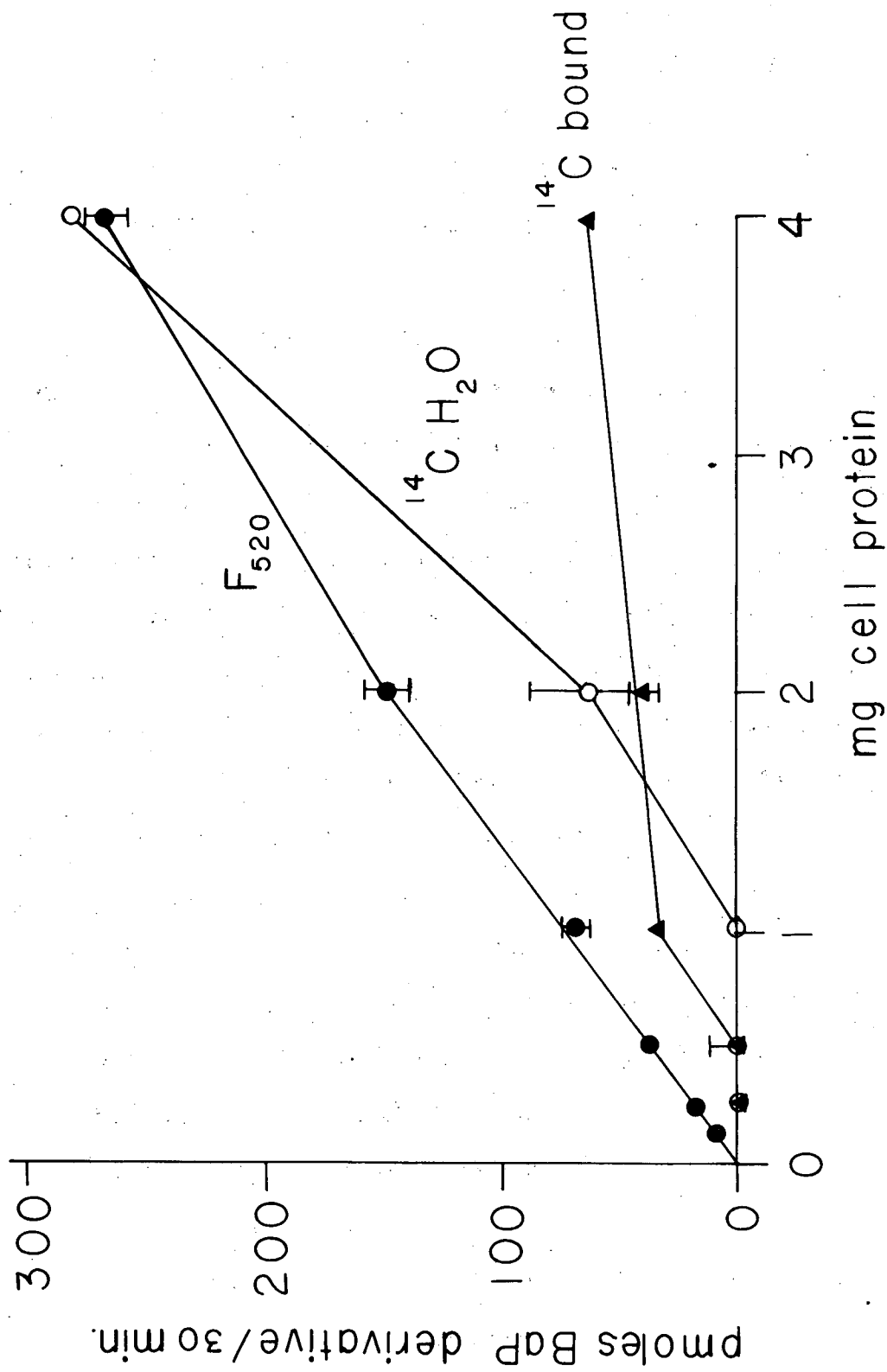
Chart 10
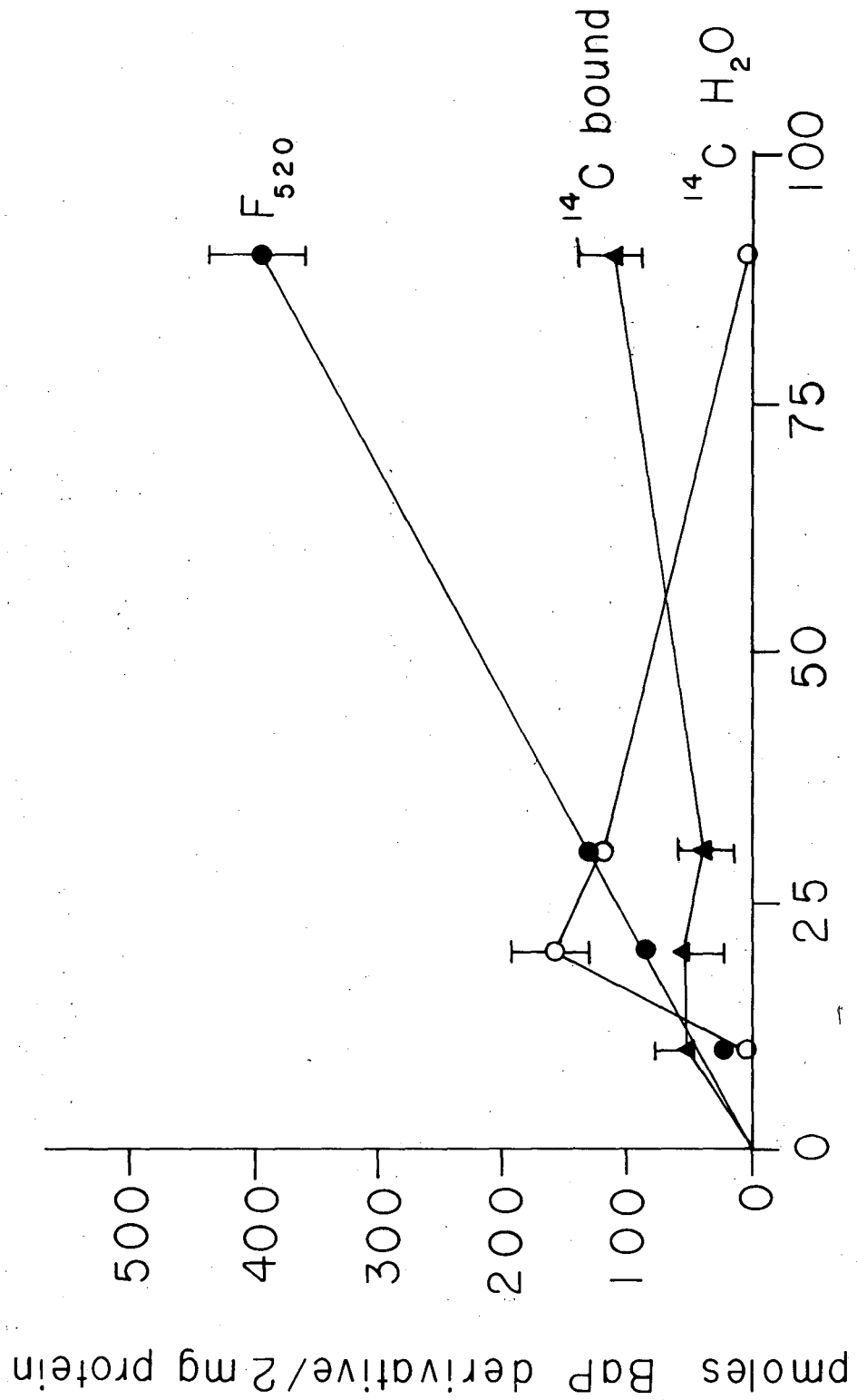
XBL 768-9526

as there was in the rat liver microsomal incubation system. In the
activity vs. time plot, there was again a lag in the production water-
acetone soluble metabolites, although for some reason these metabolites
decreased at longer times (Chart 11). This experiment will be repeated
at some future time.

A filter-binding assay (materials and methods) was used to assess
the amounts of BaP metabolites bound to TCA-precipitable cellular
macromolecules. In the activity vs. protein plot, there appears to be
a lag in the binding, and then the binding increases and then plateaus
(Chart 10). In the activity vs. time plot, the activity increases and
then slows its rate of increase (Chart 11). The activities in both these
plots were very low (around 600 counts over background), and plans are
in progress to use three-day incubations with cells on plates to measure
the binding and water-soluble metabolites.

Since the binding profile and the water-soluble metabolism seemed
to follow roughly the production of fluorescent metabolites, we decided
to use the flourescent assay as a rough measure of BaP binding capability
of the cells for cytotoxicity correlations.

7. Levels of AHH in Sensitive and Resistant Clones Derived from NMuLi

Using a 12 hour induction with 1 ug/ml of BaP and processing the
cells on day two post plating, we measured the AHH levels by the
fluorescent assay in clones 9 and 19 at early and late passages and in
resistant clone 7 and sensitive clone 8. Unfortunately, even at
passages two and three, the populations derived from clones 9 and 19
possessed roughly one half resistant variants (Table VI). In clone
19, both the basal and induced levels of AHH decreased by about two and

F_520

$^{14}C\,H_2O$

^{14}C bound

mg cell protein

pmoles BaP derivative/30 min

XBL 768 – 9524

Chart 11

Table VI. Radioactive AHH Assay: Metabolites in the Water Layers

A. Results from the Cold Induction, Hot BaP Assay

Sample	^{14}C dpm in Water-Acetone Layer
Acetone at end, cold BaP at start of Assay	0
Acetone at start, cold BaP at start of Assay	0
Cold BaP in the Assay	0
Hot BaP in the Assay	73,000 ± 8,000

B. Results from the Hot Induction, Cold BaP Assay Study

Sample	^{14}C in Water-Acetone Layer
Acetone at end, cold BaP at end	42,000 ± 900
Acetone at start, cold BaP at start	44,000 ± 1,000
Cold BaP in the Assay	43,000 ± 900
Hot BaP in the Assay	103,000 ± 3,000

Table VII. AHH Levels in Sensitive and Resistant Clones of NMuLi*

$$\text{AHH, pmoles} \times 10^{-6}/\text{cell}$$
$$-30 \text{ minutes}$$

Clone #	AHH, pmoles/ mg-30 minutes	Complete	+ 4 ug/ml BF	% Inhibition	Survival Fraction**
7, uninduced	2.6 ± 0.2	1.3 ± 0.1	N. D.***	---	
induced	35.4 ± 0.2	18.0 ± 2	11 ± 2	39 ± 9	0.8 ± 0.1
8, uninduced	12 ± 2	10.0 ± 1	N. D.	---	
induced	434 ± 4	337.0 ± 20	114 ± 11	71 ± 2	0.009 ± 0.007
9, passage two,					
uninduced	11.5 ± 0.3	2.9 ± 0.3	0.7 ± 0.1	76 ± 5	
induced	44.0 ± 0.5	32.0 ± 4	5.0 ± 1.0	85 ± 3	0.40 ± 0.05
9, passage thirteen					
uninduced	32 ± 6	7.0 ± 2	N. D.	---	
induced	114 ± 20	44.0 ± 8	10.0 ± 2.0	76 ± 3	0.9 ± 0.1
19, passage three					
uninduced	4.2 ± 0.2	3.8 ± 0.2	0.9 ± 0.1	72 ± 2	
induced	65.0 ± 15	21.0 ± 5	3.5 ± 1.0	84 ± 4	0.66 ± 0.03

Table VII (continued)

$$\text{AHH, pmoles} \times 10^{-6}/\text{cell}$$
-30 minutes

Clone #	AHH, pmoles/ mg-30 minutes	Complete	+ 4 ug/ml BF	% Inhibition	Survival Fraction**
19, passage eleven,					
uninduced	1.8 ± 0.6	0.4 ± 0.2	N. D.	---	
induced	21.0 ± 1	6.0 ± 1	0.6 ± 0.2	90 ± 10	1.0 ± 0.1

*All enzyme assays were performed in roller bottles seeded with 5 10^6 cells. Induction was with 1.0 ug/ml of BaP for 12 hours, just before the cells were processed on day two post-seeding for AHH.

**The survival fraction was performed upon two hundred cells treated with 10 ug/ml of BaP for 9 days after one day of recovery post-seeding.

***N. D. means not determined.

three-fold, respectively, as the cells became more resistant. For clone

9, the basal and induced levels of AHH actually increased by about three-

fold. Metabolism to water-soluble products in this clone might have

increased, and this study is under progress.

Clone 8, a very stably sensitive clone, possessed an induced AHH

level that was four times higher than the AHH level in any resistant

clone. Clone 7, which was resistant over many passages, possessed

the lowest basal and next to lowest induced AHH level among all clones

studied to date. Except for clone 7, the induced AHH levels among all

clones studied was inhibited at least 70% in vitro by 4 ug/ml of BF.

In clones 9 and 19 at early passages, the basal levels of AHH was

inhibited 70% by this concentration of BF as well.

Using the expression derived for the survival fraction of cells

treated with BaP that was derived from Chapter I, $\ln(N/N_c) = A + ct$

$+ B + ct$, and ignoring the second two terms because the death of

resistant clones is slow, a plot of the survival fraction vs. c, the

concentration of BaP, should be linear if the growth rates and time

of exposure of the various clones are roughly the same. In fact, the

term c should represent the BaP that is metabolized to toxic inter-

mediates, and can be replaced by the induced AHH levels of the cells.

Since the induction of AHH is a triangular function (Charts 6 and 7),

the area under the curves will be proportional to the highest induced

level of AHH, and little error will be made if that value is used

instead of the area. The data from Table VI was plotted in this

fashion, and a rough correlation of leels of AHH was shown with the

survival fraction (Chart 12). More data is needed with subclones

AHH, pmoles/mg protein-30 min.

XBL 768-9525

Chart   12
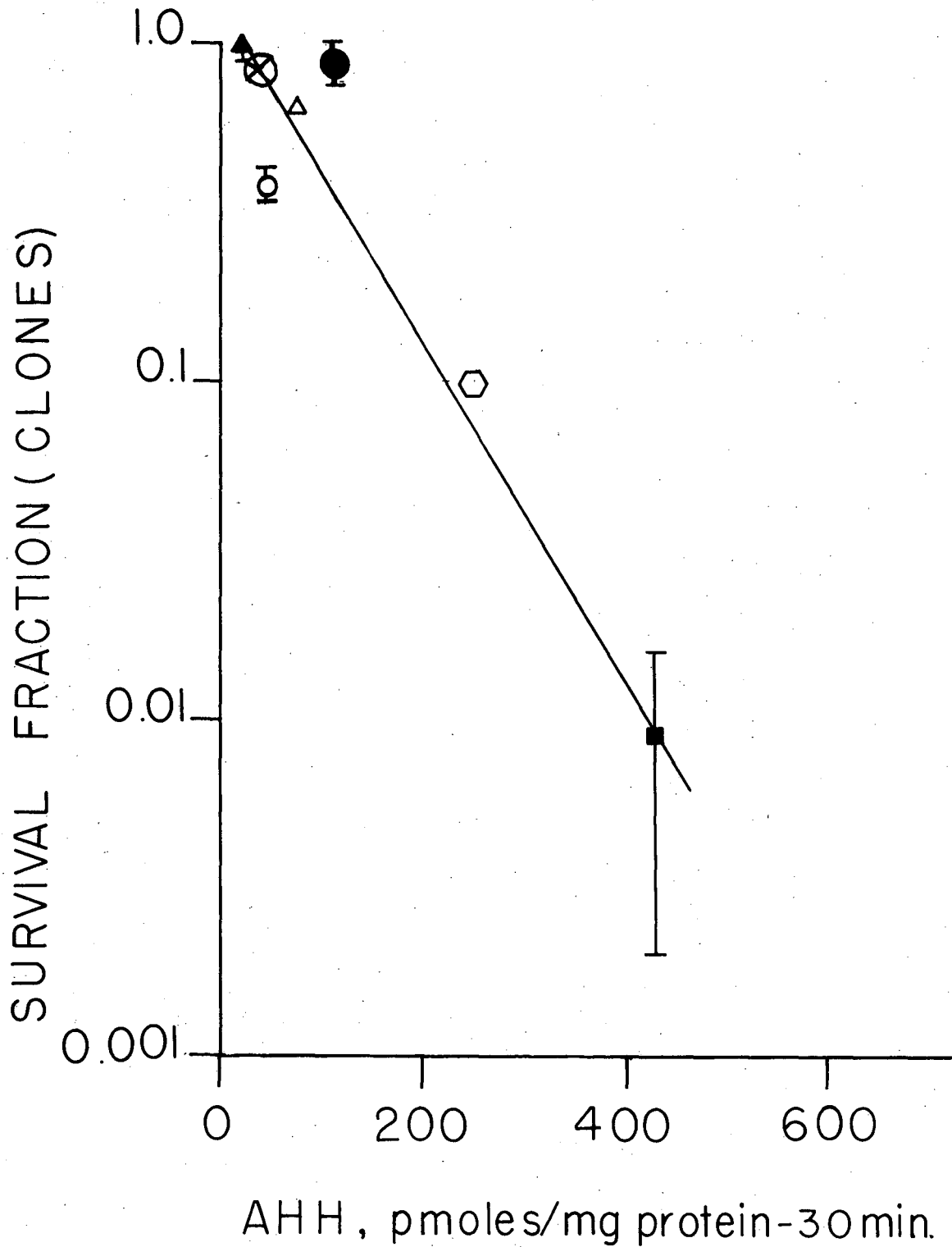
derived from a single clone, and this is in progress.

E. Discussion

Induced AHH levels in NMuLi and the most stably sensitive clone derived from NMuLi were relatively high. In a stably resistant clone and in two sensitive clones that went resistant at later passages, induced AHH levels were much less. In one of the sensitive clones that went resistant, both basal and inducible levels of AHH increased, while in the other clone basal and inducible decreased. It might be that in the former clone levels of conjugating enzymes, such as glutathione transferase, were elevated at later passages. It might also be that a certain level of induced AHH is necessary above the levels of detoxifying, conjugating enzymes before toxicity can occur. This is being investigated with subclones from a sensitive clone. Support for this is that plotting the maximum inducible AHH levels vs. the survival fraction led to a good exponential plot, suggesting that AHH levels were a major contributor to the toxicity of BaP to these cells.

In the most stably sensitive clone derived from NMuLi, variants resistant to BaP were not resistant to the 7,8-dihydro-7,8-dihydroxy-BaP (dihydrodiol). Hence, it appeared here that resistant variants generated from this sensitive clone had lost an enzyme activity that could metabolize BaP to the dihydrodiol. This enzyme activity must be BF-inhibitable, since killing by the dihydrodiol was mitigated by BF.

In another clone that was spontaneously resistant upon isolation, the killing curve with the dihydrodiol appeared qualitatively similar to the killing of the sensitive clone with the dihydrodiol in the

presence of BF, and the killing of the resistant clone was not mitigated by BF. Hence, it appeared than an enzyme was lost in this resistant clone that could efficiently epoxidate the dihydrodiol to the diol-epoxide in the sensitive clone.

On the basis of these data, we postulate that there are at least two enzymes in these cells, enzyme A that hydroxylates BaP the 7,8-epoxide of BaP, and enzyme B that hydroxylates the 7,8-dihydrodiol of BaP to the diol-epoxide. If isolated, only the former enzyme should be BF-inhibitable. The second enzyme, however, is also able to hydroxylate the dihydrodiol to the diol-epoxide, since there is some killing of the resistant clone with the dihydrodiol, although at higher concentrations than in the sensitive clone. Hence, the K_m of the second enzyme for the dihydrodiol should be greater than the K_m of the first enzyme. We further postulate that if one finds or synthesizes an inhibitor for the enzyme B, then he can successfully shut off the production of the mutagenic and toxic diol-epoxide of BaP and hence inhibit toxicity, mutagenicity, and tumor porduction by BaP. Such a goal is not unrealistic.

Of course, some of these hypotheses will be complicated by the fact that there are many toxic metabolites of BaP other than the ones just considered, and also by the possibility that in the resistant clone there might be a mutation in the enzymes from the sensitive clone. This latter possibility can be assessed by performing the thermal denaturation profiles of the enzymes that hydroxylate the dihydrodiol in the resistant and sensitive clones and by measuring the K_m values in Michaelis-Menten plots.

It was interesting that inducible levels of AHH in NMuLi in culture displayed two distinct peaks, one in log phase growth and one in resting phase. Nebert and Gelboin have examined the induction of AHH as a function of the growth curve in hamster fetus secondary cells in culture (1). They found that AHH activity maximized on day one post-plating, and then monotonically decreased as the cells grew farther. They did not obtain the same shut-off, and then turn-on, of AHH as the cells entered confluence that we observed with NMuLi. Perhaps this was due to our dealing with a permanent cell line, which is much healthier in culture, than their hamster fetus secondary cells. The two discrete peaks of AHH induction could easily be rationalized on the basis of the protein synthesizing ability of the cells. In log phase, the cells are making large quantities of protein, and it is not difficult for them to divert some of this synthetic capability toward making AHH. As the cells near confluence, they begin to shut off all protein synthesis, as if by a master damping mechanism, and hence cannot make AHH. Since there are so many growth-associated functions to close down at confluence, turning off almost all protein synthesis could be an efficient way of shutting down these functions. Once the cells have entered confluence, they can now afford to derepress some of the protein synthesizing apparatus to make such luxury proteins as AHH, and inducibility reappears. However, since the total protein capability is not turned on, the levels of AHH that they can make are a factor of 1.7 ± 0.7 times lower than those from log phase cells.

We have shown that clones sensitive to BaP do not breed true in their sensitivity (Chapter II), and here that AHH levels in these clones

also do not breed true since later passage populations generated from sensitive clones possess different AHH levels than the initial clones.

Whitlock et al. have investigated the AHH levels in subclones of a clone derived from epithelial Buffalo rat liver cells (13). Their results indicated that there was substantial variability in the induction of AHH among the subclones in the absence of any mutational stress.

The variability of AHH in these subclones could be analogous to the variability of tyrosine amino transferase (TAT) levels in the hematoma cell line, HTC. Aviv and Thompson subcloned a clone that was highly inducible for TAT and one that was miminally inducible and measured the levels of the enzyme in the subclones. They found that the distribution of inducible TAT levels in the subclones about the values of the parent clones was so broad that the levels from the two types of subclones overlapped.

Clearly, this process is not always occurring in vivo, or if it is, the variant cells are being selected out. It would be interesting to study the effects of various environmental modifications on the variability of AHH and sensitivity to BaP in various clones derived from NMuLi. In particular, it might be interesting to contrast the induction of AHH in clones 7 and 8, which seem to be stably sensitive and resistant, respectively, with regard to RNA metabolism and processing. Such studies would be particularly valuable, since at present our ability to exploit fully the advantages conferred by working in culture, such as cell cycle studies, cloning, and mutant selection, are severely hindered by the low levels of various enzymes in vitro, their eventual

loss with passage, and the loss of various differentiated functions

associated with them.

-129-

F. References

1. Aviv, D., and Thompson, E. B. Variation in Tyrosine Aminotrans-ferase Induction in HTC Cell Clones. Science, 177: 1202-1203, 1972.

2. DePierre, J. W., Moron, M. S., Hohannesen, K. A. M., and Ernster, L. A Reliable, Sensitive, and Convenient Radioactive Assay for Benzopyrene Monooxygenase. Anal. Biochem., 63: 470-484, 1975.

3. Diamond, L. The Effect of Carcinogenic Hydrocarbons on Rodent and Primate Cells in Vitro. J. Cell. and Comp. Physiol., 66: 183-198, 1965.

4. Diamond, L., Defendi, V., and Brookes, P. The Interaction of 7,12-Dimethylbenz(a)anthracene with Cells Sensitive and Resistant to Toxicity Induced by this Carcinogen. Cancer Res., 27: 890-897, 1967.

5. Diamond, L. Metabolism of Polycyclic Hydrocarbons in Mammalian Cell Cultures. Int. J. Cancer, 8: 451-462, 1971.

6. Evans, V. J., Price, F. M., Kerr, J. A., and de Oca, J. M. Effect of 7,12-Dimethylbenz(a)anthracene on Non-Neoplastic and Neoplastic Rodent Cells in Culgure. J. Nat. Cancer Inst., 45: 429-441, 1970.

7. Gelboin, H. V., Huberman, E., and Sachs, L. Enzymatic Hydroxylation of Benzopyrene and Its Relationship to Cytotoxicity. P. N. A. S., U. S., 64: 1188-1194, 1969.

8. Kit, S., Dubbs, D. R., Piekarski, L. J., and Hsu, T. C., Exp. Cell Res., 31: 297-302, 1963.

9. Mezger-Freed, L.   Effect of Ploidy and Mutagens on Bromodeoxyuridine Resistance in Haploid and Diploid Frog Cells.   Nature New Biology, 235: 245-246, 1972.

10. Nebert, D. W., and Gelboin, H. V.   Substrate-Inducible Microsomal Aryl Hydrocarbon Hydroxylase in Mammalian Cell Culture.   II. Cellular Responses During Enzyme Induction.   J. Biol. Chem., 243: 6250-6251, 1968.

11. Nebert, D. W., and Gielen, J. E.   Genetic Regulation of Aryl Hydrocarbon Hydroxylase Induction in the Mouse.   Fed. Procl, 31: 1315-1325, 1972.

12. Van Zeeland, A. A., and Simons, J. W. I. M.   Ploid Level and Mutation to Hypoxanthine-Guanine-Phosphoribosyl-Transferase (HGPRT) Deficiency in Chinese Hamster Cells.   Mut. Res., 28: 239-250, 1975.

13. Whitlock, J. P., Jr., Gelboin, H. V., and Coon, H. G.   Variation in Aryl Hydrocarbon Hydroxylase Activity in Heteroploid and Predominantly Diploid Rat Liver Cells in Culture.   J. Cell Biology, 70: 217-225, 1976.

Chart Legends — Chapter III

Chart 1. The toxicity of derivatives of BaP to NMuLi clone 8 in the colony killing assay. Two hundred single cells were plated on a 60 mm dish, allowed to recover for one day, and then treated with the various derivatives in DMSO (0.2% total in the medium, which caused no toxicity itself) for nine days. The colonies were fixed, stained, and counted. Each point represents the average of four plates. This experiment was performed on passage 11 post-isolation of this clone, passage 52 post-isolation of NMuLi.

Chart 2. The toxicity of BaP derivatives to NMuLi clone 7 was performed at the same passage number and in the same manner as for clone 8 in Chart 1.

Chart 3. The experiment of Chart 2 was repeated at passage 12, and the effect of BF on the toxicity was investigated, again in NMuLi clone 7.

Chart 4. Variants resistant to the 7,8 dihydrodiol of BaP and to BaP itself were monitored as a function of passage in NMuLi clone 8.

Chart 5.   The time course of the induction of AHH. Cells were seeded

at 5×10^6 per roller bottle, and induced with 1 ug/ml of

BaP for the times indicated before harvesting. a) Cell

counts during the assay. b) Induction at day two post-

seeding. c) Induction at day 6 post-seeding. Media was

changed at days three and five post-seeding.

Chart 6.   The inducibility of AHH throughout the growth curve.

0, cells/roller bottle. At each point, cells were induced

with 1 ug/ml of BaP for 12 hours prior harvesting. Δ,

induced AHH activity. ▲, basal (uninduced) AHH activity.

Medium was changed on days 3, 5, 7 post-seeding.

Chart 7.   The same experiment was performed as in Chart 6, except that

1 ug/ml of BaP was added to the log phase cultures on day one

post-plating and left on all cultures, enzyme levels being

measured at the points indicated. For confluent cells, BaP

was added on day 5 and remained there throughout the end of

the assay. Medium was changed on day four for the confluent

portion of the assay only.

Chart 8.   Effect of varying microsomal protein in the mdoified radio-

active assay for BaP metabolism using induced rat liver micro-

somes. □, pmoles of ^{14}C BaP metabolites in the water-acetone

layer. ●, pmoles of fluorescent BaP metabolites equivalent to

3-hydroxy-BaP in the NaOH extraction. Δ, pmoles of ^{14}C BaP

metabolites in the NaOH extraction.

Chart 9.   Effect of time of incubation on the modified radioactive assay
           using 10 ug of microsomal protein in all incubations. $\square$,
           pmoles of ^{14}C BaP metabolites in the water-acetone layer, $\bullet$,
           fluorescent metabolites of BaP equivalent to 3-hydroxy-BaP in
           the NaOH extraction. Δ, pmoles of ^{14}C BaP metabolites in the
           NaOH extraction.

Chart 10. Radioactive assay on day 2 NMuLi cells induced for 12 hours
           with 1 ug/ml of BaP. Activity as function of cellular protein
           in a 30 minute incubation. $\bullet$, pmoles of fluorescent BaP
           metabolites equivalent to 3-hydroxy-BaP in the NaOH extraction.
           0, pmoles of ^{14}C BaP metabolites in the water-acetone layer.
           $\blacktriangle$, pmoles of ^{14}C BaP metabolites bound to TCA-precipitable
           cellular macromolecules.

Chart 11. Radioactive assay on day 2 induced NMuLi cells as a function
           of time with 2 mg of cellular protein in each incubation
           flask. Same symbols as in Chart 10.

Chart 12. Correlation of clonal killing with the maximal inducible
           levels of AHH on day 2. Clones were treated with 10 ug/ml of
           BaP as in Chart 1. AHH induction as per Chart 10. 0, clone
           9, passage two. $\bullet$, clone 9, passage thirteen. Δ, clone 19,
           passage three. $\blacktriangle$, clone 19, passage eleven. $\blacksquare$, clone 8,
           passage seventeen. $\otimes$, clone 7, passage seventeen. $\bigcirc$,
           whole NMuLi population, average of five experiments.

IV.   CHARACTERIZATION OF SYNTHETIC DERIVATIVES OF BENZO(A)PYRENE

BY ABSORPTION, FLUORESCENCE, AND MASS SPECTROSCOPY

A.   Summary

The mass spectra of a number of the derivatives of BaP have been taken in an attempt to provide a further tool in identifying metabolites of BaP. Fortunately, all of the derivatives have a very significant molecular ion, attesting to the stability of the large conjugated aromatic system.

In cases where substantial fragmentation does occur, it is easily rationalizable in terms of loss of simple fragments, such as water in the case of dihydrodiols, formyl radical in the case of phenols, and carbon monoxide in the case of quinones. Since the mass spectrometer can detect down to 10 ng of compound, this technique will be extremely useful in elucidating the structures of metabolites of BaP, and providing definitive molecular weights.

The UV-visible absorption spectra of derivatives of BaP have been found to be sensitive to substituent effects. In particular, saturation of double bonds results in pronounced blue-shifts and relative intensity changes in the spectra. For the cases of single substituent substitution, it has been found that all shifts are bathochromic, and that the magnitude of the shift roughly correlates with the electron-donating inductive effect of the substituent. Where the donating effect of the substituent is small or nil, a large substituent with pi electrons that can overlap with the aromatic system also red-shifts the spectrum. Down to 40 ng of compound can be detected by absorbance.

Substituent perturbations affect the fluorescence spectra in

roughly the same way that they affect the absorption spectra. The use

of fluorescence emission spectra was found to be approximately 100

times more sensitive for detecting these derivatives than was absorption

spectra. Fluorescence excitation spectra, when corrected for lamp

output, were found to agree very well with the absorption spectra of

the compounds. Hence it will be possible to obtain spectra analogous

to absorption spectra on approximately 0.5 ng of compound.

B. Introduction

To enable us to study the metabolism of benzo(a)pyrene (BaP) in

mouse liver epithelial cells and its relationship to BaP-induced

toxicity, we first analyzed spectroscopic properties of BaP derivatives

that might be formed in the metabolism studies.

In this area, Sims has employed TLC systems to separate metabolites

of BaP produced by rat liver homogenates, and only tentatively iden-

tified the products, lacking good standards (16). No mass spectroscopy

was performed. The same author also studied the metabolism of BaP in

mouse embryo cell cultures, and again did not perform mass spectroscopy

nor fluorescence spectroscopy on the products or standards (17). Grover

et al. presented evidence for the formation of the 4,5 epoxide of BaP

by rat liver microsomes by using an inhibitor of epoxide hydrase, the

1,2 epoxy-1,2,3,4-tetrahydronaphthalene, in the incubation mixture (6).

However, evidence for the existence of the epoxide relied mainly on the

fact that microsomes converted it to a compound that co-chromatographed

with the presumed 4 or 5 phenol of BaP after an acid-catalyzed

rearrangement. Only poor quality absorption spectra and no fluorescence

or mass spectra were presented. Similarly, Flesher and Sydnor presented

a study on the metabolism of BaP and 6-methyl-BaP by rat liver homogenates, but did not employ absorbance, fluorescence, or mass spectra of their metabolites, relying only on the R_f values vs. authentic standards and the colors of the compounds to confirm their identities (5).

At this time, more synthetic standards of BaP were becoming available, and it was decided to conduct a study characterizing these derivatives as to their UV-visible absorption, fluorescence, and mass spectra. This study would lead to interesting molecular insights on the chemistry of these derivatives, as well as predicting the utility of these spectra in identifying unambiguously metabolites of BaP in cell culture systems.

During the course of this study, Wang et al. employed mass spectroscopy, R_f values, and the use of epoxide hydrase inhibitors to identify BaP 4,5 oxide as a metabolite of BaP in a hamster liver microsomal incubation system (19). Borgen et al. subsequently used co-chromatography and molecular weights determined by mass spectroscopy to identify the 9,10 dihydrodiol, the 7,8 dihydrodiol, and the 4,5 dihydrodiol of BaP, along with 3-hydroxy-BaP and the 3,6 quinone of BaP (2). These authors also compared, but did not publish, the absorption spectra of the metabolites with the authentic standards.

In a subsequent study, Kinoshita et al. studied the metabolism of BaP by rat liver microsomes and used R_f values and absorption spectra to identify the 4,5-, 7,8-, and 9,10-dihydrodiols of BaP, the 3- and 9 hydroxy-BaP's, and the 3,6 and 1,6 quinones of BaP (10).

The 4,5 oxide was again confirmed as a metabolite of BaP in a rat liver microsomal incubation system by Selkirk et al.(14). The criteria

of absorption spectra and a retention time by high pressure liquid

chromatography identical with the synthetic standard were used.

In addition, they showed the metabolite's conversion to the 4,5 dihy-

drodiol on further incubation with rat liver microsomes. This group

recently showed that the 1, 3, 7, and 9-hydroxy derivatives were

metabolites of BaP in a rat liver metabolizing system (15), proof of

identity relying on liquid chromatography retention times and absorption

spectra being identical with the synthetic standards.

Recently, Huberman et al. identified the 7α, 8β,-dihydroxy-9α,

10α-epoxy-7,8,9,10-tetrahydro-benzo(a)pyrene as an in vitro metabolite

of BaP in a rat liver microsomal incubation system, and showed that it

was the most mutagenic of the BaP derivatives tested so far in inducing

ouabain and 8-azaguanine resistant variants in Chinese hamster V79

cells (8). Finally, Meehan et al. have characterized an adduct isolated

from the microsomal reaction of BaP with poly-rG, and presented spectro-

scopic evidence that the BaP is bound to the guanine through the 9 or

10 position of BaP, and has a dihydrodiol function at the 7 and 8

positions. The similarity of the fluorescence spectra of the adduct

with that of various tetra-hydro-BaP derivatives led to this conclusion

(12).

C. Materials and Methods

1. Instrumentation

UV-visible absorption were taken on a Cary 118 recording spectro-

photometer at a scan rate of 0.2 nm/sec and with a pen response time

of 1 sec. Fluorescence emission corrected for wave length dependence of

the monochromator and photomultiplier tube and fluorescence excitation

spectra corrected for the wavelength dependence of the xenon lamp and the excitation monochromator were recorded on a Perkin Elmer Model MPF3A Fluorimeter with a corrected spectra accessory attachment. All fluorescence spectra were taken with solutions that had an optical density of less than 0.1 at the exciting wavelength, and emission were checked to verify that quenching and distortions due to self-absorption were not present by diluting the samples. All fluorescence spectra were recorded with 1 cm pathlength quartz cells. For emission spectra, emission and excitation were set to resolve bands 6 nm half width at half height; for excitation spectra, slits of 5 nm resolution were necessary. All absorption, fluorescence emission, and fluorescence excitation spectra were taken in 100% ethanol solutions; the ethanol was distilled off KOH pellets to remove carbonyl impurities.

Low resolution mass spectra were obtained on a DuPont mass spectrometer which was a hybrid between models 21491 and 21492. This instrument was interfaced to a Hewlett Packard 2100A computer and to a DuPont 21094 Data System. The spectrometer was calibrated with a mixture of perfluorokerosene, methanol, and water. All spectra were run at 70 eV ionizing potential by introducing one microgram of sample and volatilizing it as a solid through the probe inlet. Spectra presented here were taken at the point where the ion current was preferably constant or otherwise maximum, and it was verified by taking spectra at different points in the ion current trace that no saturation artifacts occurred in the spectra. Unfortunately, the relative ion intensities were found to be extremely variable among the scans taken in one run, and from run to run. Hence, they are presented here only as

approximate, and should not be taken as exact. Similarly, it was not found possible to arrive at good estimates of the C/H ratio in a compound by employing the $(M + 1)/M$ isotope ratios listed in McLafferty's reference tables (11). Consequently, only the m/e values, in particular the parent ion, M+, and those values corresponding to a smaller structure that lost a familiar molecule, such as water, are considered useful in the assignment of structures from these mass spectra.

2. Standard Reference Compounds

The following compounds were received from Dr. Harry Gelboin of the Chemistry Branch, National Cancer Institute, National Institutes of Health, Bethesda, Maryland, and their purity was verified by thin layer chromatography: on Silica Gel 6060 plates (Eastman Kodak, Rochester, New York) with 19/1 (v/v) benzene/ethanol as developing solvent: trans-7,8-dihydro-7,8-dihydroxy-BaP, 3-hydroxy-BaP, 9-hydroxy-BaP, cis-4,5-dihydro-4,5-dihydroxy-BaP, BaP-4,5-oxide, and BaP-1,6-, 3,6-, and 6,12-quinones.

BaP was purchased from Aldrich Chemicals, San Leandro, Calif., and purified by chromatography on neutral alumina (Waters Associates, Framingham, Mass.), with 19/1 (v/v) benzene-ethanol as developing solvent.

9,10-dihydro, 7-hydro, 8-ketone of BaP was also purchased from Aldrich and recrystallized from benzene-isopropanol. BaP was also recrystallized from benzene-isopropanol after the column chromatography.

6-iodo-BaP was synthesized by Dr. D. Warshawsky after the method of Johnson and Calvin (9) and purified by column chromatography on neutral alumina and recrystallization from benzene-isopropanol.

6-acetoxy-BaP was synthesized by K. Straub after the method of Fieser and Hershberg (4) and then converted to 6-hydroxy-BaP by use of $LiAlH_4$.

3-methoxy-BaP was derived from 3-hydroxy-BaP by use of ethereal diazomethane.

6-hydroxymethyl-BaP, BaP-6-aldehyde, and 6-methyl-BaP were generous gifts of Dr. E. Cavalieri, Eppley Institute for Cancer Research, Omaha, Nebraska.

9,10-dihydro-BaP was also synthesized by K. Straub (18).

D. Results and Discussion

1. Interpretation of Mass Spectral Fragmentation Patterns

For all of the compounds discussed below, tabulations of the m/e values and relative ion current values are listed in Table I.

BaP

The prominent characteristic in the fragmentation pattern of BaP is the large 252 peak, due to M+ (the radical cation), emphasizing the stability of the conjugated aromatic ring system (Chart 1-a). The 224-226 m/e peak system appears to be associated with a rearrangement series of pyrene fragments (Chart 2-a). Ions at m/e 126 are most likely a doubly-charged BaP ion, as this is common for aromatics (1).

6-hydroxy-BaP

The molecular ion is the base peak at m/e 268. Loss of CHO radical, a common fragmentation pattern in phenolic compounds (11), leads to m/e 239 by ring closure and rearomatization (Chart 2-b). M/e 134 is a doubly-charged 268 structure, and m/e 120 is most likely the doubly-charged analogue for the 239 structure. The low resolution
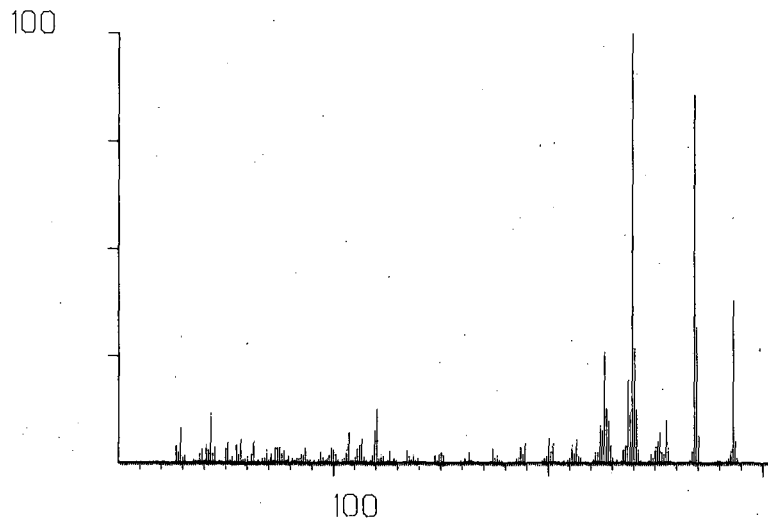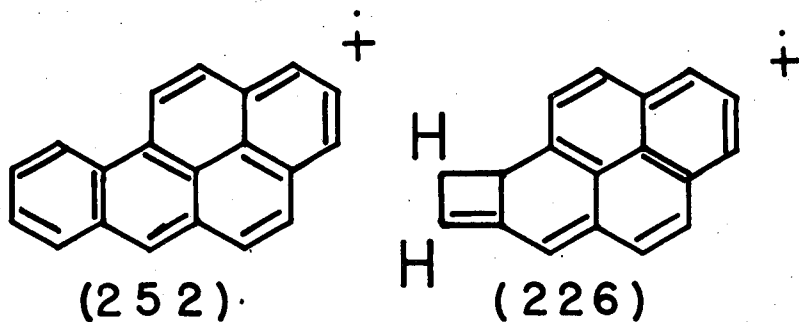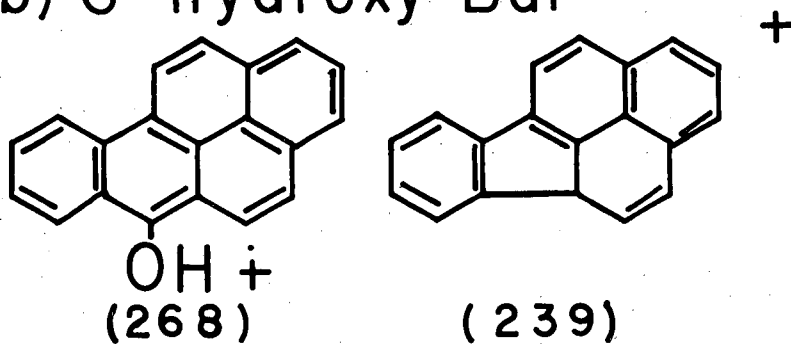
a)

100

100

b)

100

100

c)

100

100

Chart 1

a) BaP

(252)   (226)

b) 6-hydroxy-BaP

OH +
(268)   (239)

c) 6-hydroxymethyl-BaP

C=O
H
(280)

CH$_2$OH
(282)

CH$_2$
(265)
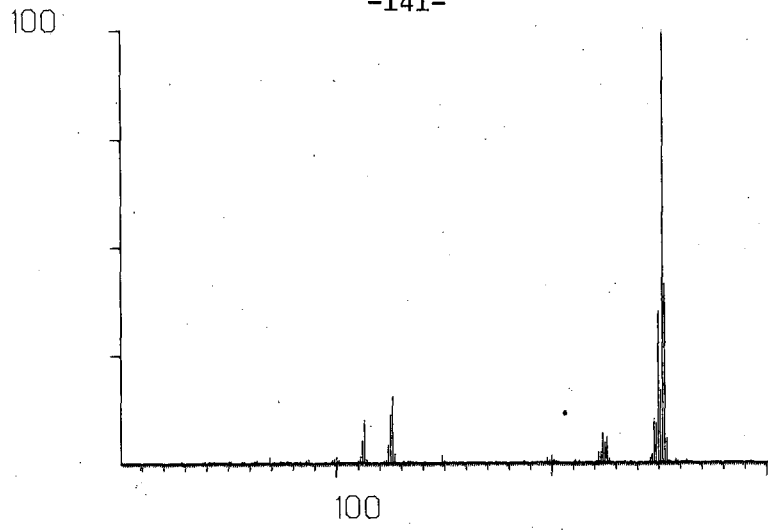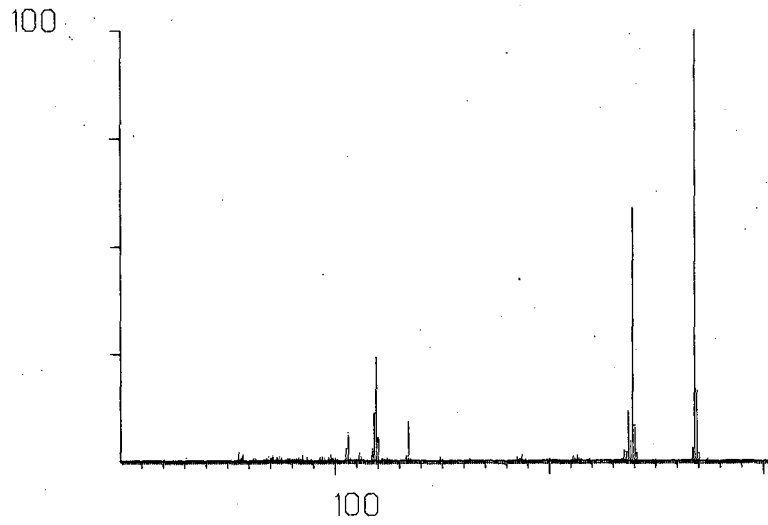
XBL 769-9547

Chart 2
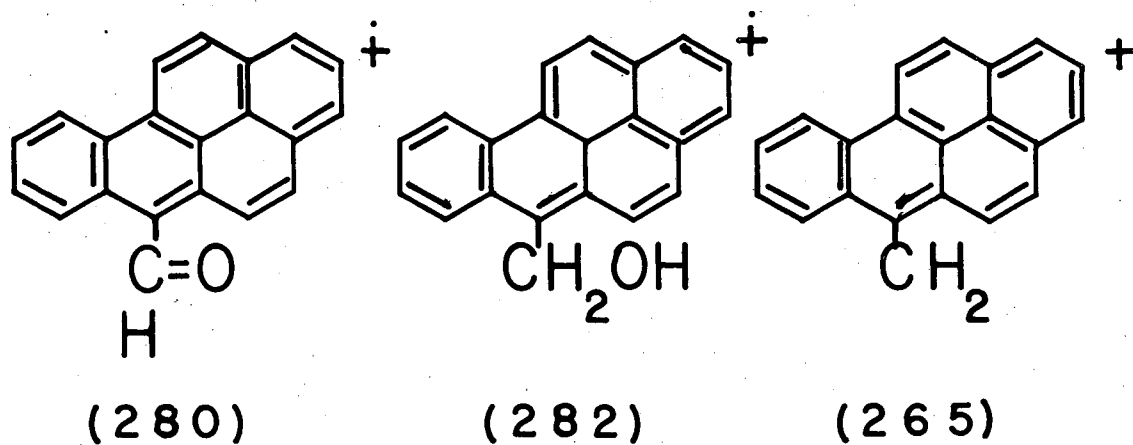
mass spectrometer only provides integral m/e values, and would round off m/e 119.5 to m/e 120. A small amount of quinone impurity is evident at m/e 282, and is probably due to the oxidation of the hydroxy-BaP.

6-hydroxymethyl-BaP

The molecular ion is the base peak at m/e 282. A peak at m/e 280 is probably due to formation of 6-aldehyde. Loss of formaldehyde gives the BaP cation at m/e 252, and loss of OH· yields the 6-CH$_2$-BaP+ ion at m/e 265, which should be stable due to its benzylic-like character. Loss of CHO· radical is responsible for m/ 253 (Chart 2-c).

6-methyl-BaP

The molecular ion forms the base peak at m/e 266. M/e 265 is also fairly intense, presumably due to loss of H· to form the same structure listed above for 6-hydroxymethyl-BaP, the benzylic-like radical.

6-acetoxy-BaP

The molecular ion, M+, is prominent but is not the base peak in the spectrum. The base peak is at m/e 268, showing that loss of ketene (CH$_2$=C=0) to form the 6-OH-BaP+ radical is favored. The ion at m/e 239 is due to loss of CHO· from the 268 m/e ion followed by ring closure as usual (Chart 3-a).

6-iodo-BaP

The predominant feature in the mass spectrum of this compound is the molecular ion at m/e 378. Loss of iodine atom leads to the BaP cation radical at m/e 251, and loss of HI results in m/e 250. Ions at m/e values 189, 126, and 125 probably result from double charges (loss of an additional electron) from the 378, 251, and 250 ions, respectively.

a) 6-acetoxy-BaP

(310)   (268)   (239)
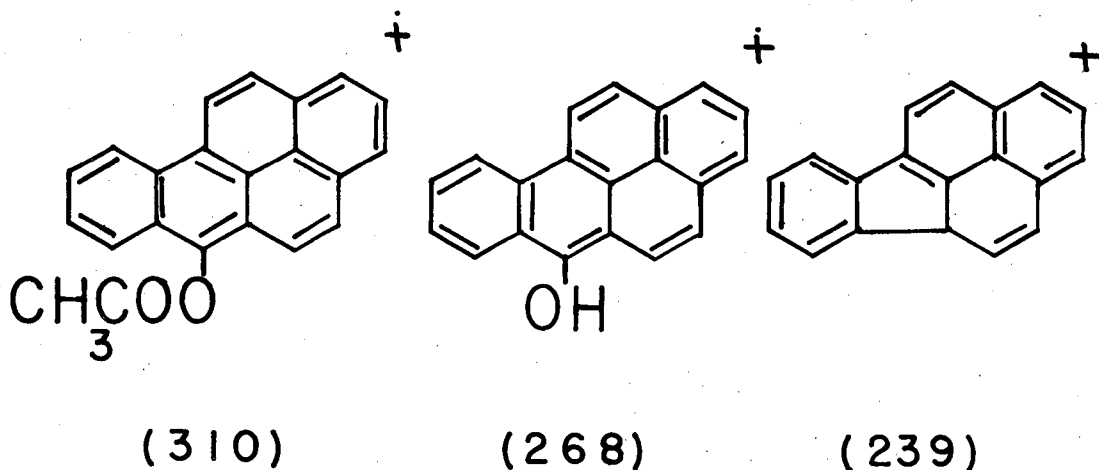
b) (cis)-4,5-dihydro-dihyroxy-BaP

(286)   (268)   (239)

XBL 769-9546

Chart 3
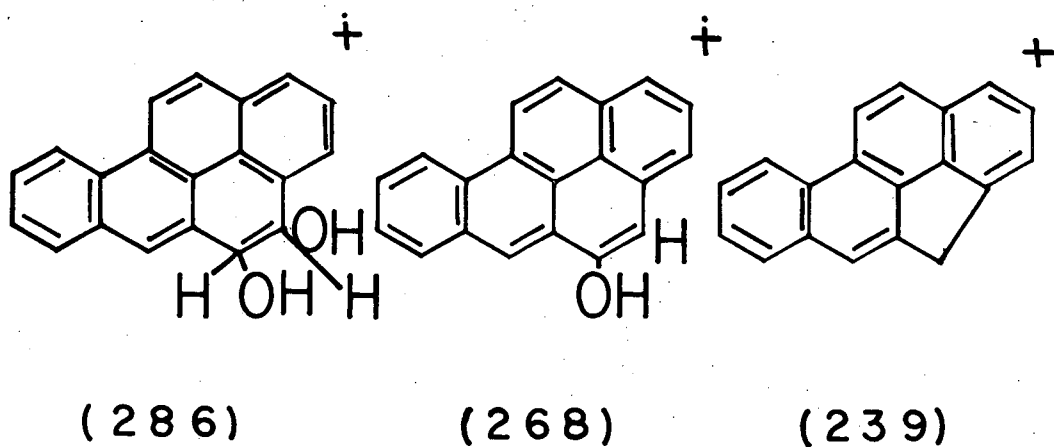
BaP-6-aldehyde

The molecular ion is the base peak in the spectrum at m/e 280. Loss of H· is favored to produce m/e 279. Loss of CO and CHO· are also favored to produce the BaP+ cation and the (BaP-1)+ ion, at m/e 252 and 251, respectively. Doubly-charged fragments are found at m/e 140, 126, and 125.

7-hydroxy-BaP

The molecular ion is the base peak at m/e 268, and again loss of formyl radical leads to m/e 239 by ring closure (Chart 1-b). The doubly-charged m/e 268 and m/e 239 structures are seen at m/e 134 and 120.

3-hydroxy-BaP and 9-hdyroxy-BaP

The mass spectra for these two derivatives are qualitatively the same as for the 7-hydroxy- and 6-hydroxy-BaP derivatives.

3-methoxy-BaP

A strong peak in the spectrum is the molecular ion at m/e 282. The base peak in the spectrum is at m/e 267, showing that loss of methyl radical is highly favored. Ions at m/e 268 and m/e 239, analogous to those seen in the spectra of all hydroxy-BaP derivatives studied so far, probably indicate that the loss of methylene (CH_2) to produce the 3-hydroxy-BaP radical followed by loss of formyl radical and ring closure yield the usual structures found in the spectra of the hydroxy-BaP derivatives.

BaP-4,5-epoxide

The base peak in this spectrum is, as usual, the molecular ion (m/e 268). The next most prominent peak occurs at m/e 239, probably

due to loss of CHO·, a loss which is common for epoxides (3). The small

m/e 252 peak is believed due to a BaP impurity, as it is difficult to

envision loss of an oxygen atom. The similar polarities of BaP and

the 4,5-oxide make recrystallization of one completely free of the

other difficult.

Cis-4,5-dihydro-dihydroxy-BaP

The molecular ion at m/e 286 is stable but is not the base peak

in the spectrum (Chart 1-c). Elimination of water with resultant

aromatization forms the stable 4- or 5-hydroxy-BaP odd electron ion, which

is responsible for the base peak in the spectrum. Further elimination

of CHO· results in the m/e 239 peak, which is also a dominant peak in

the spectrum of the 4,5-oxide and all hydroxy-BaP derivatives studied
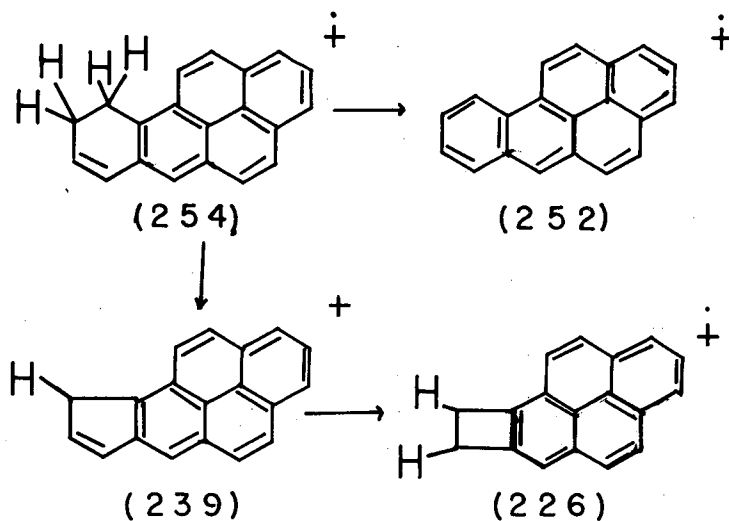
so far (Chart 3-b).

Trans-7,8-dihydro-dihydroxy-BaP

The mass spectrum of this compound is qualitatively identical to

that of the cis-4,5-dihydro-dihydroxy-BaP.

9,10-dihydro-BaP

As usual, large relative abundance of the molecular ion is the

significant feature in the mass spectrum of the compound. Rearoma-

tization by loss of H_2 leads to a substantial amount of the BaP cation,

as expected. A McLafferty rearrangement (H-transfer) followed by loss

of methyl radical and subsequent ring closure leads to the stable m/e

239 structure seen before (Chart 4-a). Loss of ethylene leads to an

ion at m/e 226, with a doubly-charged analogue at m/e 113. Doubly-

charged ions at m/e values 127, 126, and 119 are due to further ioniza-

tions of the parent ion, the BaP cation, and the m/e 239 structure.

a) 9,10-dihydro-BaP

(254)   (252)

(239)   (226)

b) 9,10-dihydro, 7-hydro, 8-ketone-BaP

(270)   (242)

(214)   (241)

XBL 769-9545

Chart 4
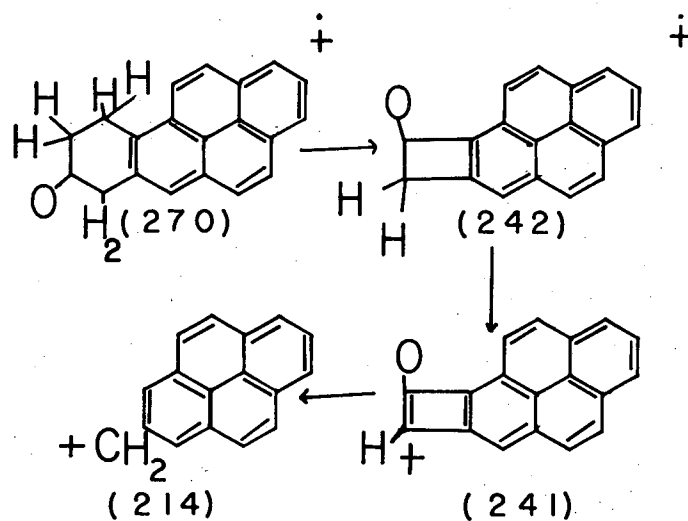
Table I. M/e Values and Normalized Relative Ion Intensities

in the Mass Spectra of Derivatives of Benzo(a)pyrene

M/e Value (Normalized Relative Ion Intensity, Percent   Mol. Wt.
                    of Base Peak)

            Benzo(a)pyrene(BaP) 252

253(24),   252(100),   251(04),   250(14),   226(02),

225(02),   224(02),   126(20),   125(10),   124(04),

113(10),   112(06),   111(03)

            6-hydroxy-BaP 268

270(03),   269(21),   268(100),   267(19),   241(02),

240(13),   239(65),   238(009),   237(16),   236(02),

235(02),   187(02),   134(006),   120(21),   119(15),

118(04),   113(02),   107(004),   106(04)

            6-hydroxymethyl-BaP 282

284(13),   283(14),   282(100),   280(20),   279(15),

267(12),   266(42),   265(70),   264(99),   263(25),

262(12),   254(21),   253(82),   252(58),   251(23),

250(30),   218(09),   217(18),   213(12),   185(13),

149(22),   135(13)

            6 Methyl-BaP 266

267(24),   266(100),   265(45),   264(08),   263(25),

262(03),   261(06),   259(03),   254(02),   252(05),

250(04),   248(02),   245(03),   239(06),   238(02),

237(04),   236(02),   235(04),   233(03),   224(03),

219(04),   217(04)

Table I (continued)

M/e Value (Normalized Relative Ion Intensity, Percent of Base Peak)   Mol. Wt.

6-Acetoxy-BaP 310

311(06),   310(22),   270(04),   269(31),   <u>268(100)</u>,

267(35),   266(02),   241(02),   240(14),   239(54),

238(13),   237(24),   236(05),   235(04),   213(02),

211(02),   119(04),   118(03)

6-Iodo-BaP 378

380(01),   379(19),   <u>378(100)</u>,   252(09),   251(30),   250(34),   249(04),

248(05),   225(03),   224(03),   223(01),   200(01),   189(04),   126(04),

125(07),   124(05),   123(01),   112(03)

BaP-6-Aldehyde 280

282(03),   281(29),   280(100),   279(34),   278(02),   268(01),   254(03),

253(13),   252(50),   251(44),   250(44),   249(05),   248(10),   247(02),

226(04),   225(05),   224(07),   155(02),   149(09),   147(02),   141(03),

140(05),   127(06),   126(37),   125(26),   124(12),   123(04),   119(02),

114(02)

7-hydroxy-BaP 268

270(02),   269(17),   <u>268(100)</u>,   267(03),   241(02),   240(09),   239(59),

238(05),   237(12),   236(02),   235(02),   213(02),   211(01),   187(02),

185(01),   149(01),   134(09),   133(01),   120(06),   119(24),   118(11),

117(03),   112(01),   111(02),   106(07),   105(03)

3-hydroxy-BaP 268

269(26),   <u>268(100)</u>,   267(21),   240(14),   239(60),

238(10),   237(13),   231(07),   219(05),   181(17),

169(14),   132(31),   120(45)

(continued)

Table I (continued)

M/e Value (Normalized Relative Ion Intensity, Percent Mol. Wt.
of Base Peak)

9-hydroxy-BaP 268

270(05), 269(30), 268(100), 267(03), 240(07), 239(36),

238(04), 237(09), 135(06), 134(26), 120(24), 119(20), 118(03),

117(04), 107(07), 105(04)

3-methoxy-BaP 282

283(18), 282(94), 268(38), 267(100), 252(07),

251(05), 250(05), 240(06), 239(46), 238(07),

237(13), 235(06), 141(06), 119(10)

BaP-4,5 oxide 268

270(02), 269(25), 268(100), 267(03), 253(07), 252(10), 250(04),

241(02), 240(08), 239(69), 238(07), 237(15), 236(03), 235(03),

227(02), 213(03), 212(02), 211(03), 187(03), 163(04), 135(02),

129(02), 125(03), 120(06), 119(09), 118(03), 113(03), 112(02),

111(05), 110(03), 109(03), 107(06), 106(04), 105(03), 99(05)

cis 4,5 dihydro-dihydroxy-BaP 286

288(02), 287(26), 286(91), 285(05), 279(02), 270(09), 269(59),

268(100), 267(03), 257(03), 256(04), 255(13), 254(02), 253(06),

252(21), 251(10), 250(08), 242(03), 241(14), 240(21), 239(65),

238(08), 237(11), 236(02), 229(05), 228(06), 227(08), 226(19),

225(04), 224(04), 213(03), 211(03), 200(03), 150(02), 149(09),

143(03), 135(02), 134(06), 129(03), 127(03), 126(05), 125(04),

124(04), 121(04), 120(24), 119(13), 118(14), 114(03), 113(09),

112(03)

Table I (continued)

M/e Value (Normalized Relative Ion Intensity, Percent   Mol. Wt.
of Base Peak)

        trans 7,8 dihydro-dihydroxy-BaP   286

287(05),   286(21),   270(05),   269(20),   268(100),   267(04),   252(03),

241(08),   240(31),   239(53),   238(04),   237(14),   226(08),   215(04),

214(04),   213(05),   211(03),   201(04),   200(03),   197(04),   135(04),

134(04),   120(03),   119(13),   118(06),   106(04)

        9,10 dihydro-BaP   254

256(04),   255(21),   254(100),   253(54),   252(81),   251(07),   250(24),

249(03),   248(04),   240(05),   239(30),   237(03),   226(07),   225(03),

224(05),   223(01),   222(01),   213(02),   211(01),   202(01),   200(03),

127(11),   126(36),   125(15),   124(06),   123(02),   120(02),   119(10),

118(03),   114(02),   113(17),   112(09),   111(04),   106(03),   105(01),

101(02),   100(04),   99(02),   78(20)

        9,10 dihydro, 7 hydro, 8 one of BaP   270

272(02),   271(25),   270(100),   269(04),   252(02),   243(02),   242(09),

241(14),   240(07),   239(16),   238(02),   237(04),   229(03),   228(09),

227(07),   226(09),   216(03),   215(13),   214(64),   213(35),   212(03),

211(03),   201(02),   200(03),   189(02),   188(02),   187(04),   107(16)

        BaP 1,6 Quinone   282

284(03),   283(21),   282(100),   256(02),   255(10),   254(54),   253(02),

227(12),   226(54),   225(15),   224(26),   223(05),   222(04),   200(06),

199(03),   198(04),   174(03),   150(02),   141(03),   127(03),   114(13),

113(35),   112(19),   119(03),   100(77)

Table I (continued)

M/e Value (Normalized Relative Ion Intensities, Percent   Mol. Wt.
of Base Peak)

     BaP 4,5 Quinone 282

284(12),   283(20),   282(100),   268(03),   258(05),   256(04),   255(10),

254(51),   239(03),   228(03),   227(06),   226(35),   225(09),   224(14),

223(03),   222(02),   218(03),   217(02),   211(03),   200(04),   199(04),

198(04),   187(03),   185(04),   175(02),   163(02),   156(02),   150(03),

149(02),   142(02),   141(04),   139(03),   137(03),   127(09),   120(05),

119(02),   115(03),   113(31),   112(31),   111(11),   100(08),   99(09),

 77(08),   71(11)

     BaP 6,12 Quinone 282

284(05),   283(27),   282(100),   281(03),   279(03),   276(02),   271(04),

270(13),   269(03),   268(03),   261(03),   257(03),   256(06),   255(17),

254(70),   252(03),   247(02),   246(05),   243(03),   242(04),   241(03),

240(03),   239(07),   227(09),   226(34),   225(14),   224(21),   223(09),

214(11),   185(10),   167(12),   149(21),   125(13),   113(34),   112(20),

111(19)

     BaP 3,6 Quinone   282

284(04),   283(21),   282(100),   270(04),   269(02),   255(06),   254(43),

241(04),   239(04),   237(03),   228(02),   227(06),   226(42),   225(12),

224(18),   223(06),   222(04),   213(04),   209(02),   200(03),   199(03),

198(04),   185(03),   181(03),   176(02),   174(02),   171(02),   150(02),

149(04),   147(03),   145(02),   143(02),   141(04),   137(04),   135(02),

130(02),   129(04),   127(05),   125(03),   124(03),   123(05),   121(04),

119(03),   117(03),   116(02),   115(02),   114(06),   113(35),   112(18),

111(07),   110(05),   109(05)

9,10-dihydro, 7-hydro, 8-ketone of BaP

The base peak is again the molecular ion at m/e 270 (Chart 5-a).
A retro-Diels-Alder cleavage (double-alpha-cleavage) followed by
formation of a cyclobutane ring accounts for the peak at m/e 242
(Chart 4-b). Loss of carbon monoxide from the m/e 242 fragment yields
another peak at m/e 214. The fragment at m/e 107 is likely due to a
doubly-charged 214 structure. The 214 m/e ion would be expected to be
fairly stable, as it is a benzylic-like carbonium ion with a stable
pyrene nucleus.

BaP-1,6-, 3,6-, 6,12-, and 4,5-quinones

All quinones show qualitatively identical mass spectra and will be
treated together by a discussion of the fragmentation pattern of the
4,5-quinone. The base peak in all spectra is the molecular ion at
m/e 282 (Chart 5-b). Two separate losses of 28 m/e units are believed
due to CO, resulting in the m/e 254 and 226 structures (Chart 6-a).
In each case, the loss of CO would probably be followed by ring closure.
Note that with a low resolution instrument, one cannot rule out two
sequential losses of ethylene as opposed to carbon monoxide. Ions at
m/e values of 141, 127, and 113 are probably the doubly-charged
analogues of the molecular ion, the 254 ion, and the 126 structure,
respectively.

2. Absorption Spectra of Various Derivatives of BaP

The absorption spectra of various derivatives of BaP have been
examined and have been found sufficiently sensitive to substituent
modifications to allow their use in identifying different metabolites
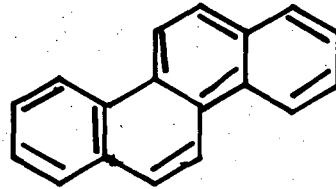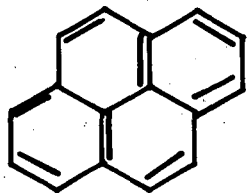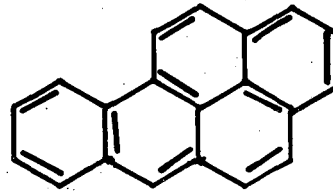of BaP. In general, spectral modifications fall into two different

a)

100

b)

100
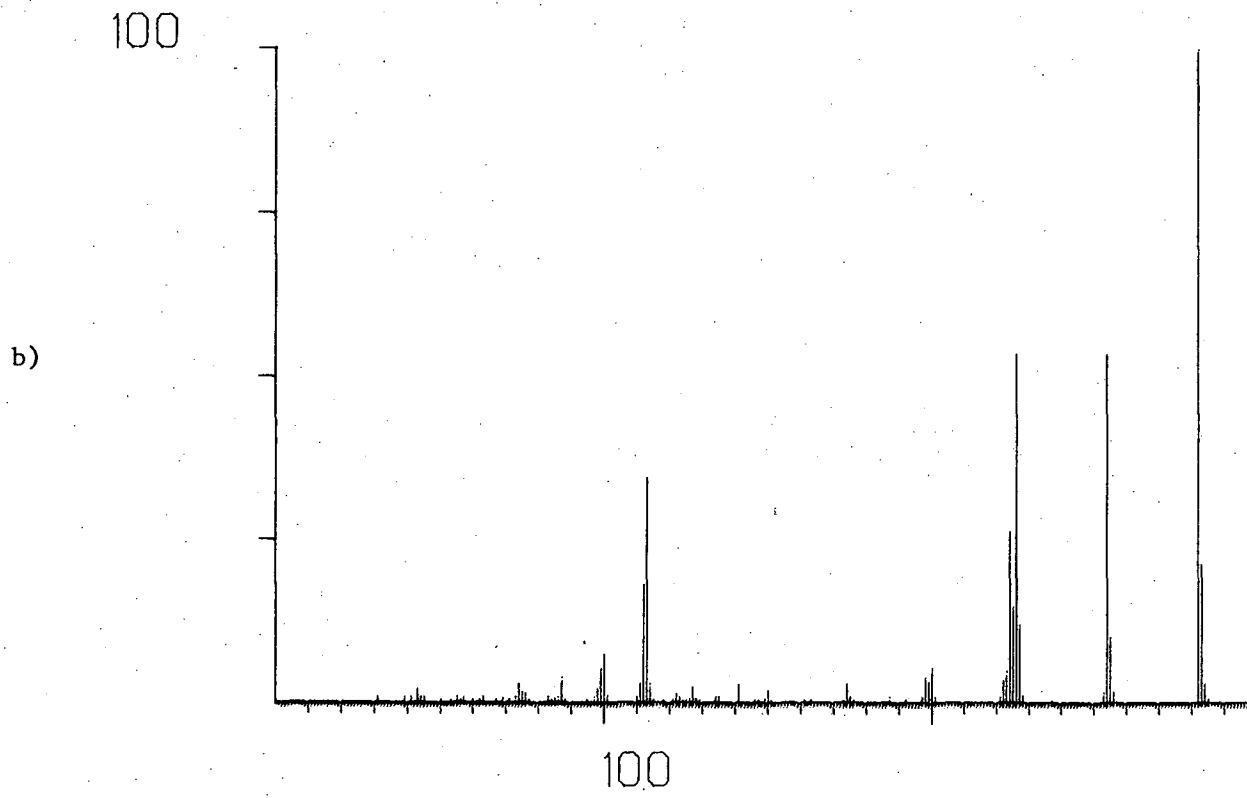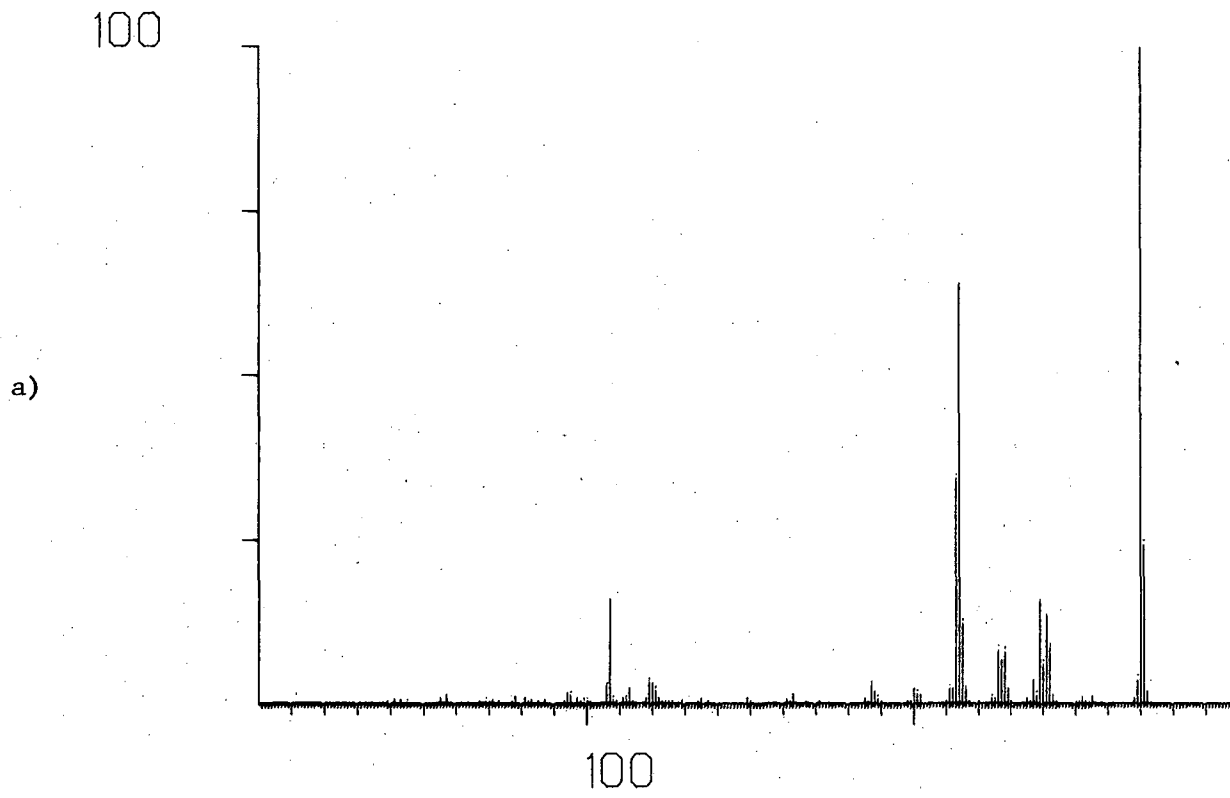
Chart 5

a) BaP-4,5-Quinone

-155-

(282) (254) (226)
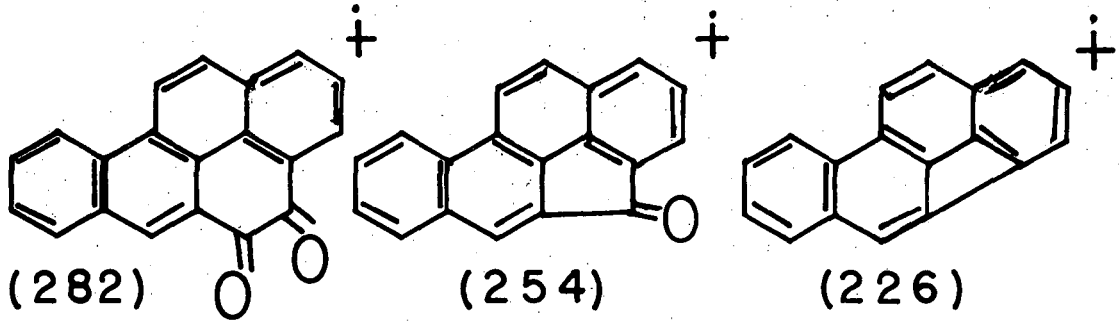
b)
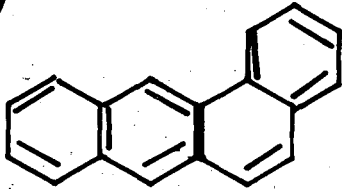
Benz(a)anthra-
cene

Chrysene

Pyrene   Benzo(a)pyrene

(BaP)

XBL 769-9548

Chart -6

a) BaP

b) Chrysene

c) Benz(a)anthracene

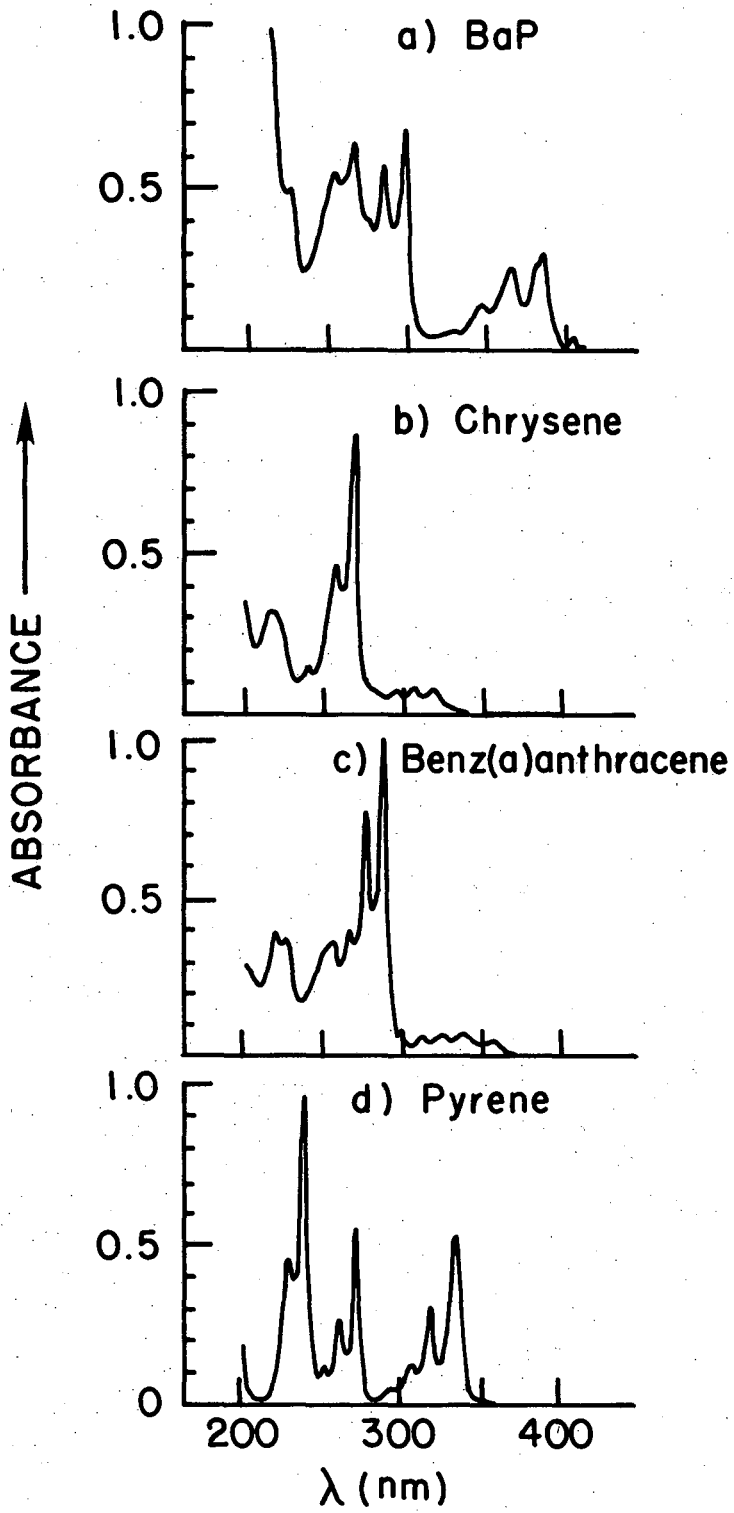d) Pyrene

ABSORBANCE

λ (nm)

XBL 768 – 9503

Chart 7

groups, which will be discussed separately. Firstly, saturation of one of the partially isolated double bonds in the molecule will substantially blue-shift the spectrum until it resembles that of one of the lower aromatic molecules from which BaP can be considered to be formally derived. Secondly, single substitution at one carbon atom of the ring will in general slightly red-shift the spectrum but preserve its relative vibronic intensity ratios.

a. Saturation of Double Bonds

There are three four-ring aromatic molecules which can be built upon to give BaP: chrysene, pyrene, and benz(a)anthracene, shown in Chart 6-b. Saturation of the 4,5-, 11,12-, or both the 7,8- and the 9,10- double bonds should give rise to molecules having the spectral properties of chrysene, benz(a)anthracene, and pyrene, respectively. The absorption of the latter molecules are shown in Chart 7, and it is seen that they are all blue-shifted relative to BaP. Further, the three spectra are all quite different from each other in terms of relative intensities of the vibrational bands.

The absorption spectrum of the cis-4,5-dihydro-dihydroxy-BaP, shown in Chart 8-a, is virtually identical to that of chrysene, as expected. Similarly, the loss of the conjugation from the 4,5 double bond in the 4,5-epoxide of BaP also results in a chrysene-like spectrum (Chart 8-b).

Trans-7,8-dihydro-dihydroxy-BaP possesses essentially a blue-shifted BaP spectrum (Chart 9-b), while the 9,10-dihydro-BaP has a spectrum intermediate between a red-shifted pyrene and a blue-shifted BaP (Table VI). The 9,10-dihydro, 7-hydro, 8-ketone of BaP again has

a) cis-4,5-dihydro-dihydroxy-BaP

b) BaP-4,5-epoxide

c) BaP-4,5-quinone

ABSORBANCE

λ (nm)
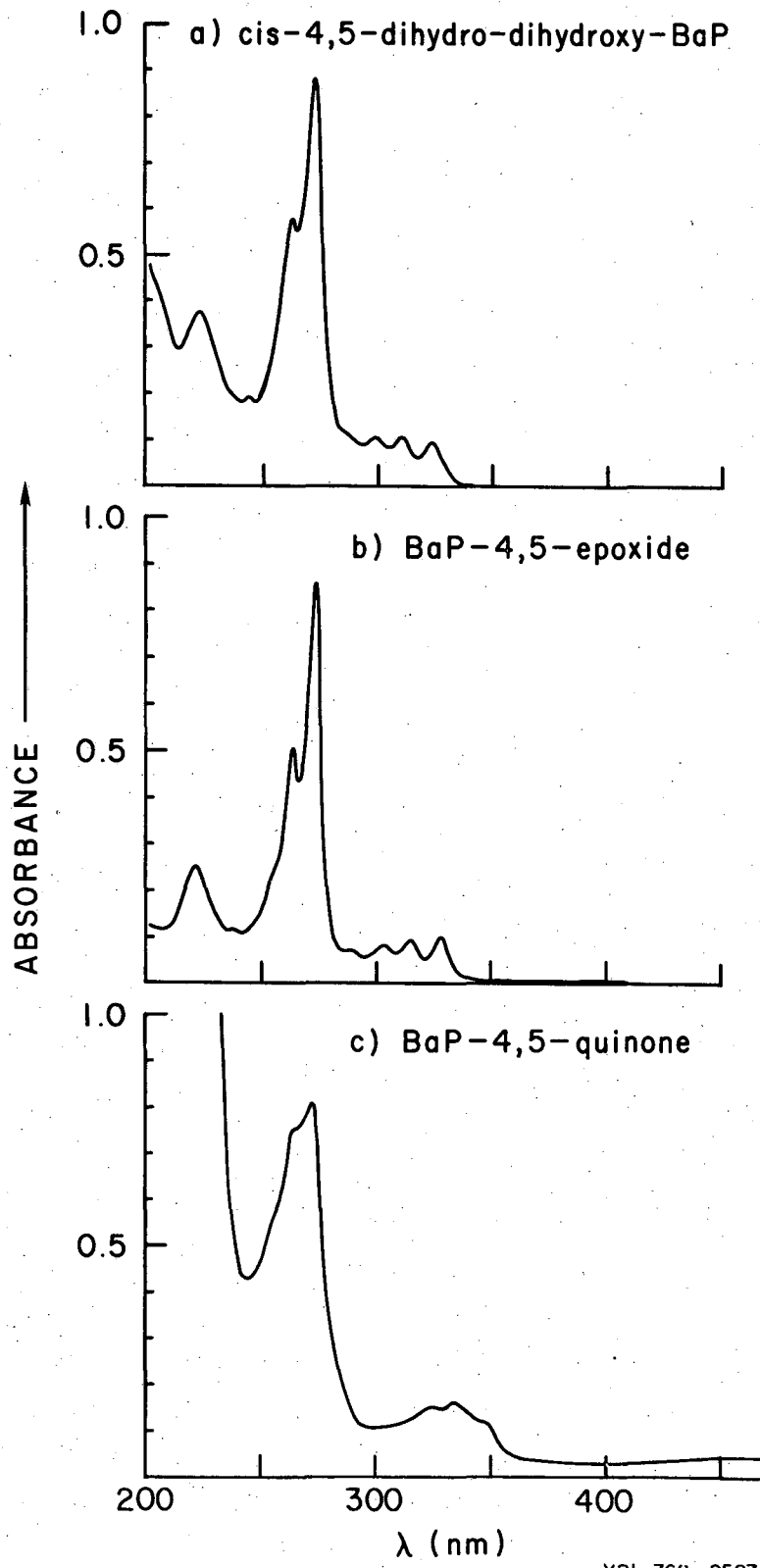
XBL 768-9507

Chart 8

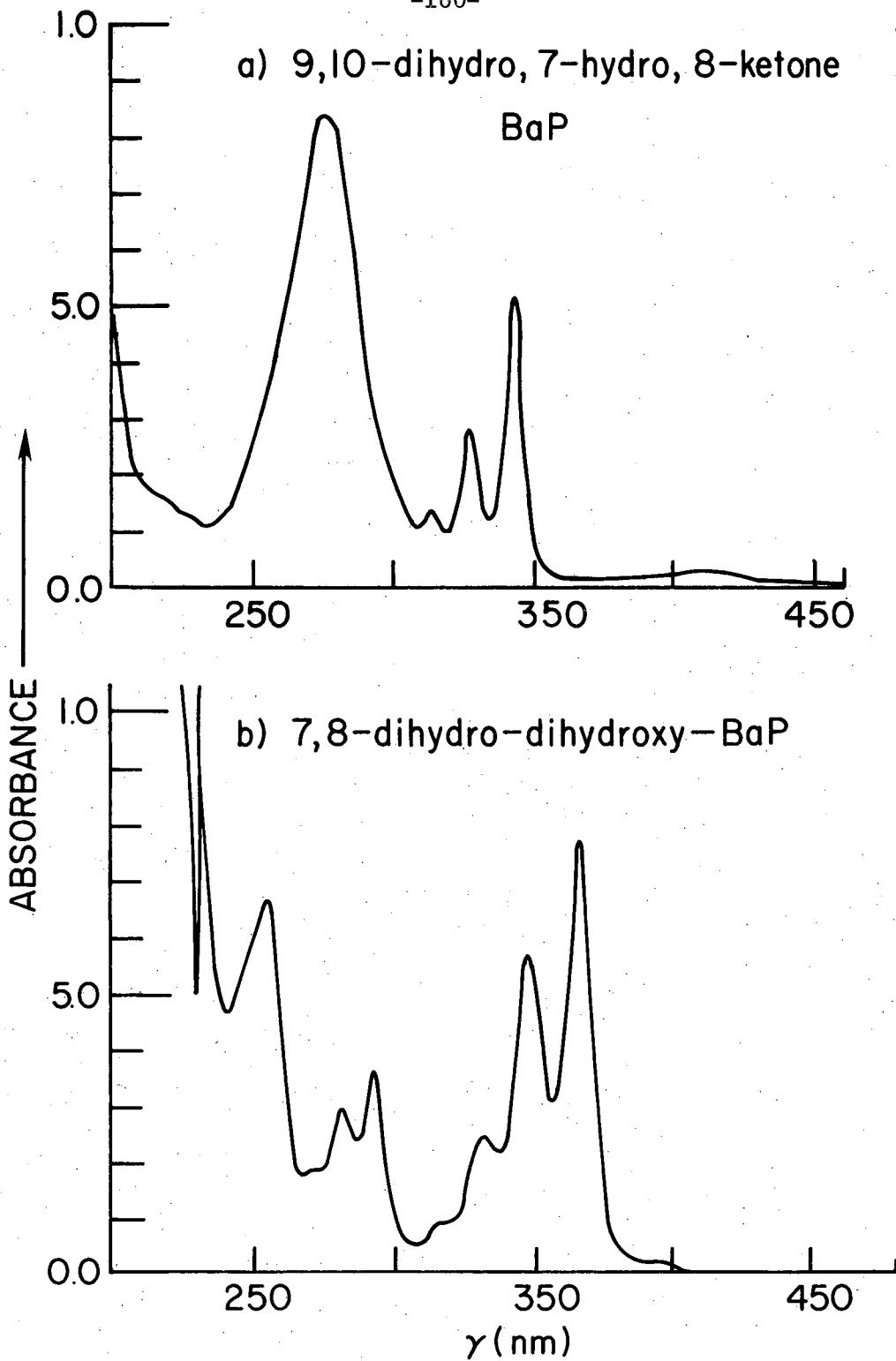an anomalous spectrum intermediate between pyrene and BaP (Chart 9-a).

The quinones are completely new spectral entities, since in these structures the aromaticity of BaP and its aromatic precursors is replaced by a new system. The 1,6-, 3,6-, and 6,12-quinones have spectra that are all far red-shifted relative to that of BaP, and there are few corresponding bands (Chart 10a-c). The 4,5-quinone appears anomalous, since in this molecule only the 4,5 double bond is saturated. Consequently, the structure maintains the semblance of chrysene, and its absorption spectrum is distinctly chrysene-like (Chart 8-c).

b. Single-Atom Substitution

The absorption spectra of the 6- and 7-hydroxy-BaP and the 3- and 9- hydroxy-BaP derivatives are all red-shifted relative to that of BaP, and many of the long-wavelength bands are either broadened or not completely resolved (Charts 11 and 12). The 3- and 9-hydroxy-BaP derivatives have very similar spectra, with the 9- being slightly to the blue of the 3-hydroxy-BaP. Minor differences in the bands around 200-300 nm allow differentiation between the two compounds. The other two hydroxy-BaP compounds are completely different from each other and from the former two in the absorption spectra. The 7-hydroxy-BaP has only two partially resolvable bands from 350-400 nm, and the 6-hydroxy-BaP spectrum in this region is completely unresolved (Chart 11).
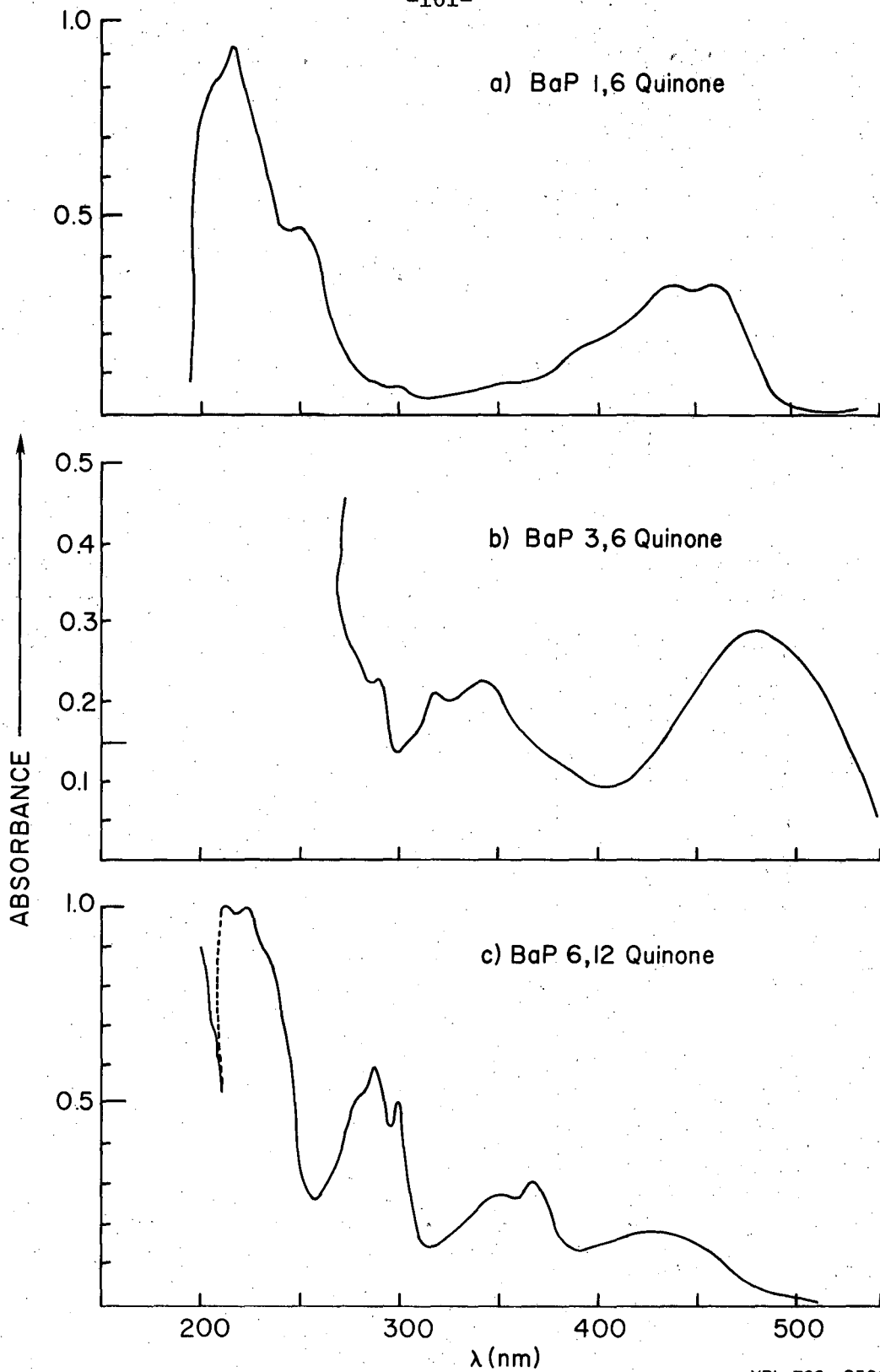
The effects of different substituents in the six position of BaP upon the absorption spectrum is straight-forward. The spectra red-shift in the order: 6-acetoxy < 6-hydroxymethyl < 6-methyl < 6-iodo < 6-hydroxy (Chart 13 and Table I). Except for the 6-hydroxy-BaP the relative intensity ratios of the bands in the spectra are roughly
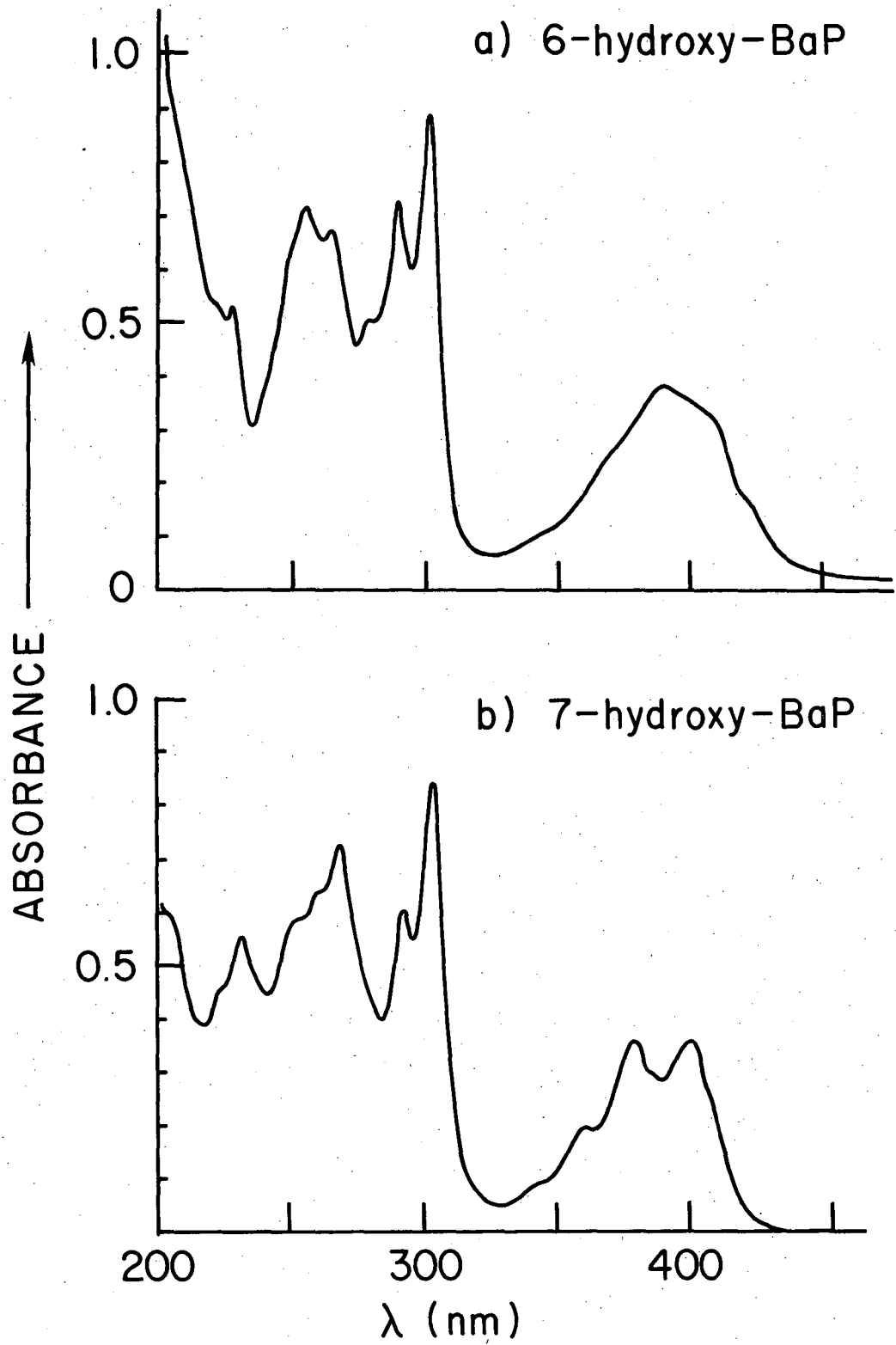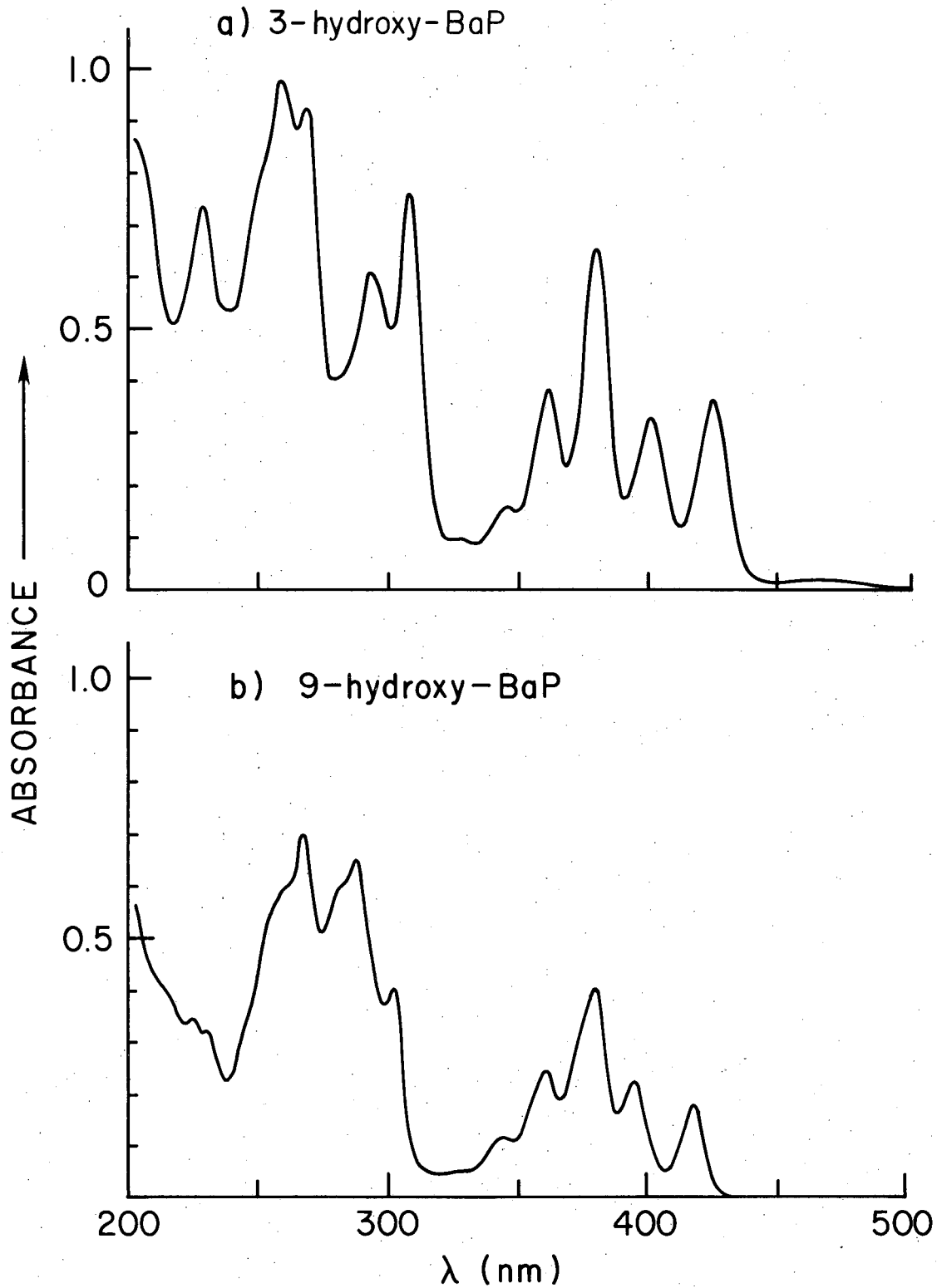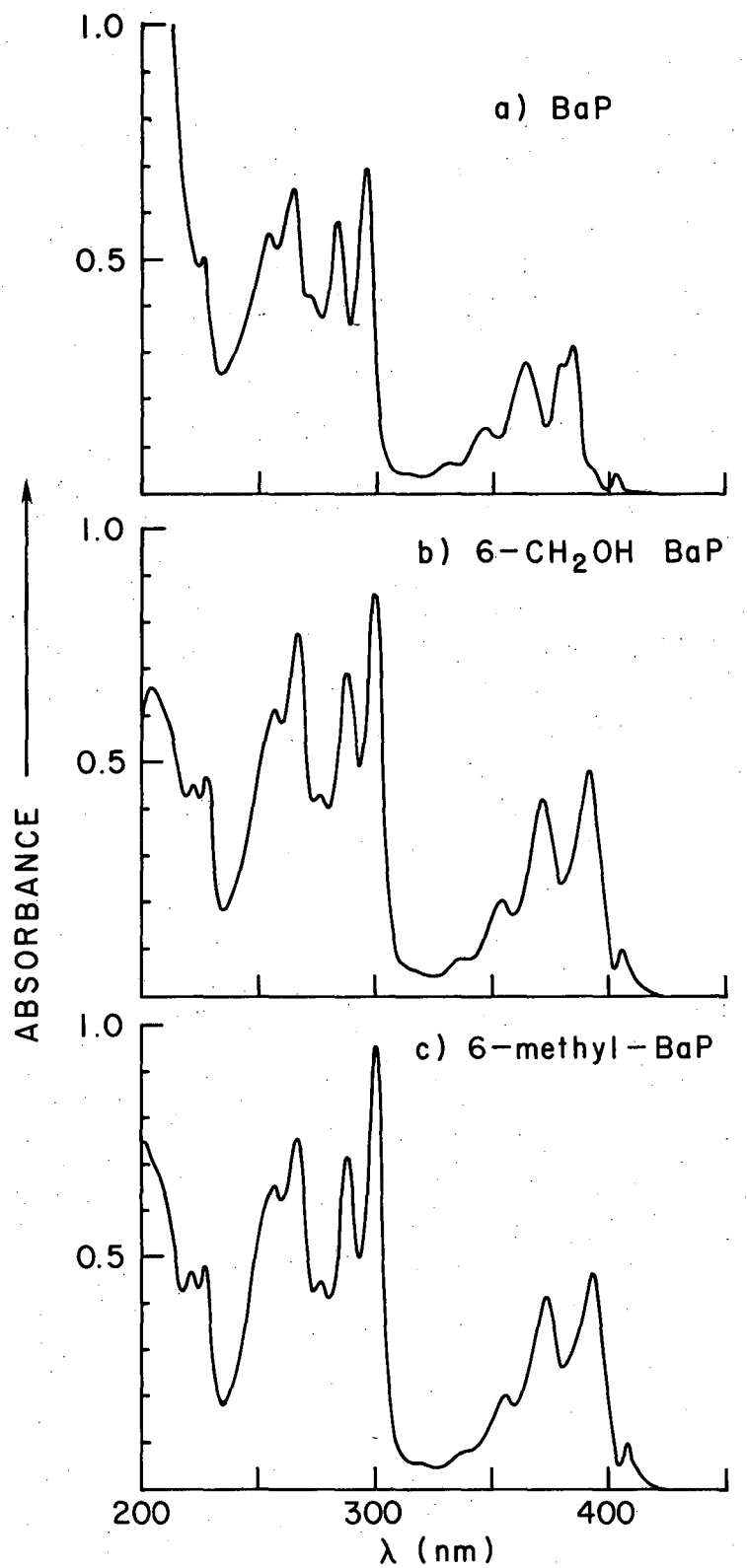
a) 9,10-dihydro, 7-hydro, 8-ketone BaP

b) 7,8-dihydro-dihydroxy-BaP

Chart 9

XBL 768 - 9504

-161-

a) BaP 1,6 Quinone

b) BaP 3,6 Quinone

c) BaP 6,12 Quinone

ABSORBANCE

λ (nm)

XBL 768 - 9509

Chart 10

a) 6-hydroxy-BaP

b) 7-hydroxy-BaP

XBL 768-9505

Chart 11

a) 3-hydroxy-BaP

b) 9-hydroxy-BaP

ABSORBANCE

λ (nm)

XBL 768-9506

Chart 12

a) BaP

b) 6-CH$_2$OH BaP

c) 6-methyl-BaP

ABSORBANCE

λ (nm)

XBL 768-9508

Chart 13

equal to those of BaP. The large red-shift for the hydroxyl derivative
is probably due to conjugation of the 2p pi electrons of oxygen with
the conjugated aromatic pi system, and to what is usually called an
electron-donating inductive effect. The same effect, although weaker,
is responsible for the red-shift due to the methyl group. This is
reasonable, since hydroxyl group has a stronger electron-donating
inductive effect than does methyl. The lesser red-shift in hydroxymethyl
is explainable by the fact that the oxygen-carbon bond is polarized,
with a resulting partial positive charge on the carbon. Since the
carbon is adjacent to the ring, this partial positive charge exerts
an electron-withdrawing inductive effect, which increases the energy
of the transition. The situation is even more pronounced in 6-acetoxy-
BaP, since the carbonyl carbon is even more positive than the carbon
in the hydroxymethyl group, and hence the spectrum is the most blue-
shifted of the six-substituted derivatives.

In 6-iodo-BaP, it is presumed that the red-shift is due to the
conjugation of the iodine 5p electron cloud with the aromatic pi cloud
of the BaP system. Otherwise, iodine would exert an electron-with-
drawing inductive effect and increase the energy of the transition.
An intuitive guess would be that the donating inductive effect would
serve to stabilize a polar excited state of the transition, although
such arguments do not rule out destabilization of the ground state by
the polar substituent.

c. Quantitative Aspects of the Absorption Spectra

Ideally, one should discuss the spectra of these molecules in
terms of the oscillator strength of the transition:

$$F = A_{exp}/A_{HO} = 4.33 \times 10^{-9} \ \varepsilon(\bar{v})\overline{dv}$$

Here, F is the oscillator strength, which is the ratio of the integrated absorption intensity measured for an absorption ban experimentally to that calculated for a harmonic oscillator (13). ε is the extinction coefficient, and the integration represents an average over the vibrational sublevels of the band. The value F=1 is considered a very strong transition. Since many of the bands in the spectra of these molecules in ethanol solution are not resolved, we will make the assumption that $(\bar{v})\overline{dv} = \Delta v$, if the band is not too broad. Further assuming that the band widths for a series of closely allied derivatives are the same, we will then be able to compare ε's for these derivatives as a measure of the strength of the transition.

Except for the quinones, the derivatives of BaP all show roughly the same resolution and the bands are not appreciably broadened. There does not appear to be any good correlation between the red-shifts in the spectra and the extinction coefficient at the absorption maximum. This is not surprising, since a red-shift is due to the usual potential energy well diagrams of the ground and excited states approaching each other, while the extinction coefficient is a rough measure of the probability of the transition and represents the potential diagrams being aligned directly underneath each other.

It is true that for many of the compounds the extinction coefficients are all increased relative to BaP and that they are all red-shifted. In the series 6-acetoxy, 6-hydroxymethyl, and 6-methyl-BaP,

Table II.   Absorption Spectra Maxima and Extinction Coefficients

at These Maxima for Substituted Derivatives of BaP/EtOH

BaP[†]		$\overset{O}{\overset{\|}{6\text{-}CH_3C\text{-}O\text{-}BaP}}$		$6\text{-}CH_2OH$ BaP		$6\text{-}CH_3$ BaP		6-Iodo-BaP	
λ,nm	$\epsilon \times 10^4$*	λ,nm	$\epsilon \times 10^4$	λ,nm	$\epsilon \times 10^4$	λ,nm	$\epsilon \times 10^4$	λ,nm	$\epsilon \times 10^4$
403	0.27	406	1.05	407	0.656	409	0.433	409.5	1.39
384	2.00	392	4.75	392	3.11	394	2.11	401.5	3.32
364	1.874	371	4.12	371	2.72	373	1.94	380.5	2.72
347	0.986	353	2.08	353	1.33	355	1.04	361.5	1.29
332	0.40	337	0.822	338	0.508	339	--	345	0.491
296	5.45	299	10.1	300	5.39	300	4.58	304	5.37
284	5.08	287	7.70	288	4.29	288	3.31	291.5	4.14
272	4.05	275	4.41	277	2.77	277	2.04	280	2.31
265	5.64	266	7.63	267	4.83	267	3.49	267	3.93
255	4.52	255	6.79	257	3.84	256	3.03	258	3.75
226	--	226	--	228	2.84	227	2.16	s(226)	--
219	2.00	220	--	221	2.64	221	--	s(220)	--
				204	--				

*Entry of 0.501 means $\epsilon = 0.501 \times 10^4 \cdot \dfrac{\ell}{cm - mole}$: absorbance was linear with conc. from 1.0 OD to 0.01 OD.

[†] The values for BaP are in agreement with those from Hirayama, 1967.

the extinction coefficients are all decreased relative to BaP and that

the red-shift seems to correlate with the decrease (Table II). 6-iodo-BaP

does not fit this series, presumably because of the large perturbation

induced by the large iodine atom and its pi cloud. All of the bands of

low energy, above 332 nm, have greater extinction coefficients than BaP.

The inner bands or higher energy bands are affected but not as much.

The hydroxyl substituents in general seem to have higher extinction

coefficients than BaP, which correlates with the red-shifts in the

spectra, although it is difficult to match up the corresponding bands

in these compounds with those of BaP (Table III). The 3-hydroxy-BaP and

9-hydroxy-BaP have very similar spectra, and corresponding bands can be

matched fairly well. It is seen that the spectrum of the 3-hydroxy-BaP

is more red-shifted than that of 9-hydroxy-BaP, and its extinction

coefficients are all greater. There is some correspondence between the

7-hydroxy-BaP and 6-hydroxy-BaP absorption bands, and it is seen that

the more red-shifted 6-hydroxy-BaP has the greater extinction coefficients.

The quinone spectra all have similar extinction coefficients in

the long wavelength bands. Here, there is no correspondence between the

red-shift and the size of the extinction coefficient (Table IV).

The 4,5 quinone, the 4,5-dihydrodiol, and the 4,5-epoxide of BaP

all have spectra that are qualitatively very similar to chrysene (Table V).

The extinction coefficients of the dihydrodiol are almost identical to

those of chrysene itself, given the uncertainty in the measurements ($\pm 5\%$).

In the 4,5-quinone, the long wavelength bands, from 330 to 366 nm, are

of the same order of magnitude as those of chrysene itself. However,

the 272 nm band system is markedly depressed in extinction values. The

Table III.   Extinction Coefficients of Hydroxy Derivatives of BaP.

3-OH-BaP		9-OH-BaP		7-OH-BaP		6-OH-BaP	
λ,nm	$\epsilon \times 10^4$	λ,nm	$\epsilon \times 10^4$	λ,nm	$\epsilon \times 10^4$	λ,nm	$\epsilon \times 10^4$
425	1.7	418	1.03	400	1.31	s(420)	--
401	1.5	395	1.27			s(410)	--
380	3.1	380	2.47	378	1.33	390	3.10
361	1.8	361	1.38	360	0.745	s(370)	--
345	0.75	343	0.626	343	0.340	s(344)	--
308	3.7	327	0.284				
293	2.9	302	2.45	303	3.32	302	7.15
		287	3.70	292	2.29	290	5.88
268	4.4	s(282)	3.41			279	4.05
257	4.6	267	3.98	268	2.78	265	5.44
228	3.5	260	3.44	260	2.38	255	5.79
		s(254)	3.01	252	2.12		
		s(225)	2.00	231	1.92	227	4.29
				223	1.49		

Table IV.   Extinction Coefficients of Quinones of BaP.

BaP-1,6	Quinone	BaP-6,12	Quinone	BaP-3,6	Quinone
λ, nm	$\epsilon \times 10^4$	λ, nm	$\epsilon \times 10^4$	λ, nm	$\epsilon \times 10^4$
459	1.57	429	0.632	471	0.881
439	1.58	368	1.12	342	0.681
s(355)	0.426	350	0.995	318	0.729
s(300)	0.416	300	1.89	289	0.590
251	2.46	288	2.30		
218	4.63				

Table V. Extinction Coefficients of Chrysene-Like Derivatives of BaP (cis)-4,5 dihydro

Chrysene		4,5 dihydroxy-BaP		BaP-4,5 Quinone		BaP-4,5 oxide	
λ,nm	$\epsilon \times 10^4$	λ,nm	$\epsilon \times 10^4$	λ,nm	$\epsilon \times 10^4$	λ,nm	$\epsilon \times 10^4$
217	2.46	222	3.81	218	2.33	222	4.10
241	1.48	244	2.02	233	2.13	238	1.97
258	5.48	263	6.59	264	2.69	264	8.82
267	10.05	273	9.60	272	2.76	274	11.6
282	0.923					290	1.15
294	0.900	299	1.13	300	0.563	302	1.31
306	0.945	310	1.14			316	1.51
319	0.923	324	1.08	326	0.610	328	1.64
343	0.118			335	0.665	350	0.164
351	0.0712	347	0.0689	350	0.564	368	0.164
361	0.100	365	0.0620	366	0.362		
				438	0.575		
				457	0.597		

extinction coefficient values for the 438 and 457 nm band systems are the same order of magnitude as those of the other three quinones. Note that at the longer wavelengths, the bands of the quinones are appreciably broadened, and hence comparison of the extinction coefficient values with those of BaP or simple derivatives is not valid without performing the integration of extinction coefficients over the entire band.

Since the spectrum of the trans-7,8-dihydro-dihydroxy-BaP resembles a blue-shifted BaP spectrally, it is reasonable to compare these two in their extinction coefficients. In general, the band system centered on 350 nm has higher extinction coefficients than those of BaP, while the higher energy band system beginning at 300 nm has in general lower extinction coefficients than those of BaP (Table VI).

The 9,10-dihydro-, 7 hydro-, 8-ketone of BaP resembles pyrene more closely in its absorption spectrum. A comparison of the extinction coefficients from the 343 band system in the former with the 334 nm system in pyrene shows that they are very close (Table VI). No comparison is valid at energies higher than 313 nm because the transition of the carbonyl group appears in this region and complicates the spectrum.

The 9,10-dihydro-BaP is at the transition point between pyrene and BaP in its absorption spectra, but if one compares the 310 nm to 350 nm system in this compound with the bands compared above for the ketone and for pyrene, it is seen that the extinction coefficients are very close.

As a calibration, we present some of the values of extinction coefficients for pyrene, BaP, and chrysene from the literature (7), and compare them to ours (Table VII). The values for BaP are in very good agreement, while those for the extinction coefficients of pyrene and

Table VI.   Extinction Coefficients of Derivatives of BaP.

Pyrene		9,10 dihydro, 7-hydro, 8 ketone of BaP		9,10 dihydro-BaP		7,8(trans)-dihydro- 7,8 dihydroxy-BaP	
λ,nm	$\epsilon \times 10^4$	λ,nm	$\epsilon \times 10^4$	λ,nm	$\epsilon \times 10^4$	λ,nm	$\epsilon \times 10^4$
				403	0.0689	395	0.114
				s(393)	0.0737	366	4.42
		410	0.157	384	0.325	347	3.48
		391	0.114	379	0.302	332	1.41
		372	0.0575	s(363)	0.305	318	0.533
344	3.60	343	3.51	345	3.15	293	2.02
318	2.16	327	1.80	329	1.78	281	1.69
306	0.815	313	0.912	316	0.953	271	1.05
295	0.272	276	4.38	299	2.68	254	3.77
272	3.72	227	0.0340	279	6.57	s(246)	--
261	1.80	219	0.725	269	5.00		
251	0.735			s(220)	1.32		
240	6.45						
231	3.04						

Table VII. Comparison of Extinction Coefficients

for Aromatic Compounds with Literature Values[*]

a. BaP

λ,nm	$\epsilon \times 10^4$	
	Ours	Hirayama's
225	--	2.51
265	5.64	5.02
284	5.08	5.02
284	5.08	5.02
296	5.45	5.02
383	2.00	2.51
403	0.27	0.40

b. Pyrene

λ,nm	$\epsilon \times 10^4$	
	Ours	Hirayama's
241	6.45	7.95
272	3.72	3.98
333	3.60	5.01

c. Chrysene

λ,nm	$\epsilon \times 10^4$	
	Ours	Hirayama's
220	2.46	3.98
267	10.1	10.6
319	0.92	1.59
360	0.100	0.100

[*]Literature values taken from Hirayama, reference 7.

chrysene are not quite as good, but serve to validate the results obtained here.

3. Corrected Fluorescence Spectra of Derivatives of BaP

a. Corrected Emission Spectra

The corrected emission spectra of BaP derivatives are as sensitive or more so than the absorption spectra to substituent effects. As for the absorption spectra, the saturation or substitution of double bonds has profound effects on the fluorescence spectra. The emission spectra corresponding to BaP, chrysene, benz(a)anthracene, and pyrene are all distinctly different, in both relative intensities of the vibronic bands and in that the latter three are all blue-shifted relative to BaP (Chart 14). The spectrum of the cis-4,5-dihydro-dihydroxy-BaP is qualitatively identical to that of chrysene, and red-shifted by about 5 nm (Chart 15). The 9,10-dihydro, 7-hydro, 8-ketone of BaP has a very large red shift, and unusual vibronic intensity ratios (Chart 16a). The spectrum of the 9,10-dihydro-BaP is virtually identical to that of BaP, showing that the additional ketone group and the loss of the 7,8 double bond in the previously mentioned ketone are responsible for the anomalies in its spectrum (Chart 16b). The trans-7,8-dihydro-dihydroxy-BaP has a spectrum with the rough relative vibronic intensity ratios of BaP, but is shifted to the blue of BaP (Chart 16c).

The effects of hydroxy substituents is essentially the same as that for the absorption spectra. The 3- and 9-hydroxy-BaP derivatives have spectra shifted to the red of BaP, but retain the same rough relative vibronic intensity ratios (Charts 17a and b). This in contrast to the alteration of the intensities of the vibronic bands in the absorption

XBL 768 – 9501

Chart 14

BaP cis-4,5-dihydro-diol

XBL 769-9587

Chart 15

a) 9,10-dihydro, 8-hydro, 7-one of BaP

b) 9,10-dihydro-BaP

c) trans-7,8-dihydro-dihydroxy-BaP

FLUORESCENCE INTENSITY (arb. units)

λ (nm)

XBL 769-9588

Chart 16

a) 9-hydroxy-BaP

b) 3-hydroxy-BaP

FLUORESCENCE INTENSITY (arb. units)

λ (nm)
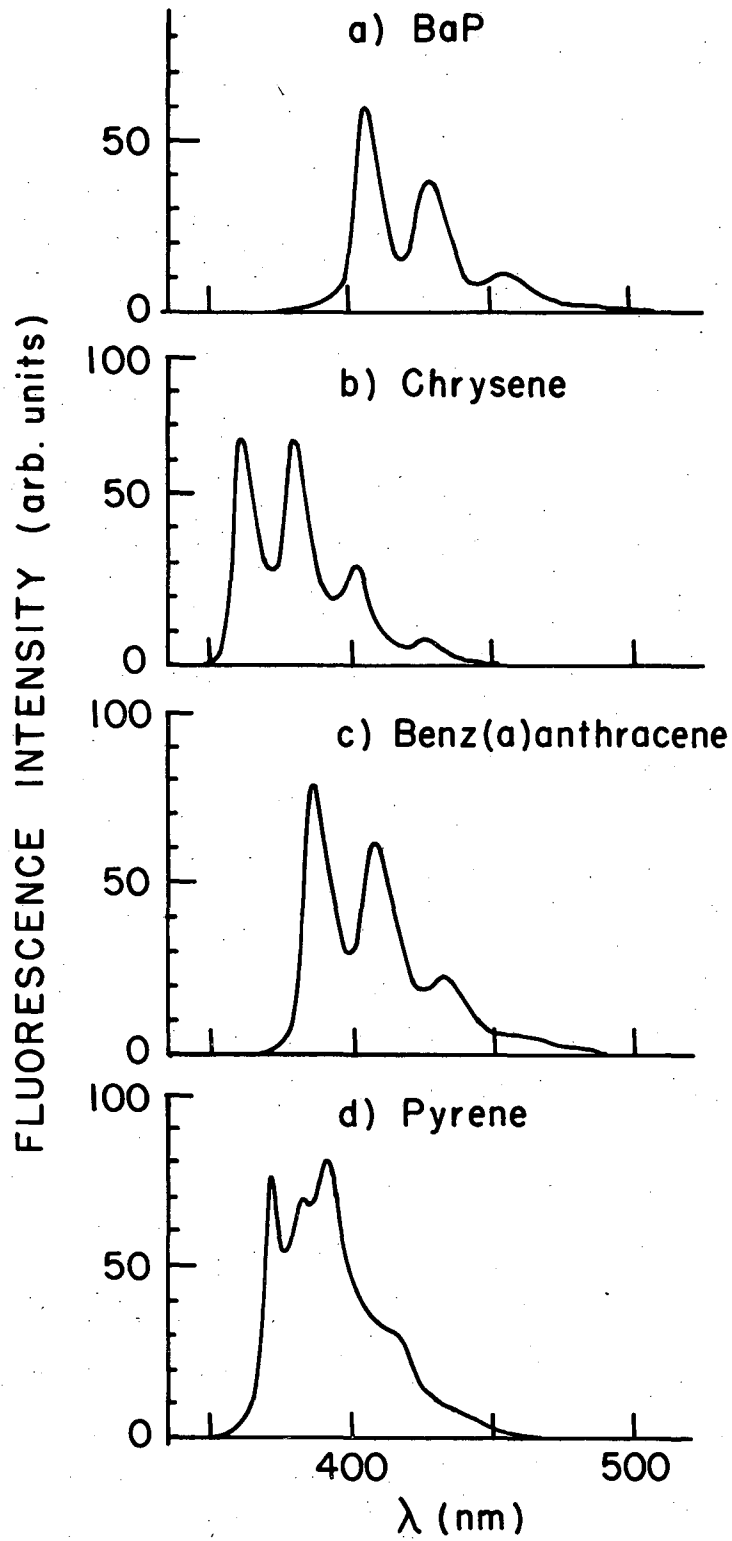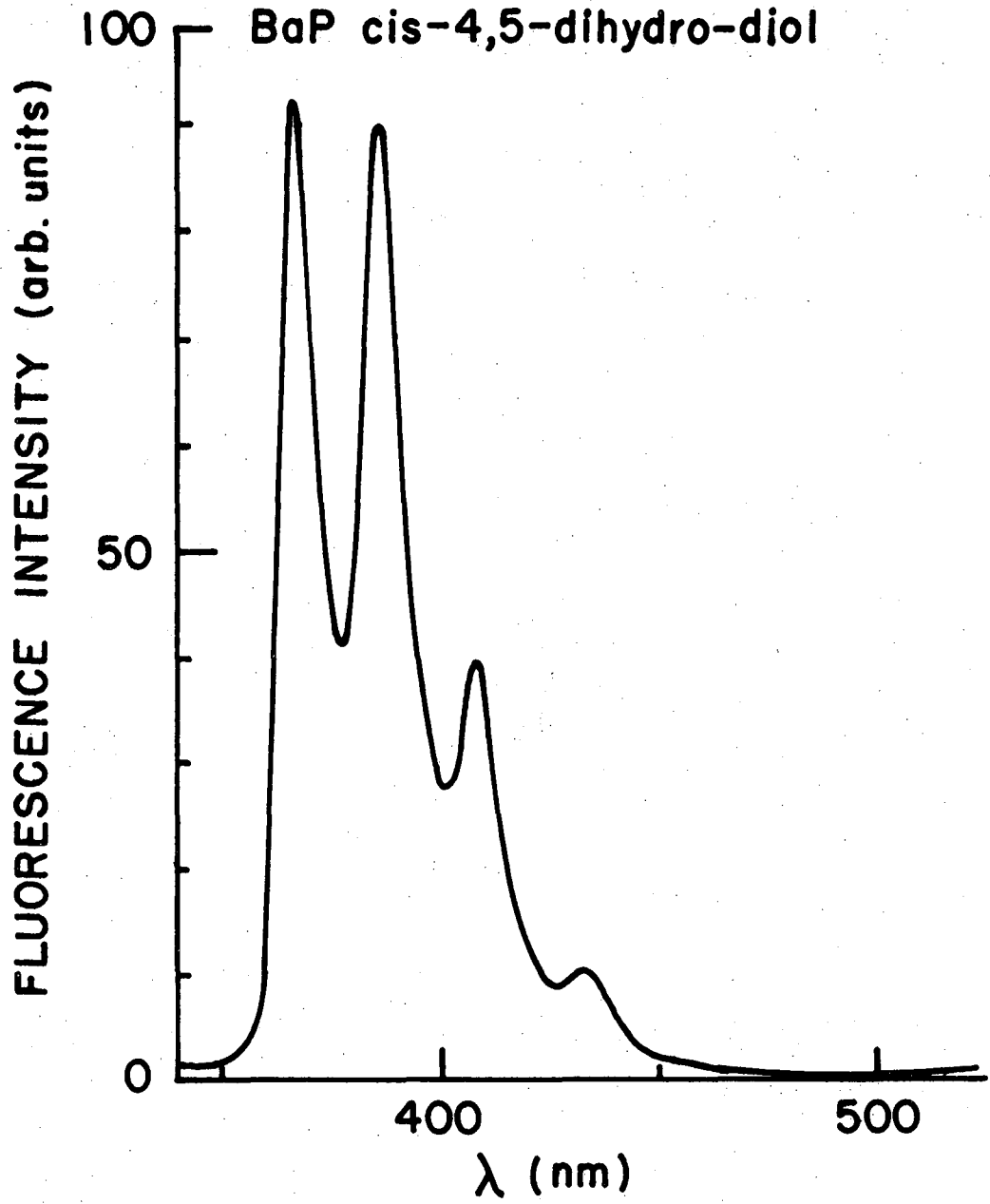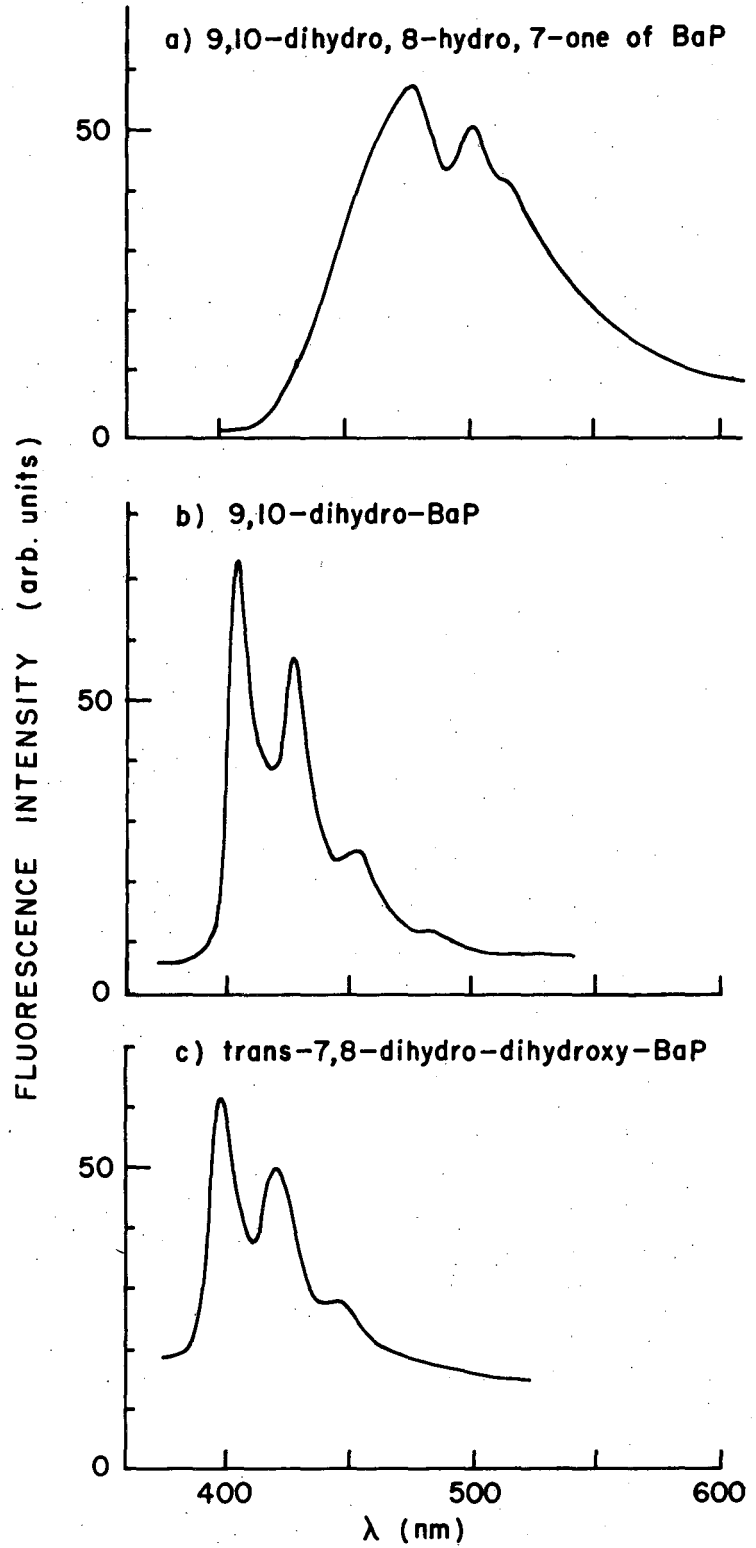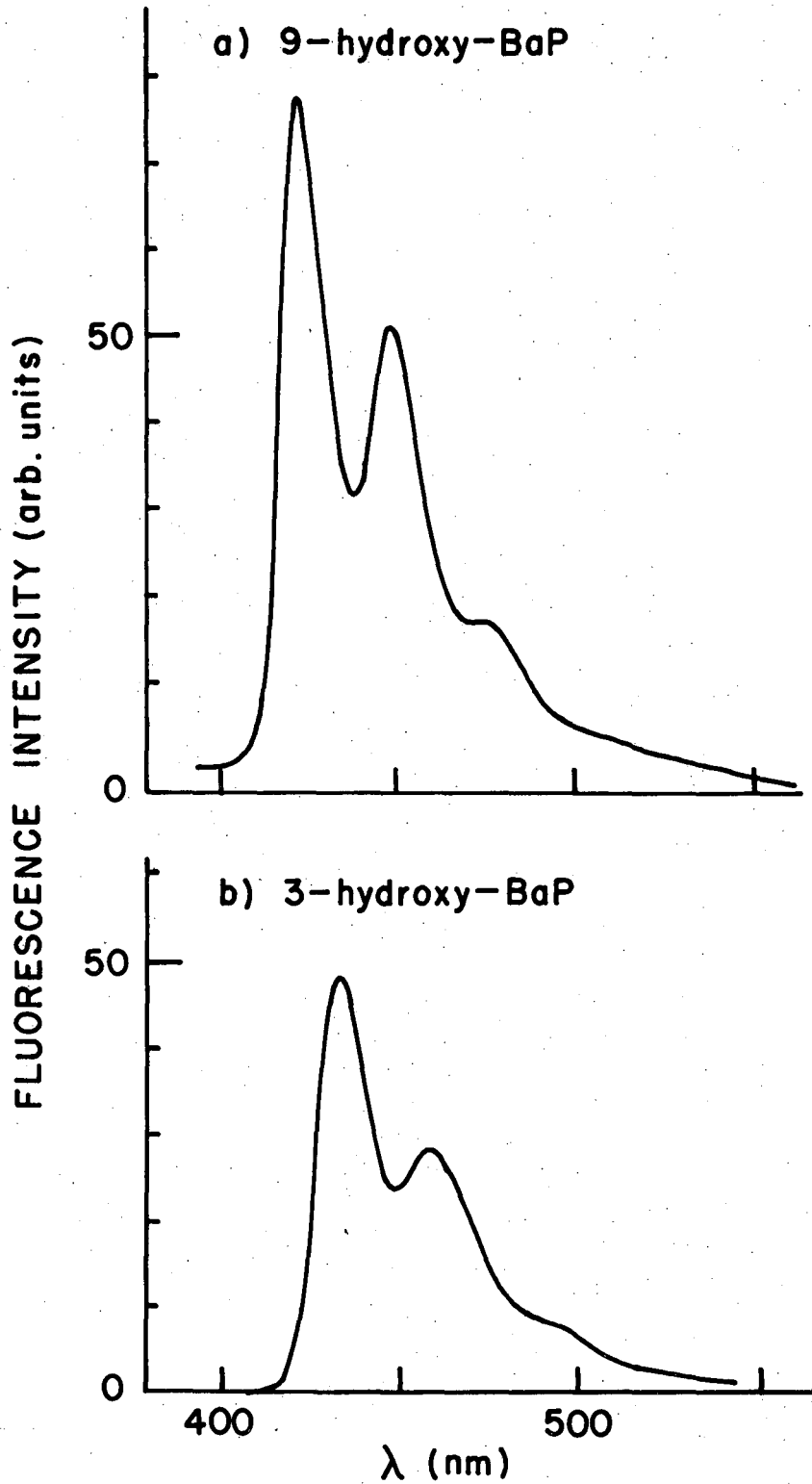
XBL 769-9581

Chart 17

spectra of these compounds. The spectrum of the 3-hydroxy-BaP is slightly to the red of the 9-hydroxy-BaP. In a comparison of the 6- and 7-hydroxy-BaP compounds, it is interesting that the emission spectra results are reversed relative to the absorption spectra, since the 7-hydroxy-BaP loses most of its fine structure while the 6-hydroxy-BaP has partially resolved vibronic bands (Chart 18).

None of the quinones was found to be fluorescent, and so no spectra are reported for them.

Again, the effects of single substitution at the six position of BaP are in parallel with these effects in the absorption spectra. The red-shift increases in the same substituent order, and the spectra retain the BaP vibronic structure (Charts 19 and 20). Emission maxima for all these compounds are listed in Table IX.

b. Corrected Fluorescence Excitation Spectra of the Derivatives

In metabolism studies one deals with ng to ug quantities of materials. Since fluorescence is more sensitive than absorption, it would be useful to employ fluorescence in the identification of metabolites of BaP. For instance, in the detection of BaP itself, Tables VIII and X show that fluorescence is 100 times more sensitive than absorbance. However, if fluorescence is employed, it would also be useful to take excitation spectra as well as emission spectra, since the corrected excitation spectra of compounds frequently resemble the absorption spectra.

Fortunately, the corrected fluorescence excitation spectra of BaP, chrysene, benz(a)anthracene, and pyrene are almost identical to the absorption spectra of these compounds, although there is a slight loss of resolution in the fluorescence spectra (Charts 21-24). All of the
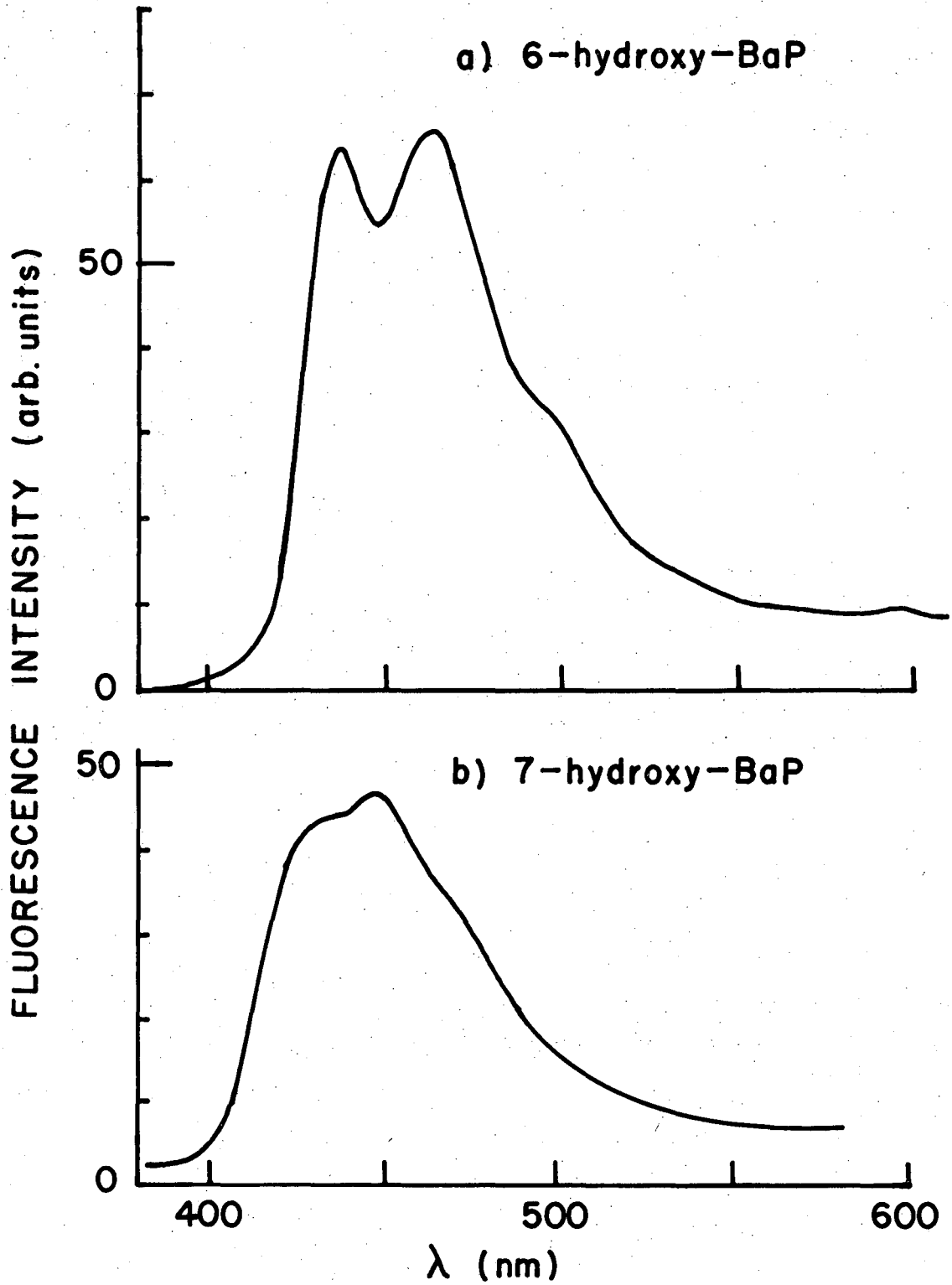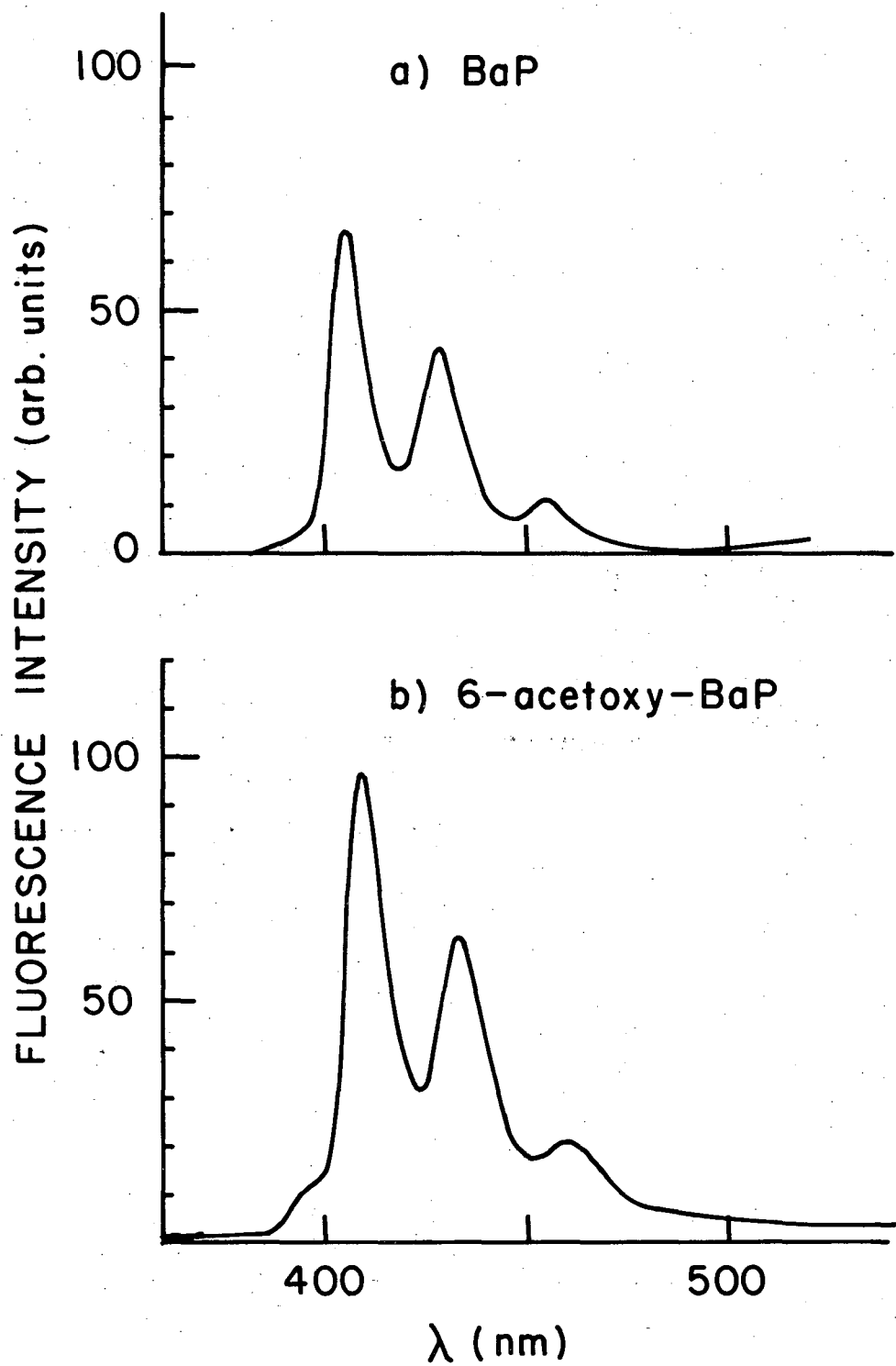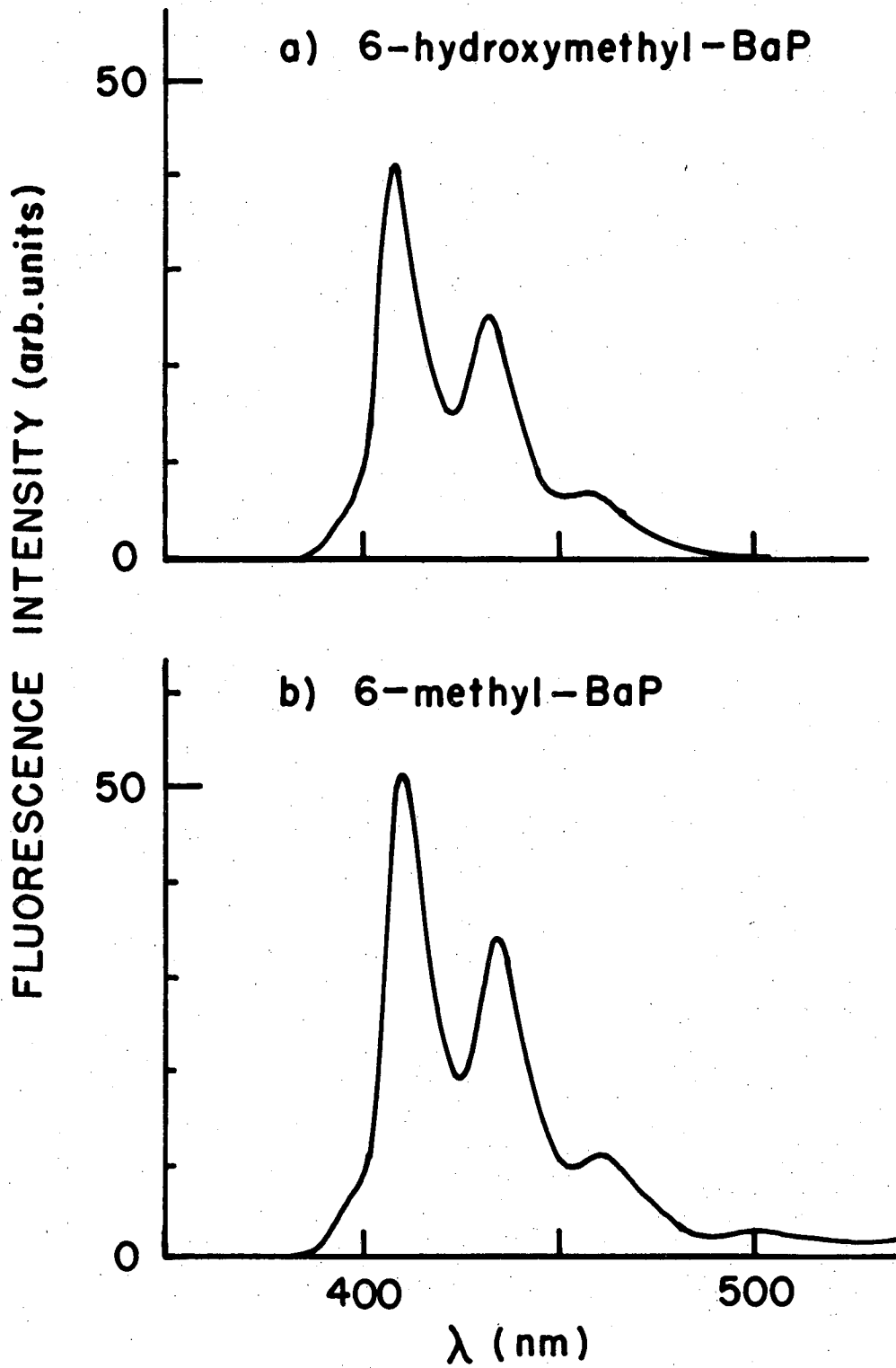
a) 6-hydroxy–BaP

b) 7-hydroxy–BaP

FLUORESCENCE INTENSITY (arb. units)

λ (nm)

XBL 769-9580

Chart 18

a) BaP

b) 6-acetoxy-BaP

FLUORESCENCE INTENSITY (arb. units)

λ (nm)

XBL 768-9502

Chart 19

Chart 20

XBL 769-9582

BaP

XBL 769-9584

Chart 21

Chrysene

XBL 769-9583

Chart 22

Benz(a)anthracene

a)

b)

ABSORBANCE

FLUORESCENCE INTENSITY (arb. units)

1.0

0.5

100

50

200   300   400

λ (nm)

XBL 769-9585

Chart 23

Pyrene

a)

b)

XBL 769-9586

Chart 24
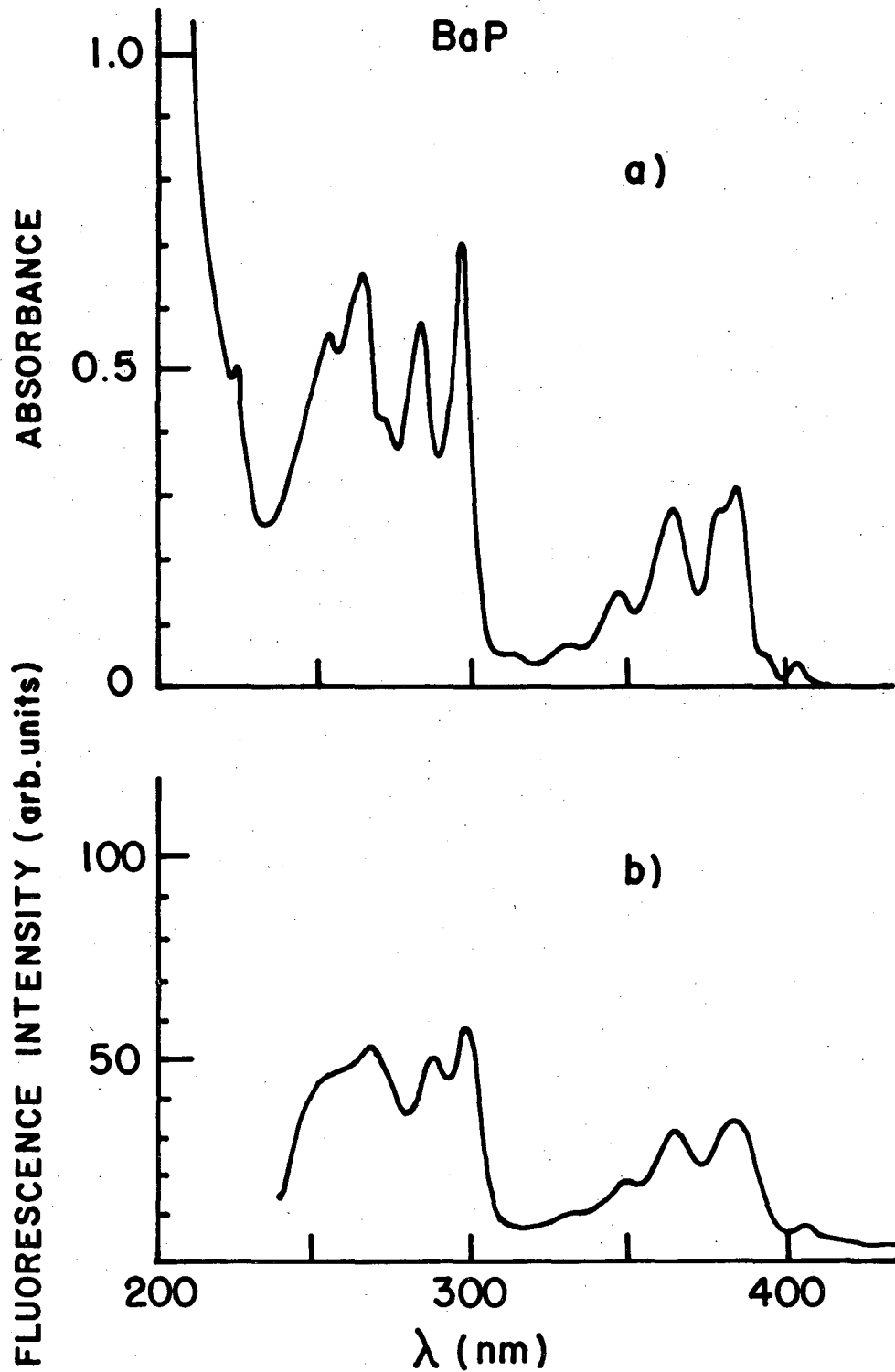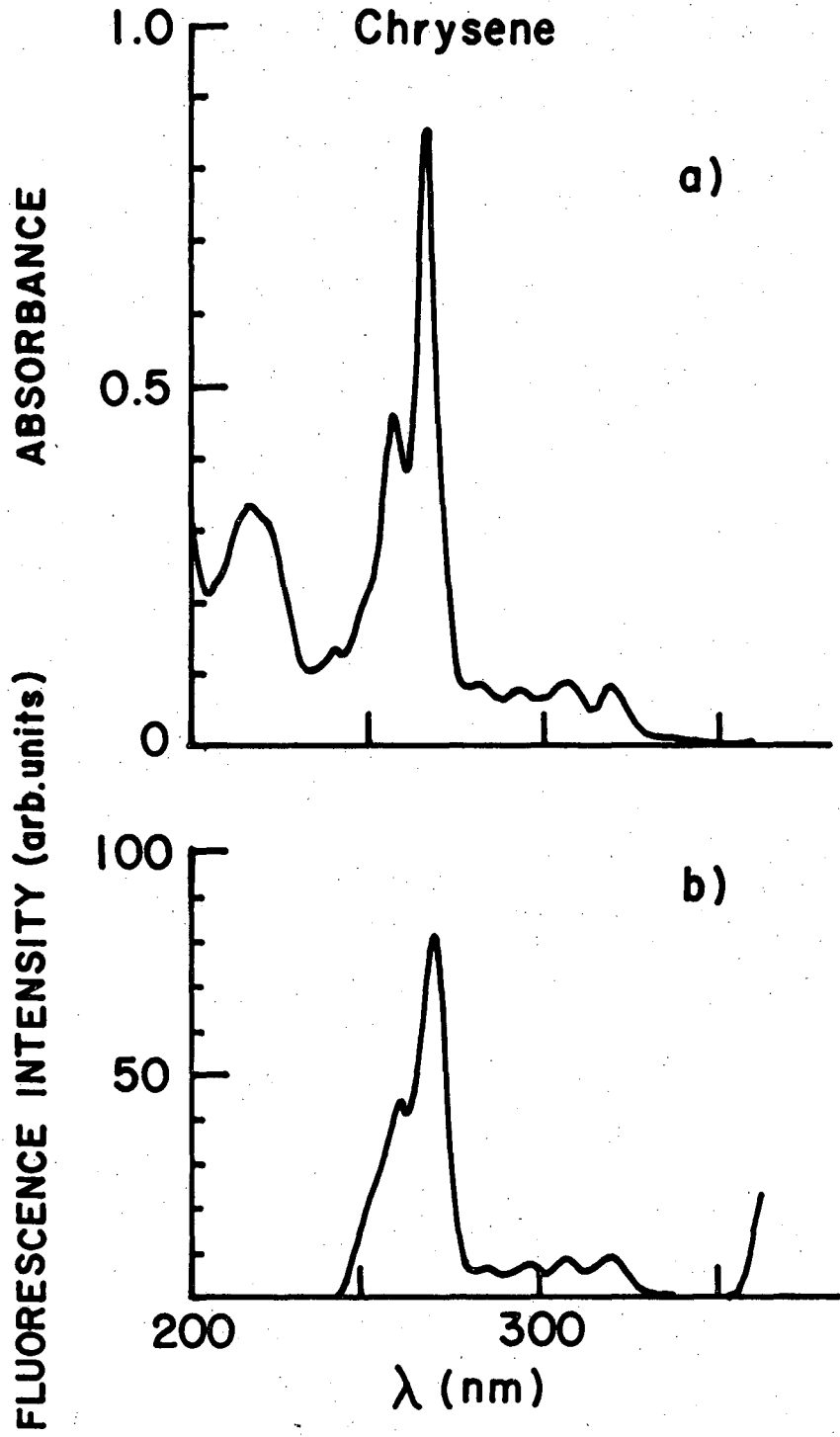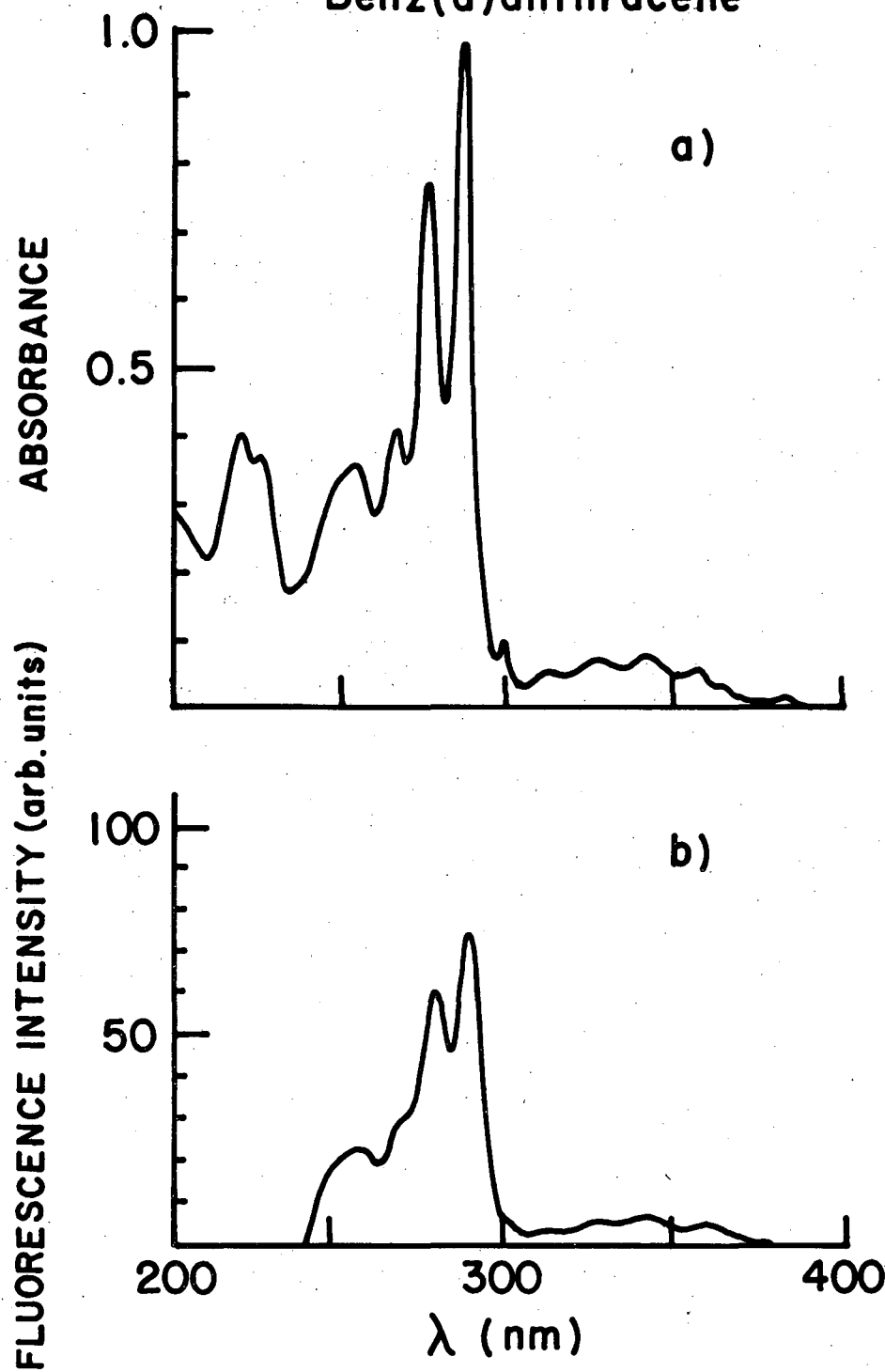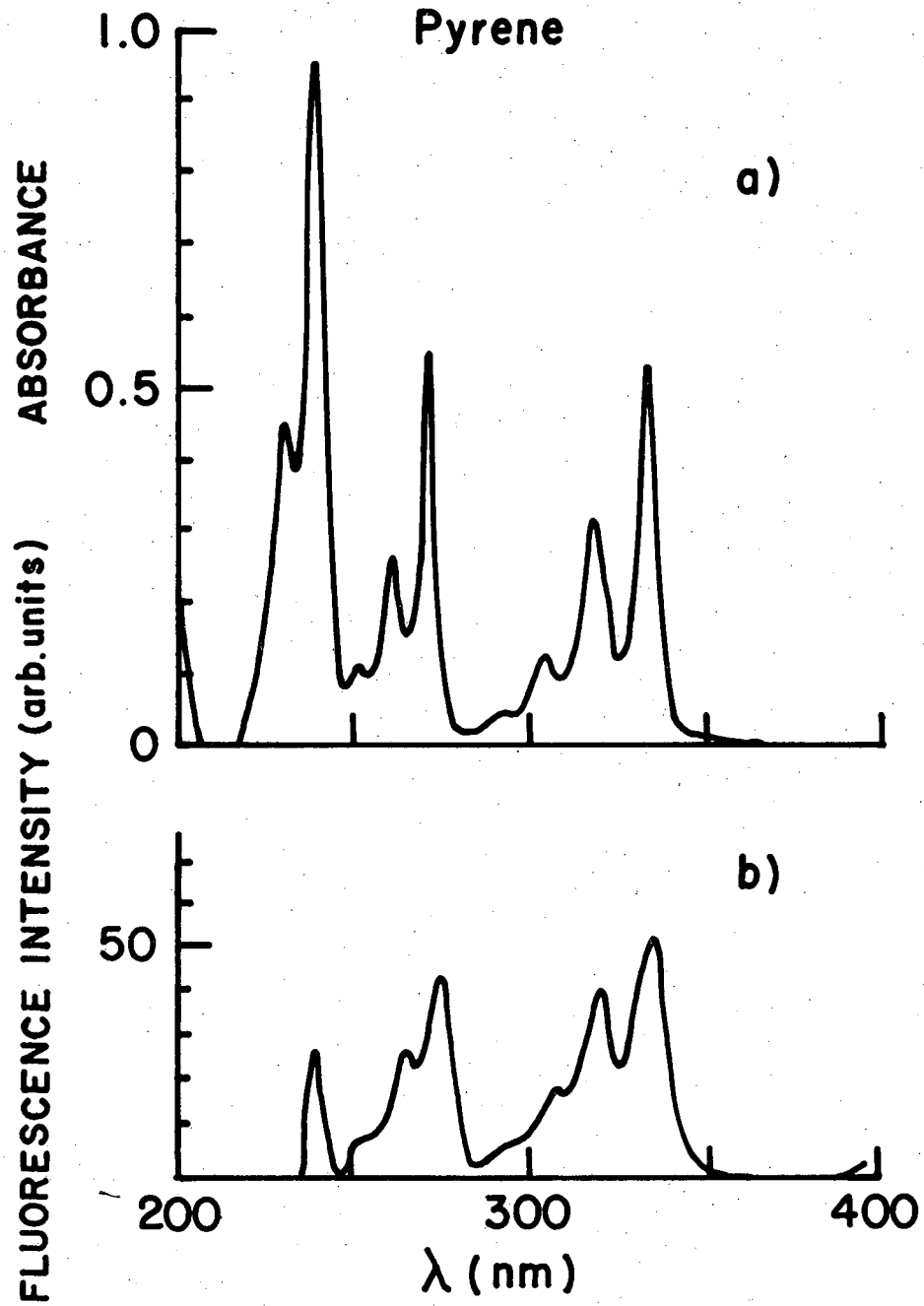
other derivatives of BaP were tested for the match of the absorption

and fluroescence excitation spectra, and it was found that the agreement

was as good as in the figures just presented; this can be seen by

comparing Tables XI and XII.

c. Miminum Detectable Levels of Metabolites

Unfortunately, the amounts of BaP metabolized by cell culture micro-

somal preparations will be at the ng level. Therefore, absorption

spectra will be stretched to the limit, and sometimes are not sensitive

enough. Table VIII depicts the minimum levels of BaP derivatives

detectable in a one ml sample with a 1 cm pathlength using the Cary 118

absorption spectrophotometer, which can accurately measure 0.01

absorbance.

Table VIII. Minimum Detectable Limits of Derivatives of BaP by Absorption Measurements, Assuming Highest Spectra Peak at Have OD of 0.01

Compound	$\lambda_{(highest)}$	C_{min}, molar $\times 10^{-7}$	Amount min, ng
BaP	296	1.07	26.9
9,10 di[H], 7[H] 8-one of BaP	308	2.28	61.5
6-acetoxy BaP	299	0.99	30.6
6-aldehyde + acetal of BaP	308	3.32	93.0
6-hydroxymethyl BaP	300	1.86	52.4
6-methyl BaP	300	2.18	58.0
BaP 1,6-quinone	460	151.0	4,260.0
BaP 3,6-quinone	478	264.0	7,450.0
BaP 6,12-quinone	--	--	--
BaP 4,5-quinone	272	1.31	36.9
BaP 4,5-epoxide	272	2.91	78.0

*Rough calculation based on one measured concentration and one absorbance value, not done by least squares fit.

Table IX. The Effect of Substituents on the Corrected Fluorescence.

Emission Spectra of BaP Derivatives in Ethanol Solution.

Compound	Emission Maxima, nm
BaP	405, 428, 455
6-Acetoxy-BaP	408, 433, 459
6-hydroxymethyl-BaP	409, 433, 458
6-methyl-BaP	411, 435, 463
6-hydroxy-BaP	439, 459
Hemiacetal of 6-aldehyde of BaP	410, 435, s(460)
6-aldehyde of BaP	s(480), s(505), 517
4 and/or 5-hydroxy-BaP[†]	421, 444, s(470)
cis 4,5 dihydro-dihydroxy-BaP	367, 387, 408, 433
9,10 dihydro, 8 hydro, 7 one of BaP	478, 502
3-hydroxy-BaP	434, 459, s(496)
Pyrene	372, 383, 392, s(410)
Chrysene	362, 380, 401, 424
Benz(a)anthracene	386, 407, 432
trans 7,8 dihydro-dihydroxy-BaP	398, 420, 445, s(470)
9-hydroxy-BaP	422, 449, 477
7-hydroxy-BaP	450, s(430)
9,10 dihydro-BaP	405, 426, 453, 482

[†]Generated by the spontaneous isomerization of
BaP-4,5 epoxide.

Table X. Calibration and Lower Limits of Detectability

for BaP Derivatives Using Emission Spectroscopy.

Compound	Emission	nm Constant*	Ex., nm	Min.Det. Conc., M.	Min.Det. Wt.,ng.
BaP	405	1.09×10^{-2}	300	1.51×10^{-9}	0.38
	428	2.33×10^{-3}			
6-Acetoxy-BaP	408	9.23×10^{-3}	300	2.55×10^{-9}	0.79
	432	2.51×10^{-3}			
6-hydroxymethyl-BaP	409	4.74×10^{-3}	300	1.02×10^{-8}	2.85
	433	1.11×10^{-3}			
6-methyl-BaP	411	2.71×10^{-3}	300	2.12×10^{-9}	0.56
	435	7.96×10^{-4}			
6-aldehyde-BaP	410	9.51×10^{-4}	300	1.16×10^{-8}	3.25
(as hemiacetal)	433	2.48×10^{-3}			
9,10 dihydro-, 7 hydro-	478	4.64×10^{-5}	343	4.80×10^{-8}	13.0
8 one of BaP	503	6.11×10^{-4}			
cis 4,5 dihydro-,	387	2.12×10^{-2}	273	1.01×10^{-8}	2.87
dihydroxy-BaP	408	1.97×10^{-3}			
BaP 4,5 oxide (as	423	8.91×10^{-3}	274	2.03×10^{-9}	0.52
4 and/or 5 OH-BaP)	447	3.02×10^{-3}			

*This constant is the slope of the line derived from plotting
the fluorescence intensity of the compound divided by the
fluorescence intensity of 8.45×10^{-6} M quinine sulfate
dihydrate in 1N H_2SO_4 vs concentration. It has units of
$cm^{-1} nM^{-1}$.

Table XI.   Maxima in the Absorption Spectra for

BaP Derivatives/Ethanol

Compound	Maxima
BaP	226, 255, 265, 272, 284, 296, 332, 347, 364, 378, 381, 384, 403
6-hydroxymethyl-BaP	204, 221, 228, 257, 267, 277, 288, 300, 338, 353, 371, 392, 407
6-acetoxy-BaP	220, 226, 255, 266, 275, 287, 299, 337, 353, 371, 392, 406
6-methyl-BaP	221, 227, 256, 267, 277, 288, 300, 339, 355, 373, 393, 410
3-hydroxy-BaP	228, 257, 268, 293, 308, 345, 361, 380, 401
9,10 dihydro, 8 hydro, 7 one of BaP	219, 227, 276, 313, 327, 343, 372, 391, 410
cis 4,5 dihydro-dihydroxy-BaP	222, 244, 263, 273, 299, 310, 324, 347, 365
trans 7,8-dihydro-dihydroxy-BaP	246, 254, 271, 281, 293, 318, 332, 347, 366, 395
9-hydroxy-BaP	225, 254, 260, 267, 282, 287, 302, 327, 343, 361, 380, 395, 418
7-hydroxy-BaP	223, 231, 252, 260, 268, 292, 303, 343, 360, 378, 400
9,10-dihydro-BaP	s(220), 269, 279, 299, 316, 329, 345, s(363), 379, 384, s(393), 403

Table XII.   Maxima in the Corrected Fluorescence

Excitation Spectra of BaP Derivatives in Ethanol.

Compound	Maxima	Em.	Conc.
BaP	s(260), 268, 288, 299, s(334), 349, 365, 383, 403	427	7.42×10^{-8}
6-hydroxymethyl-BaP	s(261), 271, 291, 302, s(337), 355, 372, 392, 407	432	4.10×10^{-7}
6-acetoxy-BaP	s(258), 269, 290, 302, s(339), 355, 372, 391, 407	430	2.55×10^{-7}
Hemiacetal of 6-aldehyde of BaP	271, 291, 303, s(339), 356, 374, 394, s(407)	433	1.16×10^{-7}
6-methyl-BaP	272, 292, 303, s(339), 358, 374, 394, 410	432	2.12×10^{-7}
3-hydroxy-BaP	272, 299, 307, 349, 362, 381, 402, 427	456	5.55×10^{-7}
9,10 dihydro, 8 hydro, 7 one of BaP	280, 314, 328, 345, 416 (broad)	472	4.80×10^{-7}
cis 4,5 dihydro-dihydroxy-BaP	268, 277, 300, 310, 310, 315	387	1.00×10^{-6}
trans 7,8 dihydro-dihydroxy-BaP	258, 286, 296, 318, 334, 349, 366, s(395)	398	8.75×10^{-7}
9-hydroxy-BaP	272, 292, 304, 327, s(344), 363, 381, 396, 420	440	7.02×10^{-7}
7-hydroxy-BaP	270, s(295), 304, s(340), s(360), 379, 400	450	5.26×10^{-6}
9,10 dihydro-BaP	270, 285, 297, 328, 356, 363, 403	405	2.09×10^{-6}

E. References

1. Beynon, J. H., Saunders, R. A., and Williams, A. E. The Mass Spectra of Organic Molecules. Elsevier Publishing Company, New York, 1968, pg. 129.

2. Borgen, A., Darvey, H., Castagnoli, N., Crocker, T. T., Rasmussen, R. E., and Wang, I. Metabolic Conversion of Benzo(a)pyrene by Syrian Hamster Liver Microsomes and Binding of Metabolites to Deoxyribonucleic Acid. J. Med. Chem., 16: 502-505, 1973.

3. Budzkiewicz, H., Djerassi, C., and Williams, D. H. Mass Spectrometry of Organic Compounds. Holden-Day, Inc. 1967, pg. 462.

4. Fieser, L., and Hershberg, E. B. The Orientation of 3.4 Benzpyrene in Substitution Reactions. J.A.C.S., 61: 1565-1573, 1939.

5. Flesher, J. W., and Sydnor, K. L. Possible Role of 6-Hydroxymethyl-Benzo(a)pyrene as a Proximate Carcinogen of Benzo(a)pyrene and 6-Methyl-Benzo(a)pyrene. Int. J. Cancer, 11: 433-437, 1973.

6. Grover, P. L., Hewer, A., and Sims, P. Formation of K-Region Epoxides as Microsomal Metabolites of Pyrene and Benzo(a)pyrene. Biochem. Pharmacol., 21: 2713-2726, 1972.

7. Hirayama, K. Handbook of Ultraviolet and Visible Absorption Spectra of Organic Compounds. Plenum Press, 1967.

8. Huberman, E., Sachs, L., Yang, S. K., and Gelboin, H. V. Identification of Mutagenic Metabolites of Benzo(a)pyrene in Mammalian Cells. P.N.A.S., U.S., 73: 607-611, 1976.

9. Johnson, M., and Calvin, M. Induced Nucleophilic Substitution in Benzo(a)pyrene. Nature, 241: 271-272, 1973.

10. Kinoshita, N., Shears, B., and Gelboin, H. V. K-Region and
Non-K-Region Metabolism of Benzo(a)pyrene by Rat Liver Microsomes.
Cancer Res., 33: 1937-1944, 1973.

11. McLafferty, F. W. Interpretation of Mass Spectra. Second Edition.
W. A. Benjamin, Inc. 1973. pg. 118.

12. Meehan, T., Straub, K., and Calvin, M. Elucidation of Hydrocarbon
Structure in an Enzyme-Catalyzed Benzo(a)pyrene-Poly(G) Covalent
Complex. P.N.A.S., U.S., 73: 1437-1441, 1976.

13. Pilar, F. Elementary Quantum Chemistry, 1968, McGraw-Hill. pg, 441.

14. Selkirk, J. K., Croy, R. G., and Gelboin, H. V. Isolation by High
Pressure Liquid Chromatography and Characterization of Benzo(a)pyrene-
4,5-Epoxide as a Metabolite of Benzo(a)pyrene. Arch. Biochem. Biophys.,
168: 322-326, 1975.

15. Selkrk, J. K., Croy, R. G., and Gelboin, H. V. High-Pressure
Liquid Chromatographic Separation of 10 Benz(a)pyrene Phenols and
the Identification of 1-Phenol and 7-Phenol as New Metabolites.
Cancer Res., 36: 922-926, 1976.

16. Sims, P. The Metabolism of Benzo(a)pyrene by Rat-Liver Homogenates.
Biochem. Pharmacol., 16: 613-618, 1967.

17. Sims, P. The Metabolism of Some Aromatic Hydrocarbons by Mouse
Embryo Cell Cultures. Biochem. Pharmacol., 19: 285-297, 1970.

18. Straub, K. Thesis, University of California, Berkeley, California.
1977.

19. Wang, I. Y., Rasmussen, R. E., and Crocker, T. T. Isolation and
Characterization of an Active DNA-Binding Metabolite of Benzo(a)-
pyrene from Hamster Liver Microsomal Incubation Systems. Biochem.
Pharmacol., 49: 1142-1149, 1972.

Chart Legends — Chapter IV

Chart 1. Low resolution mass spectra of a) BaP, b) 7-hydroxy-BaP, and cis-4,5-dihydro-4,5-dihydroxy-BaP.

Chart 2. Postulated structures of ion fragments appearing in the low resolution mass spectra of a) BaP, b) 6-hydroxy-BaP, and c) 6-hydroxymethyl-BaP.

Chart 3. Postulated structures of ion fragments appearing in the low resolution mass spectra of a) 6-acetoxy-BaP and b) cis-4,5-dihydro-4,5-dihydroxy-BaP.

Chart 4. Postulated structures of ion fragments appearing in the low resolution mass spectra of a) 9,10-dihydro-BaP and b) 9,10-dihydro-, 7-hydro, 8-ketone of BaP.

Chart 5. Low resolution mass spectra of a) 9,10-dihydro, 7-hydro, 8-ketone of BaP and b) BaP-4,5-quinone.

Chart 6. Postulated structures of ion fragments appearing in the low resolution mass spectra of a) BaP-4,5-quinone and b) molecular structures of BaP and the lower aromatic hydrocarbons from which BaP may be formally derived.

Chart 7. The UV-visible absorption spectra in ethanol of a) 7.42×10^{-6} M BaP, b) 8.45×10^{-6} M Chrysene, c) 1.51×10^{-5} M Benz(a)anthracene, and d) 1.47×10^{-4} M Pyrene.

Chart 8.   The UV-visible absorption spectra of a) 9.04×10^{-6} M cis-4,5-dihydro-4,5-dihydroxy-BaP, b) BaP-4,5-oxide, and c) 1.06×10^{-5} M BaP-4,5-quinone.

Chart 9.   The UV-visible absorption spectra of a) 1.92×10^{-5} M 9,10-dihydro-, 7-hydro-, 8-ketone of BaP and b) trans-7,8-dihydro-7,8-dihydroxy-BaP, 1.75×10^{-5} M.

Chart 10.   The UV-visible absorption spectra of a) 4.85×10^{-4} M BaP-1,6-quinone,   b) 7.39×10^{-4} M BaP-3,6-quinone, and c) 3.1×10^{-5} M BaP-6,12-quinone.

Chart 11.   The UV-visible absorption spectra of a) 1.30×10^{-5} M 6-hydroxy-BaP and b) 3.05×10^{-5} M 7-hydroxy-BaP.

Chart 12.   The UV-visible absorption spectra of a) 2.23×10^{-5} M 3-hydroxy-BaP and b) 1.75×10^{-5} M 9-hydroxy-BaP.

Chart 13.   The UV-visible absorption spectra of a) 7.42×10^{-6} M BaP, b) 1.64×10^{-5} M 6-hydroxy-methyl-BaP, and c) 2.15×10^{-5} M 6-methyl-BaP.

Chart 14.   Fluorescence emission spectra of a) BaP, 2.97×10^{-6} M, excitation 300 nm, sample sens. 1.0,   b) Chrysene, 6.75×10^{-7} M, excitation 272 nm, sample sens. 30,   c) Benz(a)anthracene, 1.39×10^{-6} M, excitation 290 nm, sample sens. 3.0,   and d) Pyrene, 1.30×10^{-5} M, excitation 334 nm, sample sens. 3.0.

Chart 22. Comparison of a) the absorption spectrum of Chrysene,
8.45×10^{-6} M, with b) the corrected fluorescence excitation
spectrum of Chrysene, 6.75×10^{-7} M, emission at 362 nm,
reference ratio 2, sample sens. 10.

Chart 23. Comparison of a) the absorption spectrum of Benz(a)anthracene,
1.51×10^{-5} M, with b) the corrected fluorescence excitation
spectrum of benz(a)anthracene, 1.39×10^{-6} M, emission 409 nm,
sample sens. 30, reference ratio 2.

Chart 24. Comparison of a) the absorption spectrum of Pyrene, 1.47×10^{-4}
M, with b) the corrected fluorescence excitation spectrum of
Pyrene, 1.30×10^{-5} M, emission at 394 nm, reference ratio 2,
sample sens. 3.0.

Acknowledgments

The help and encouragement of many people made this thesis possible.

Firstly, I would like to thank Dr. Melvin Calvin for sponsoring my thesis work in the Chemistry Department, for his generosity in sending me to two Cell Biology Meetings, to Los Alamos Laboratory, and to a liquid chromatography training course, and for allowing me considerable latitude in my investigations. He is also to be commended for providing one of the best equipped laboratories in the world, one in which an investigator is not equipment- or money-limited, but instead, self-limited.

I would like to thank Dr. Richard Lemmon for accepting me into the laboratory on a temporary basis for a job before I started graduate school, and for the numerous favors and help in the purchase of equipment that he has provided. In addition, I am grateful to Wally Irwin and Ben Gordon for showing me the rudiments of liquid scintillation counting and gas chromatography.

I am especially grateful to Dr. Paul Philp for running mass spectra for me and showing me some fundamentals of the technique, and to both he and Kelly for their friendship.

Drs. Tom Meehan, Sue Hawkes, Mina Bissell, and Al Bassham were extremely helpful to me in the writing of my first paper with their criticisms and encouragement. The acceptance of this paper gave me the confidence to finish the work.

Dr. Steve Cooper, my special friend and confidant, who listened patiently to most of my data, contributed assessments and encouragements toward it, taught me some inorganic chemistry, and in general made it